3GPP TR 25.892 V2.0.0 (2004-06)

Technical Report

3rd Generation Partnership Project;
Technical Specification Group Radio Access Network;
Feasibility Study for OFDM for UTRAN enhancement;
(Release 6)

OFDM for UTRAN enhancement

<keyword[, keyword]>

3GPP

Postal address

3GPP support office address

650 Route des Lucioles - Sophia Antipolis
Valbonne - FRANCE
Tel.: +33 4 92 94 42 00 Fax: +33 4 93 65 47 16

Internet

http://www.3gpp.org

Contents

Foreword

This Technical Report has been produced by the 3rd Generation Partnership Project (3GPP).

The contents of the present document are subject to continuing work within the TSG and may change following formal TSG approval. Should the TSG modify the contents of the present document, it will be re-released by the TSG with an identifying change of release date and an increase in version number as follows:

Version x.y.z

where:

x   the first digit:

1   presented to TSG for information;

2   presented to TSG for approval;

3   or greater indicates TSG approved document under change control.

y   the second digit is incremented for all changes of substance, i.e. technical enhancements, corrections, updates, etc.

z   the third digit is incremented when editorial only changes have been incorporated in the document.

Introduction

This technical report presents the results of the 3GPP system Study Item to consider the application of OFDM techniques to 3GPP-based systems. This study includes an analysis of the feasibility and potential benefits of introducing OFDM in UTRAN and a recommendation to RAN Plenary on a potential standardisation work plan and time frame.

As the mobile radio systems evolve and become more integrated with daily activities, there is an increasing requirement for additional services requiring very high bit rates and higher system capacity. These include both services to individuals as well as multimedia broadcast and multi-cast services. OFDM (Orthogonal Frequency Division Multiplexing) is a technology that has been shown to be well suited to the mobile radio environment for high rate and multimedia services. Examples of commercial OFDM systems include the Digital Audio Broadcast (DAB), Digital Video Broadcast Terrestrial (DVB-T) and the HiperLAN and IEEE WLAN (802.11a) wireless local area network systems.

Editor's notes : Provides a high-level outline of report, and summary of the rational, conclusions and recommendations. Important considerations are why the new technology might be needed, compatibility with previous releases of UTRAN, aspects of new service requirements, constraints of spectrum. It is a study of physical layer aspects only and does not include changes in UTRAN architectures beyond those needed to support an additional physical layer.

1 Scope

The scope of this Study Item is to consider the performance of OFDM in the mobile environment and to consider scenarios in which OFDM may be introduced in UTRAN 3GPP based systems. This activity involves the Radio Access work area of the 3GPP studies and has some effect on the Mobile Equipment and Access Network of the 3GPP systems.

The aims of this study are:

- to consider the advantages that may be gained by introducing a new modulation technique in 3GPP RAN systems,

- to estimate possible benefits and complexity and

- to recommend to 3GPP RAN if further standardisation development work should be undertaken by 3GPP.

As a starting point, OFDM will be considered in the downlink only. It should be possible to operate in a 5MHz spectrum allocation i.e. coupled with W-CDMA in the uplink for a 2*5MHz deployment scenario.

The following list provides examples of areas that are to be considered in the study:

- Throughput for data services . To be compared with throughput of current UTRAN releases;

- Complexity aspects of multimode UEs supporting both OFDM and release 99/release 5 UMTS;

- Deployment scenarios including frequency re-use aspects within diverse spectrum allocations;

The study should consider performance aspects, aspects linked to the evolution of UMTS (high level architecture, diverse spectrum arrangements and allocations), impacts on signalling in UTRAN , aspects of capacity/cost/complexity/coverage and aspects of co-existence with the existing UMTS modes.

The purpose of the study is to consider the feasibility of introducing OFDM in UTRAN and to compare OFDM performance with HSDPA. The analysis of OFDM performance and its comparison with reference HSDPA performance should be based on a basic OFDM design (often referred as textbook OFDM). More elaborate OFDM techniques should not be considered. However the use of text book OFDM in the feasibility study phase does not restrict the design when moving to the specification phase. It is a study of physical layer aspects only and does not include changes in UTRAN architecture. Changes are to be restricted to the physical layer and not extend beyond those needed to support an additional modulation. Principles as provided in TS 25.302 (Services provided by the physical layer) are to be respected where possible.

This study item was approved by the TSG RAN#16 (Marco Island Fl USA 4th – 7th June 2002).

2 References

The following documents contain provisions which, through reference in this text, constitute provisions of the present document.

- References are either specific (identified by date of publication, edition number, version number, etc.) or non-specific.

- For a specific reference, subsequent revisions do not apply.

- For a non-specific reference, the latest version applies. In the case of a reference to a 3GPP document (including a GSM document), a non-specific reference implicitly refers to the latest version of that document *in the same Release as the present document*.

[1]   3GPP, "TR 25.848: Physical layer aspects of UTRA High Speed Downlink Packet Access", Version 4.0.0, March/2001.

[2]   3GPP, "TR 25.855: High Speed Downlink Packet Access: Overall UTRAN Description", Version 5.0.0, September/2001.

[3]   3GPP, "TR 25.858: High Speed Downlink Packet Access: Physical Layer Aspects", Version 5.0.0, March/2002.

[4] 3GPP, "TS 25.212: Multiplexing and channel coding (FDD)", Version 5.0.0, March/2002.

[5] 3GPP2, "1xEV-DV Evaluation Methodology – Addendum (V6)", July 2001.

[6] 3GPP, "TS 25.141: Base station conformance testing (FDD)", Version 5.4.0, September/2002.

[7] Huawei, "Time-frequency mappings of OFDM units for full frequency reuse without resource planning", Tdoc R1-030799, New York, NY, USA, August 25-29, 2003.

[8] Huawei, "Link-level OFDM performances under realistic inter-cell interference", Tdoc R1-031171, Lisbon, Portugal, November 17-21, 2003.

[9] 3GPP, TSG-RAN1, Nortel Networks, "Effective SIR Computation for WCDMA System-Level Simulations", Document R1-03-1299, Meeting #35, Lisbon, Portugal, November 17-21, 2003.

[10] R4-021406, "Problem on PN9 seed setting in Test Model 5", Lucent, RAN4#25, Nov 2002.

[11] 3GPP, "TS25.104: Base Station (BS) radio transmission and reception (FDD)", v6.5.0, Mar 2004.

3 Definitions, symbols and abbreviations

3.1 Definitions

For the purpose of this document, the definitions in 3GPP TR 21.905 as well as the following definitions apply.

Guard interval / Guard time: A number of samples inserted between useful OFDM symbols, in order to combat inter-OFDM-symbol-interference induced by channel dispersion and to assist receiver synchronization. It may also be used to aid spectral shaping. The guard interval may be divided into a prefix (inserted at the beginning of the useful OFDM symbol) and a postfix (inserted at the end of the previous OFDM symbol).

Inter-carrier frequency / Sub-carrier separation: The frequency separation between OFDM sub-carriers, defined as the OFDM sampling frequency divided by the FFT size.

OFDM samples: The discrete-time complex values generated at the output of the IFFT, which may be complemented by the insertion of additional complex values (such as samples for pre/post fix and time windowing). Additional digital signal processing (such as filtering) may be applied to the resulting samples, prior to being fed to a digital-to-analog converter.

OFDM sampling frequency: The total number of samples, including guard interval samples, transmitted during one OFDM symbol interval, divided by the symbol period.

Prefix/Postfix: See **Guard interval**.

Sub-carrier: The frequency over which the low data rate information is modulated; it also often refers to the related modulated carrier.

Sub-carrier separation: See **Inter-carrier frequency**.

Useful OFDM symbol: The time domain signal corresponding to the IFFT/FFT window, excluding the guard time.

Useful OFDM symbol duration: The time duration of the useful OFDM symbol.

3.2 Symbols

F_o OFDM sampling frequency.

f_d Maximum Doppler shift.

N Total number of IFFT/FFT bins (sub-carriers).

N_p Number of prefix samples.

N_u Number of modulated sub-carriers (i.e. sub-carriers carrying information).

T_s OFDM symbol period.

T_g OFDM prefix duration

T_u OFDM useful symbol duration

Δf Sub-carrier separation.

τ Channel total delay spread.

$g(t)$ Prototype function

$\Im(t)$ IOTA function

τ_0 OFDM/OQAM symbol period

3.3 Abbreviations

For the purpose of the present document, the following abbreviations apply:

FDM Frequency Division Multiplexing

FFT Fast Fourier Transform

IFFT Inverse Fast Fourier Transform

ISI Inter-Symbol Interference

IOTA Isotropic Orthogonal Transform Algorithm

MIMO Multiple-Input Multiple-Output

OFDM Orthogonal Frequency Division Multiplexing

OQAM Offset Quadrature Amplitude Modulation

PAPR Peak-to-Average Power Ratio

PSK Phase Shift Keying

QAM Quadrature Amplitude Modulation

4 OFDM Technology

4.1 OFDM Fundamentals

4.1.1 OFDM Definition

The technique of Orthogonal Frequency Division Multiplexing (OFDM) is based on the well-known technique of Frequency Division Multiplexing (FDM). In FDM different streams of information are mapped onto separate parallel frequency channels. Each FDM channel is separated from the others by a frequency guard band to reduce interference between adjacent channels.

The OFDM technique differs from traditional FDM in the following interrelated ways:

1. multiple carriers (called sub-carriers) carry the information stream,

2. the sub-carriers are orthogonal to each other, and

3.   a guard time may be added to each symbol to combat the channel delay spread.

These concepts are illustrated in the time-frequency representation of OFDM presented in Figure 1.
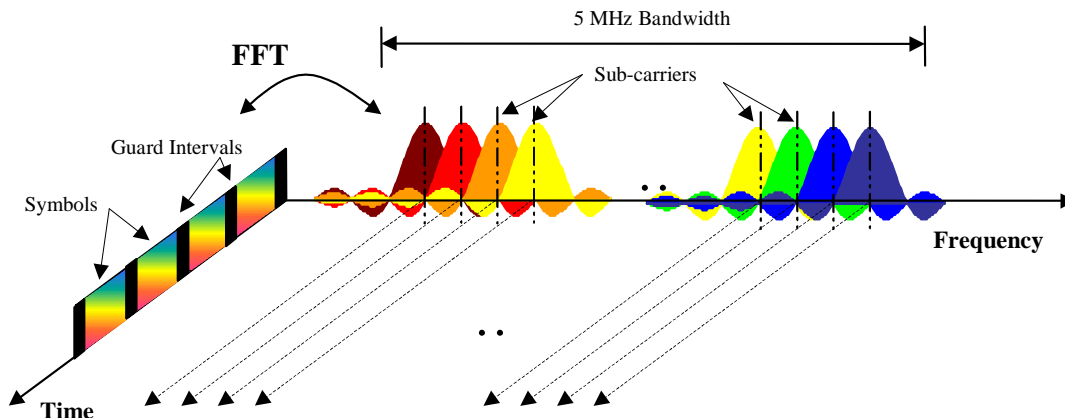
Figure 1: Frequency-Time Representation of an OFDM Signal

Since the orthogonality is guaranteed between overlapping sub-carriers and between consecutive OFDM symbols in the presence of time/frequency dispersive channels the data symbol density in the time-frequency plane can be maximized.

4.1.2   Conceptual OFDM Signal Generation

Data symbols are synchronously and independently transmitted over a high number of closely spaced orthogonal sub-carriers using linear modulation (either PSK or QAM). The generation of the OFDM signal can be conceptually illustrated as in Figure 2,
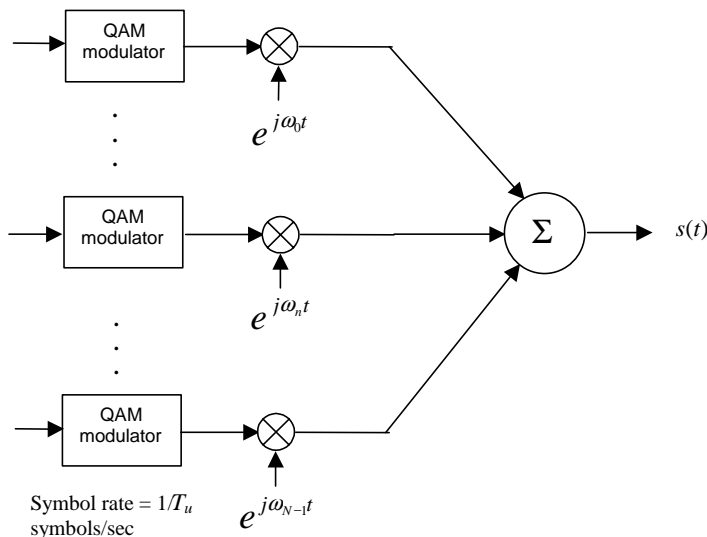
Figure 2: Conceptual Representation of OFDM Symbol Generation

where ω_n is the nth sub-carrier frequency (in rad/s) and $1/T_u$ is the QAM symbol rate. Note that the sub-carriers frequencies are equally spaced, and hence the sub-carrier separation is constant. That is:

$$\frac{\left|\omega_n - \omega_{n-1}\right|}{2\pi} = \Delta f, \qquad n \in [1, N-1].$$

4.1.3 Practical OFDM Signal Generation Using IFFT Processing

In practice, the OFDM signal can be generated using IFFT digital signal processing. The baseband representation of the OFDM signal generation using an N-point IFFT is illustrated in Figure 3, where $a(mN+n)$ refers to the nth sub-channel modulated data symbol, during the time period $mT_u < t \leq (m+1)T_u$.
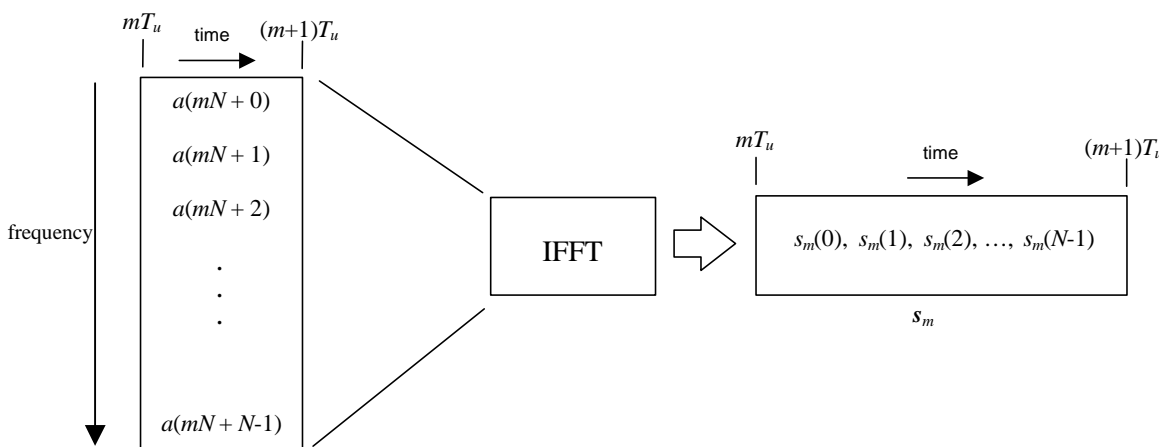
Figure 3: OFDM Useful Symbol Generation Using an IFFT

The vector s_m is defined as the useful OFDM symbol. Note that the vector s_m is in fact the time superposition of the N narrowband modulated sub-carriers.

It is therefore easy to realize that, from a parallel stream of N sources of data, each one modulated with QAM useful symbol period T_u, a waveform composed of N orthogonal sub-carriers is obtained, with each narrowband sub-carrier having the shape of a frequency *sinc* function (see Figure 1). Figure 4 illustrates the mapping from a serial stream of QAM symbols to N parallel streams, used as frequency domain bins for the IFFT. The N-point time domain blocks obtained from the IFFT are then serialized to create a time domain signal.
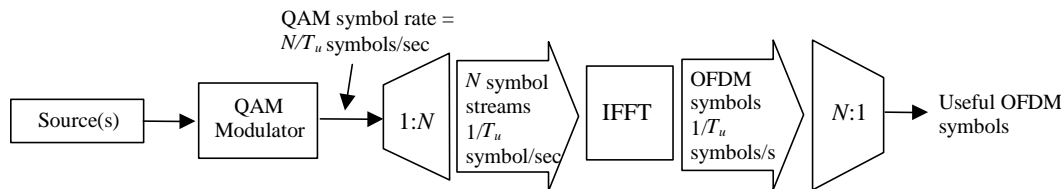
Figure 4: OFDM Signal Generation Chain

4.1.4 Guard Interval

A guard interval may be added prior to each useful OFDM symbol. This guard time is introduced to minimize the inter-OFDM-symbol-interference power caused by time-dispersive channels. The guard interval duration T_g (which corresponds to N_p prefix samples) must hence be sufficient to cover the most of the delay-spread energy of a radio channel impulse response. In addition, such a guard time interval can be used to allow soft-handover.

A prefix is generated using the last block of N_p samples from the useful OFDM symbol. The prefix insertion operation is illustrated in Figure 5. Note that since the prefix is a cyclic extension to the OFDM symbol, it is often termed cyclic prefix. Similarly, a cyclic postfix could be appended to the OFDM symbol.
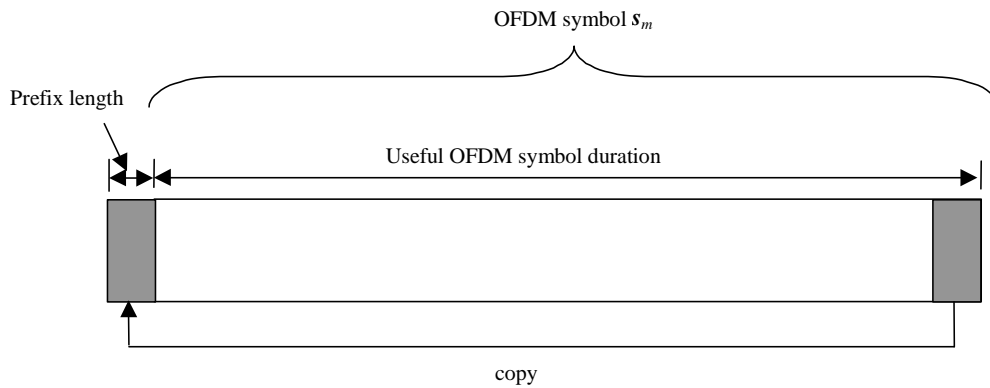
Figure 5: Cyclic Prefix Insertion

After the insertion of the guard interval the OFDM symbol duration becomes $T_s = T_g + T_u$

The OFDM sampling frequency F_o can therefore be expressed as

$$F_o = \frac{N + N_p}{T_s} \ .$$

Hence, the sub-carrier separation becomes:

$$\Delta f = \frac{F_o}{N} \ .$$

It is also worth noting that time-windowing and/or filtering is necessary to reduce the transmitted out-of-band power produced by the ramp-down and ramp-up at the OFDM symbol boundaries in order to meet the spectral mask requirement specified in TS 25.141.

4.1.5 Impact of Guard Interval

The cyclic prefix should absorb most of the signal energy dispersed by the multi-path channel. The entire the inter-OFDM-symbol-interference energy is contained within the prefix if the prefix length is greater than that of the channel total delay spread, i.e.

$$T_g > \tau ,$$

where τ is the channel total delay spread. In general, it is sufficient to have most of the energy spread absorbed by the guard interval, given the inherent robustness of large OFDM symbols to time dispersion, as detailed in the next section.

4.1.6 Impact of Symbol Duration

The mapping of the modulated data symbol onto multiple sub-carriers also allows an increase in the symbol duration. Since the throughput on each sub-carrier is greatly reduced, the symbol duration obtained through an OFDM scheme is much larger than that of a single carrier modulation technique with a similar overall transmission bandwidth. In general, when the channel delay spread exceeds the guard time, the energy contained in the ISI will be much smaller with respect to the useful OFDM symbol energy, as long as the symbol duration is much larger than the channel delay spread, that is:

$$T_s \gg \tau.$$

Although large OFDM symbol duration is desirable to combat time-dispersion caused ISI, however, the large OFDM symbol duration can reduce the ability to combat the fast temporal fading, specially, if the symbol period is large compared to the channel coherence time, then the channel can no longer be considered as constant through the OFDM symbol, therefore will introduce the inter-sub-carrier orthogonality loss This can affect the performance in fast fading conditions. Hence, the symbol duration should be kept smaller than the minimum channel coherence time. Since the channel coherence time is inversely proportional to the maximum Doppler shift f_d, the symbol duration T_s must, in general, be chosen such that:

$$T_s \ll \frac{1}{f_d}.$$

4.1.7 Impact of Inter-Carrier Spacing

Because of the time-frequency duality, some of the time-domain arguments of Section 4.1.6 can be translated to the frequency domain in a straightforward manner. The large number of OFDM sub-carriers makes the bandwidth of the individual sub-carriers small relative to the overall signal bandwidth. With an adequate number of sub-carriers, the inter-carrier spacing is much narrower than the channel coherence bandwidth. Since the channel coherence bandwidth is inversely proportional to the channel delay spread τ, the sub-carrier separation is generally designed such that:

$$\Delta f \ll \frac{1}{\tau}.$$

In this case, the fading on each sub-carrier is frequency flat and can be modelled as a constant complex channel gain. The individual reception of the QAM symbols transmitted on each sub-carrier is therefore simplified to the case of a flat-fading channel. This enables a straightforward introduction of advanced MIMO schemes.

Moreover, in order to combat Doppler effects, the inter-carrier spacing should be much larger than the maximum Doppler shift f_d:

$$\Delta f \gg f_d.$$

4.1.8 OFDM Inactive Sub-Carriers

Since the OFDM sampling frequency is larger than the actual signal bandwidth, only a sub-set of sub-carriers is used to carry QAM symbols. The remaining sub-carriers are left inactive prior to the IFFT, as illustrated in Figure 6. The split

between the active and the inactive sub-carriers is determined based on the spectral constraints, such as the bandwidth allocation and the spectral mask.

Transmitted Power

N_u

Inactive Sub-Carriers

Inactive Sub-Carriers

1 N

Frequency (Sub-Carrier)
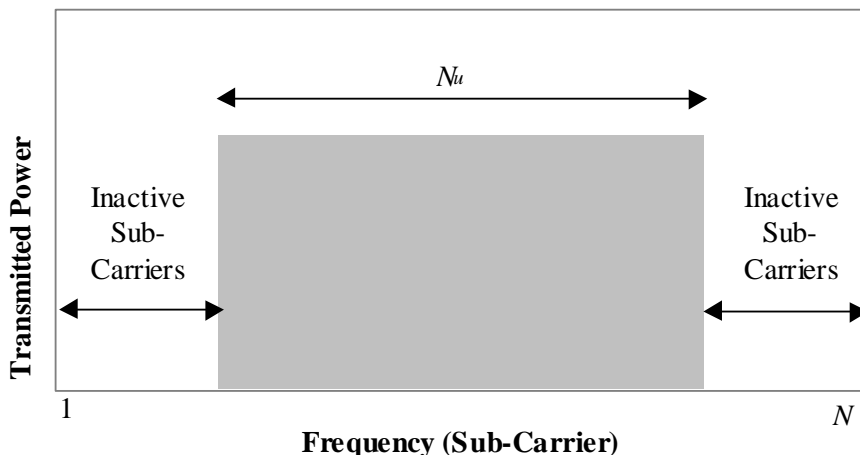
Figure 6: OFDM Spectrum with Incative Sub-carriers

The N_u mdulated sub-carriers (i.e. carrying information), are centered in the N FFT bins, with the remaining inactive sub-carriers, on either side of the modulated sub-carriers.

4.1.9 Time-Frequency Multiplexing

Multiple users can be multiplexed, both in time and in frequency, with pilot and signalling information. In the frequency dimension (i.e. the sub-carrier dimension), users data symbol can be multiplexed on different numbers of useful sub-carriers. In addition, sub-carriers or group of sub-carriers can be reserved to transmit pilot, signaling or other kind of symbols. Multiplexing can also be performed in the time dimension, as long as it occurs at the OFDM symbol rate or at a multiple of the symbol rate (i.e. from one IFFT computation to the other, every k*T_s seconds). The modulation scheme (modulation level) used for each sub-carrier can also be changed at the corresponding rate, keeping the computational simplicity of the FFT-based implementation. This allows 2-dimensional time-frequency multiplexing, of the form shown in Figure 7.

Frequency (Useful sub-carriers) →

←Time

D_4	D_4	D_4	D_4	D_4	D_4	D_4	D_4	D_4		D_6	D_6	D_6	D_6	D_6	D_6	D_6	D_6
D_4	D_4	D_4	D_4	D_4	D_4	D_4	D_4	D_4		D_6	D_6	D_6	D_6	D_6	D_6	D_6	D_6
D_4	P	D_4	D_4	D_4	D_4	D_4	P	D_4		P	D_6	D_6	D_6	D_6	D_6	P	D_6
D_4	D_4	D_4	D_4	D_4	D_4	D_4	D_4	D_4		D_6	D_6	D_6	D_6	D_6	D_6	D_6	D_6
D_4	D_4	D_4	D_4	D_4	D_4	D_4	D_4	D_4		D_6	D_6	D_6	D_6	D_6	D_6	D_6	D_6
D_4	D_4	D_4	D_4	P	D_4	D_4	D_4	D_4		D_6	D_6	D_6	P	D_6	D_6	D_6	D_6
D_4	D_4	D_4	D_4	D_4	D_4	D_4	D_4	D_4		D_6	D_6	D_6	D_6	D_6	D_6	D_6	D_6
D_2	D_2	D_2	D_2	D_2	D_2	D_2	D_2	D_2		D_2	D_2	D_2	D_2	D_2	D_2	D_2	D_2
D_2	D_2	D_2	D_2	D_2	D_2	D_2	D_2	D_2		D_2	D_2	D_2	D_2	D_2	D_2	D_2	D_2

T_s

D_2	D_2	D_2	D_2	D_2	D_2	D_2	D_2	D_2		D_2	D_2	D_2	D_2	D_2	D_2	D_2	D_2
D_2	P	D_2	D_2	D_2	D_2	D_2	P	D		P	D_2	D_2	D_2	D_2	D_2	P	D_2
D_2	D_2	D_2	D_2	D_2	D_2	D_2	D_2	D_2		D_2	D_2	D_2	D_2	D_2	D_2	D_2	D_2

Figure 7: Example of OFDM 2-D structure; P = pilot or signaling, D = data. The subscript indicates the modulation level M=2,4 or 6 (QPSK, 16QAM or 64QAM).

4.1.10   OFDM Signal Reception Using the FFT

At the receiver, a computationally efficient Fast Fourier Transform (FFT) is used to demodulate the multi-carrier information and to recover the transmitted data.

4.2   OFDM/IOTA Fundamentals

OFDM/IOTA is an OFDM/OQAM modulation using a particular function, called IOTA, modulating each sub-carrier. First, the general principle of OFDM/OQAM is introduced, and then IOTA filter is presented

4.2.1   OFDM/OQAM Principles

OFDM/OffsetQAM modulation is an alternative to classical OFDM modulation. Contrary to it, OFDM/OQAM modulation does not require a guard interval (also called cyclic prefix).

For this purpose, the prototype function modulating each sub-carrier must be very well localized in the time domain, to limit the inter-symbol interference[1]. Moreover, it can be chosen very well localized in the frequency domain, to limit the inter-carrier interferences (Doppler effects, phase noise…). This function must also guarantee orthogonality among sub-carriers and among multi-carrier symbols. Functions having these characteristics exist, which guarantee the orthogonality only in *real* domain. Consequently, the complex QAM data stream (c_{mn}) must be separated into its two real components: real part (a_{mn}) and imaginary part ($b_{mn.}$) (see Figure 8), the imaginary part being modulated with a half-symbol-duration ($T_u/2$) shifted version of the modulation filter (thus the connotation Offset). The classical OFDM signal (without cyclic prefix) can be written as:

$$s(t) = \sum_{n=-\infty}^{n=+\infty} \sum_{m=0}^{m=N_u-1} c_{mn} e^{(2i\pi n \, \Delta f \, t)} g(t - nT_u),$$

where g(t) is a rectangular filter.

By separating the two parts of (c_{mn}), the corresponding OFDM/OQAM modulated signal can be written as:

$$s(t) = \sum_{n=-\infty}^{n=+\infty} \sum_{m=0}^{m=N_u-1} a_{mn} i^m e^{(2i\pi n \Delta ft)} g(t - nT_u) + i b_{mn} i^m e^{(2i\pi n \Delta ft)} g\left(t + \frac{T_u}{2} - nT_u\right)$$

where g(t) is the prototype function (noted $\Im(t)$ in the case of IOTA). In a more concise writing, this gives:

$$s(t) = \sum_{n} \sum_{m=0}^{N_u-1} d_{m,n} i^{m+n} e^{2i\pi n \Delta ft} \Im(t - n\tau_0), \qquad d_{m,n} = a_{m,n} \ or \ b_{m,n}$$

---

[1] For comparison, in classical OFDM with guard interval, the prototype function modulating the sub-carriers is the rectangular function.

Note that data is multiplied by i^{m+n} prior to modulation in order to have orthogonality in real domain.

Notation: in OFDM/OQAM, the symbol period is usually noted τ_0 and $\boldsymbol{\tau_0 = T_u/2}$
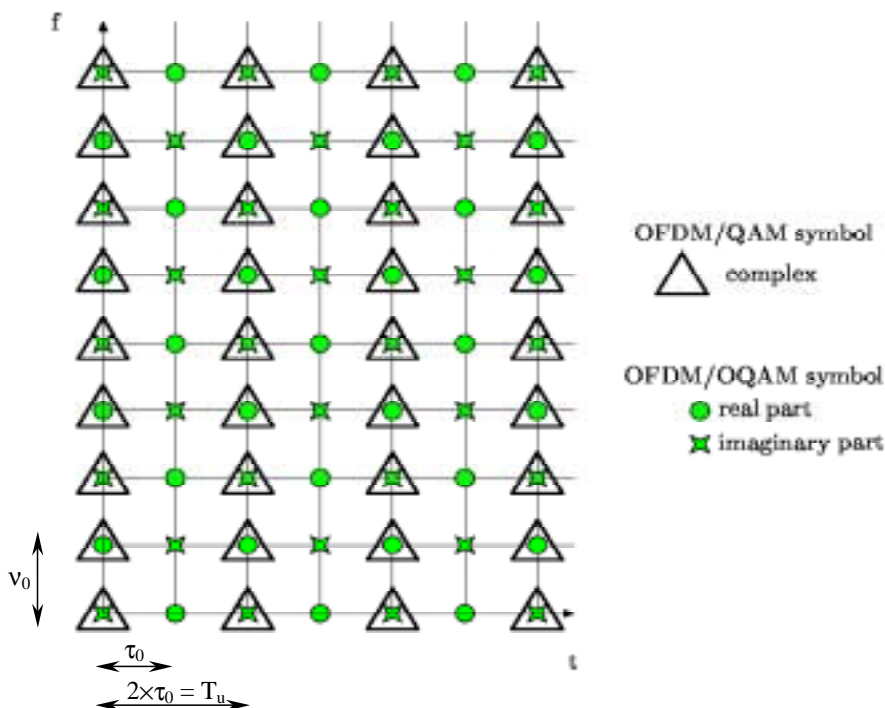
Figure 8: OFDM/OQAM time and frequency lattices (compared to OFDM w/o guard interval)

Figure 9 represents the OFDM/OQAM transmitter.
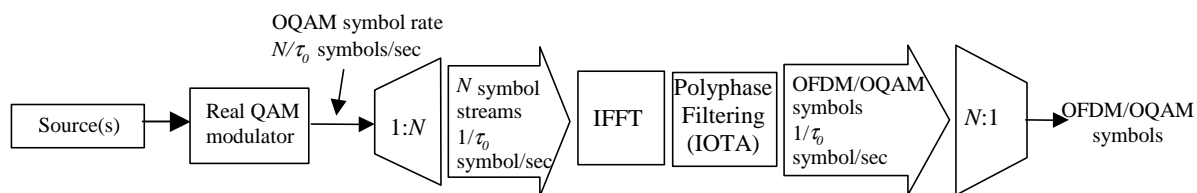
Figure 9: OFDM/OQAM Signal Generation Chain

The "real OQAM modulator" is simply a Pulse Amplitude Modulator. Thanks to the Inverse Fourier Transform, the time filtering is implemented in its polyphase form, in order to reduce the complexity of the filtering.

4.2.2 IOTA filter

IOTA filter guarantees a quasi-optimal localisation in time/frequency domain; it is obtained by applying the Isotropic Orthogonal Transform Algorithm to the Gaussian function aiming at orthogonalizing this function.

Thus, the IOTA function has the following properties:

- it is identical to its Fourier Transform, so, the OFDM/IOTA signal is affected similarly by the time and frequency spreading due to propagation conditions (if parameters are adapted to the channel),
- the time-frequency localization is quasi optimal as the IOTA function does not differ a lot from the Gaussian function (optimally localized).

Figure 10 and Figure 11 show various representations of the IOTA function. On Figure 11, the frequency response of the IOTA function is represented, as well as the rectangular function (used in classical OFDM).
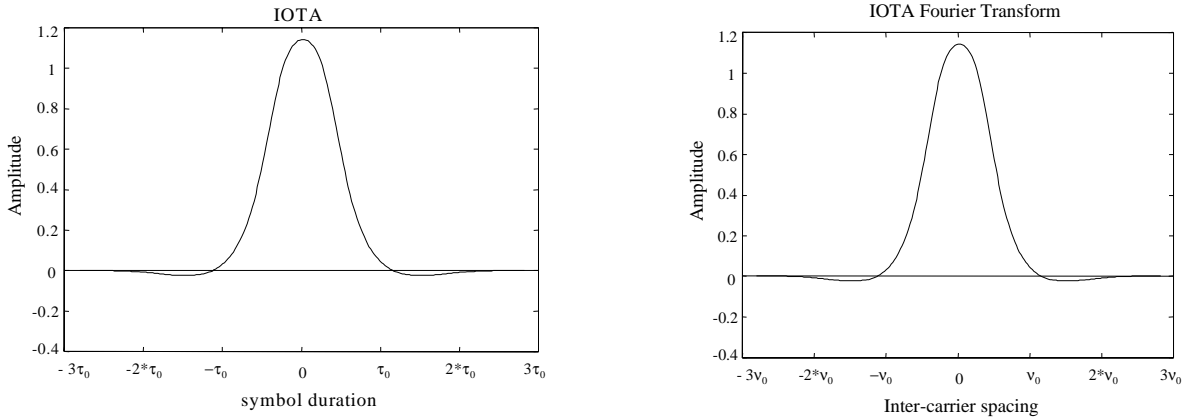
Figure 10: IOTA function and its Fourier transform
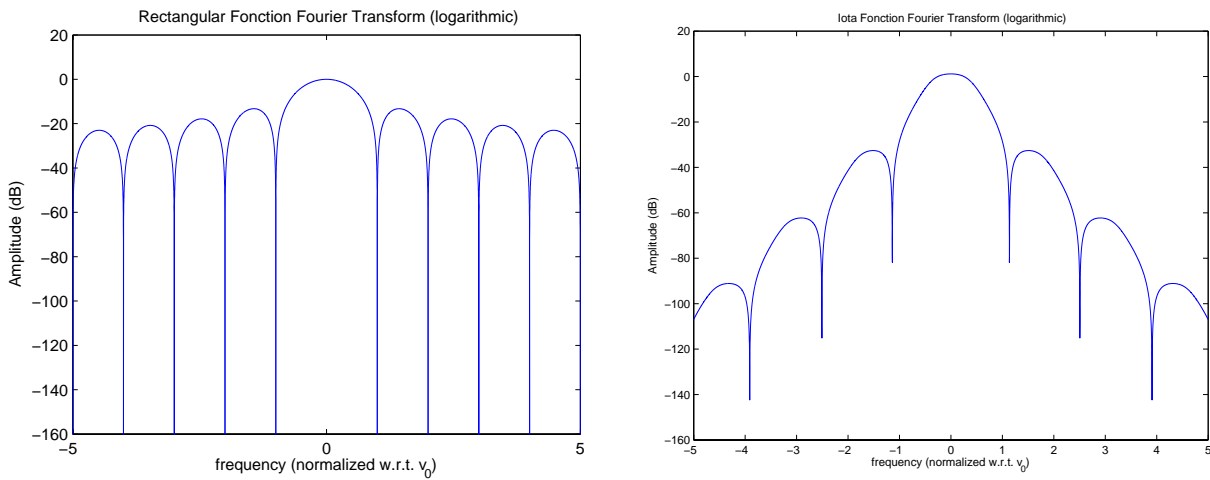
Figure 11: IOTA and Rectangular Function Fourier transforms

Orthogonality of IOTA function is expressed as:

$$\text{Re}\left(\int_{\Re} \Im_{m,n}(t).\Im_{m',n'}^{*}(t)dt\right) = \delta_{m,m'}\delta_{n,n'}$$

with $\Im_{m,n}(t) = i^{m+n} e^{2i\pi\Delta ft} \Im(t - n\tau_0)$.

OFDM/OQAM using the IOTA filter is noted OFDM/IOTA.

4.2.3 OFDM/ IOTA parameters

As for classical OFDM, the OFDM/IOTA parameters have to be designed according to the channel constraints. Conditions from sections 4.1.6 and 4.1.7 are still relevant in the IOTA case:

We need to have $\tau_0 \gg \tau$ and $\tau_0 \ll \dfrac{1}{f_d}$ in time domain, or $\Delta f \ll \dfrac{1}{\tau}$ and $\Delta f \gg f_d$ in frequency domain.

According to the channel environment (Doppler frequency f_d, delay-spread τ), the value of $\Delta f = \dfrac{1}{2\tau_0}$ is chosen in such a way that the FFT size is a power of two.

With the IOTA filter flexibility, as there is no guard interval, the design of the parameter set leads to an integer number of symbols per TTI (2 ms) with a frequency sampling of 7.68 MHz. The configuration can be done by soft means. For examples, a 512 points FFT leads to 60 symbols in a TTI and a 1024 points FFT leads to 30 symbols per TTI.

4.3 OFDM for Mobile Systems

OFDM has intrinsic features that are generally acknowledged to be well suited to the mobile radio environment. The following channel, signal or receiver characteristics are worth noting:

- **Time dispersion**

   The use of several parallel sub-carriers in OFDM enables longer symbol duration, which makes the signal inherently robust to time dispersion. Furthermore, a guard time may be added to combat further the ISI.

- **Spectral Efficiency**

   OFDM is constructed with fully orthogonal carriers, hence allowing tight frequency separation and high spectral efficiency. The resulting spectrum also has good roll-off properties, given that cross-symbol discontinuities can be handled through time windowing alone, filtering alone, or through a combination of the two techniques.

- **Reception**

   Even in relatively large time dispersion scenarios, the reception of an OFDM signal requires only an FFT implementation in the UE. No intra-cell interference cancellation scheme is required. Furthermore, because of prefix insertion, OFDM is relatively insensitive to timing acquisition errors. On the other hand, OFDM requires to perform frequency offset correction.

- **Extension to MIMO**

   Since the OFDM sub-carriers are constructed as parallel narrow band channels, the fading process experienced by each sub-carrier is close to frequency flat, and therefore, can be modelled as a constant complex gain. This may simplify the implementation of a MIMO scheme if this is applied on a sub-carrier or subset of carrier basis.

5 OFDM performance analysis

5.1 Reference System Scenario for High Speed Data Services Capacity Evaluation

This section describes equivalent reference scenarios for comparing the throughput of WCDMA and OFDM radio interfaces in the context of high speed data services. While such a comparison forms an essential part of the Study Item, it is recognized that the Study Item will not be concluded based on the performance of the radio interface alone. The remaining issues include the drawbacks associated with the additional HSDPA carrier, frequency availability and planning, carrier access and handover issues. Such issues are addressed in section 6.

5.1.1 OFDM Downlink

In the Section, an initial reference system configuration is proposed to evaluate an OFDM downlink. The reference architecture is generic, and is compatible with the current 3GPP Rel 5 configuration. In the proposed configuration, new data services are provided through the use of a separate 5 MHz downlink carrier, supporting the OFDM HS-DSCH transmission. The reference architecture is shown in Figure 12**Error! Reference source not found.**.
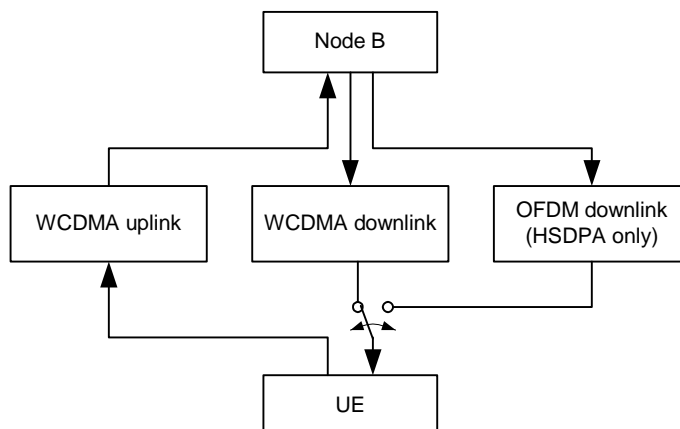
Figure 12: Network deployment for the OFDM HS-DSCH transmission

The separate OFDM DL carrier is operated using HSDPA features, such as link adaptation and HARQ. At this stage, it is assumed that network access is performed through the WCDMA architecture, and handover to the OFDM carrier occurs, when needed, for interactive background and streaming data services. In this case, a UE with OFDM HS-DSCH receiving capabilities would also have WCDMA receiving capabilities. In the first stage, the WCDMA link would be used to achieve the initial network access. However, when there is a requirement for high bit rate traffic, the HS-DSCH mode may be initiated, using either the WCDMA DL carrier (Rel 5 HSDPA) or the separate OFDM DL carrier.

Based on this initial reference scenario, a UE with OFDM HS-DSCH receiving capabilities is not required to receive the WCDMA and OFDM carriers simultaneously. This implies that, if there is a need for real time services, such as voice communications supported only on the WCDMA carrier, the UE would use the WCDMA mode. Note however that if OFDM proves to be useful in the HS-DSCH scenario, other services could also be mapped to the OFDM downlink in future work. In the proposed configuration, the current UMTS uplink carrier is reused and is considered to have sufficient capacity to support either a Rel 5 WCDMA DL carrier, or the separate OFDM DL carrier. There is no special assumption about the separate carrier frequency.

5.1.2 Equivalent WCDMA Scenario

Since the objective of the study item is to evaluate the potential benefits of OFDM as a radio interface for UTRAN, the evaluation should be decoupled from the impact of other factors. To achieve this, the proposed OFDM HSDPA-only carrier is compared to an equivalent HSDPA-only carrier, which employs the existing UTRAN radio interface. This is shown in Figure 13**Error! Reference source not found.**, where a speculative WCDMA HSDPA-only carrier was added to the Release-5 system, ensuring a 'like-with-like' comparison of the two radio interfaces. It should be recognised that the introduction of the standalone WCDMA HS-DSCH carrier within the OFDM study item is speculative and serves purely to aid the evaluation process.
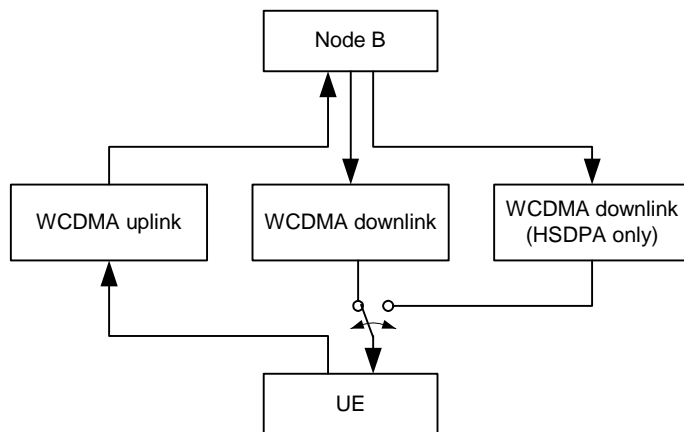
Figure 13: Release-5 system with an 'HSDPA only' WCDMA downlink

It is assumed that the UE is not required to receive the Release-5 downlink and the additional HSDPA-only downlink (whether WCDMA or OFDM) simultaneously. The network access is performed through the Release-5 architecture, and handover to the HSDPA-only carrier occurs when needed.

The second downlink is also assumed to be entirely available for HS-DSCH transfers, i.e. 15 out of 16 codes (with SF = 16) are available for data services.

5.2 Reference OFDM configuration for the evaluation

Two sets of reference OFDM configuration parameters are listed in Table 1.

Parameters	**Set 1**	**Set 2**
TTI duration (msec)	2	2
FFT size (points)	512	1024
OFDM sampling rate (Msamples/sec)	7.68	6.528
Ratio of OFDM sampling rate to UMTS chip rate	2	17/10
Guard time interval (cyclic prefix) (samples/μsec)	56 / 7.29 57 / 7.42[2]	64/9.803
Subcarrier separation (kHz)	15	6.375
# of OFDM symbols per TTI	27	12

---

[2] Requires one extra prefix sample for 8 out of 9 OFDM symbols.

OFDM symbol duration (μsec)	73.96/74.09[3]	166.67
# of useful subcarriers per OFDM symbol	299	705
OFDM bandwidth (MHz)	4.485	4.495

Table 1: Reference OFDM configuration parameter sets

The parameter set 1 consists of nine OFDM symbols that fit into a 0.667 us timeslot. The useful symbol duration is equal to 512 samples. The guard interval is equal to 56 samples for the 0th symbol, and 57 samples for symbols 1..8 of every timeslot, as illustrated in figure 14. The actual position of the 56-sample GI symbol is believed to be inconsequential as long as it is known by both the transmitter and receiver. Therefore, it may be revisited in future, should a different location be deemed more favourable.

It should be noted that spectral shaping of the OFDM signal is required for out-of-band emission compliance. The implications of spectral shaping on delay spread robustness are discussed in a separate section of this report.
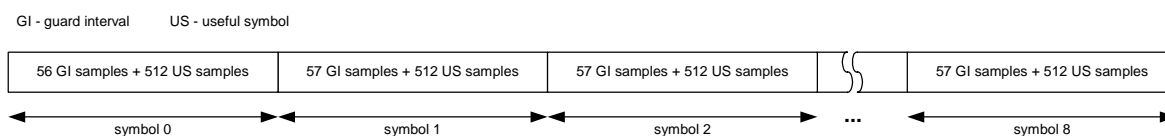
Figure 14: Temporal structure of the OFDM signal (one timeslot), parameter set 1.

5.3   Performance Analysis Results

Detailed results can be found in annex A.5.

6   OFDM feasibility

Editor's note : This chapter discusses a number of specific technical and operational issues related to the application of OFDM within the framework of 3GPP systems.   These are not in any particular order of presentation.

6.1   Spectrum compatibility

To minimize the impact of the introduction of OFDM in UTRAN and to ensure the coexistence of OFDM with WCDMA in UTRAN, the OFDM carriers should be spectrally compatible with current WCDMA UMTS carriers.

6.1.1 UMTS Spectrum Emission Mask

The OFDM signal spectrum should be shaped prior to transmission to meet the UMTS spectrum emission mask. The OFDM spectrum roll-off can be controlled at baseband by using the windowing and overlapping of consecutive OFDM symbols, as illustrated in Figure 15.

---

[3]Depending on guard interval duration
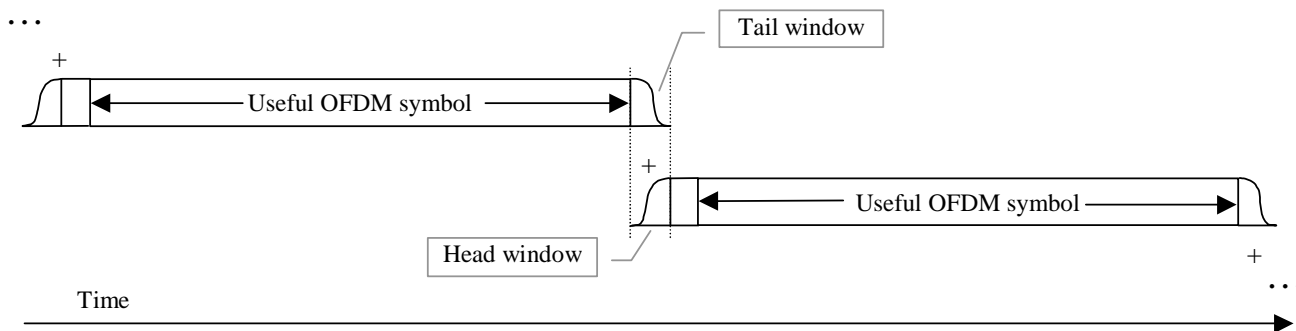
Figure 15: Windowing in consecutive OFDM symbols.

Several different windowing functions can be used. The spectrum obtained using a straightforward trapezoidal window (i.e. using linear head and tail weighting functions) is illustrated in Figure 16 and Figure 17, for the two sets of OFDM parameters proposed in Section 5.2. In both Figures, the spectrum of an OFDM signal without windowing is also illustrated. It is clear that in the absence of a spectrum shaping method, the intrinsic spectrum of the OFDM signal would not meet the required emission mask. However, the use of linear ramp-up and ramp-down weighting functions does bring a significant reduction in the out-of-band energy present at baseband.
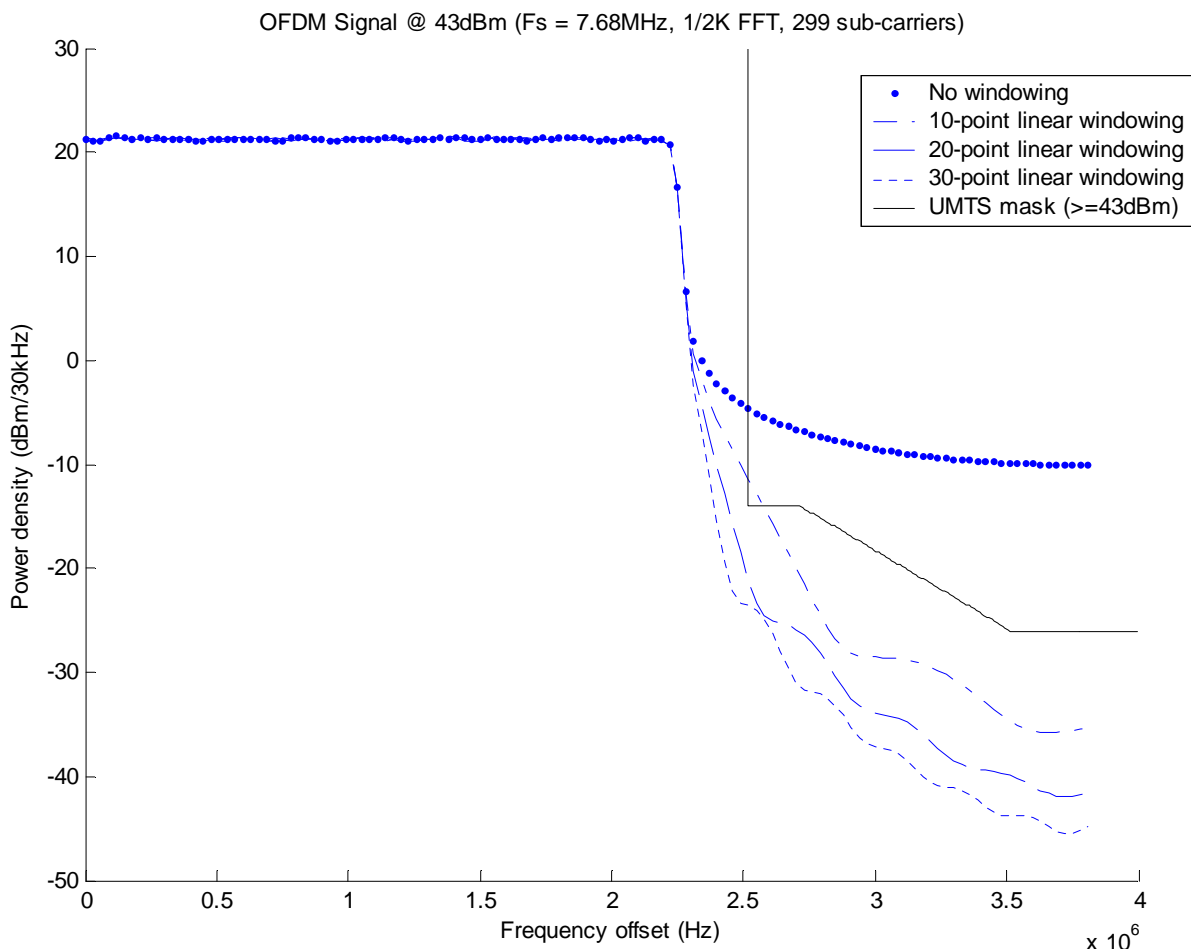
Figure 16: OFDM Spectrum for parameter Set 1 (@ 43dBm)

OFDM Signal @ 43dBm (Fs = 6.528MHz, 1K FFT, 705 sub-carriers)
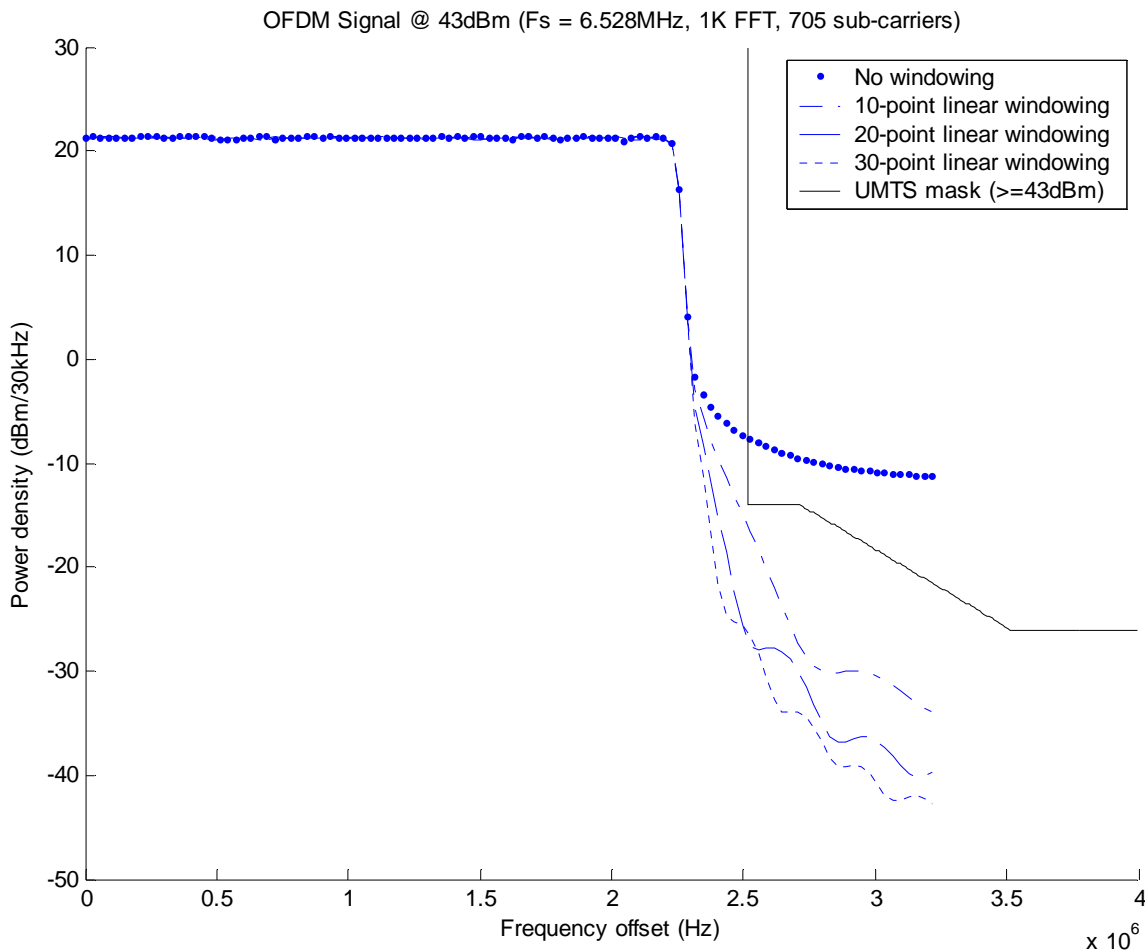
Figure 17: OFDM Spectrum for parameter Set 2 (@ 43dBm)

According to the previous Figure 16 and Figure 17, using a window size in the range of 20 to 30 samples for the overlapping head and tail windows should be sufficient to meet the UMTS spectrum emission mask.

In the case of OFDM/IOTA (see section 4.2), thanks to the very high localization both in time and frequency of the IOTA filter, the transmitted signal meets the UMTS emission spectrum masks without requiring any additional filtering.

6.1.2 Comparison with WCDMA Carriers

To compare the impact of the introduction of OFDM signals in terms of spectral compatibility, it is important to look at the adjacent channel interference generated by OFDM signals. This is particularly important if a channel spacing inferior to 5MHz is considered. In that case, the impact of the spectrum shape can be analysed via the Adjacent Channel Leakage Ratio (ACLR), as defined in [11]. An example of ACLR impact is presented in Figure 18 for OFDM parameter set 2 with 641 and 705 sub-carriers. The case with 641 sub-carriers correspond to symbol rate equal to that of WCDMA (3.84×10^6 symbols/sec), while the 705 sub-carriers case corresponds to the number of sub-carriers proposed in the previous section to respect the UMTS emission mask. These two scenarios are compared to the ACLR for WCDMA. It is important to note that all of these ACLR figures are obtained for idealised conditions, and that they may not accurately represent practical implementations, where other factors influence the ACLR (e.g. fixed-point precision, PA non-linearity, etc.). Nevertheless, with this idealised case, it can be seen that meeting the UMTS spectrum emission mask does not guarantee an ACLR figure comparable to that of WCDMA for carrier offsets inferior to 5MHz. For instance, the case of OFDM set 2 with 705 sub-carriers, while it does seem to meet the UMTS spectrum emission mask (as presented in the previous section), does require a larger carrier offset for a given ACLR. The number of sub-carriers used in an OFDM system should therefore take into account the target channel spacing. Note also that the number of OFDM sub-carriers could be adapted to fit actual deployment scenarios, while the WCDMA spectrum is fixed to maintain compatibility (i.e. chip rate and RRC roll-off).
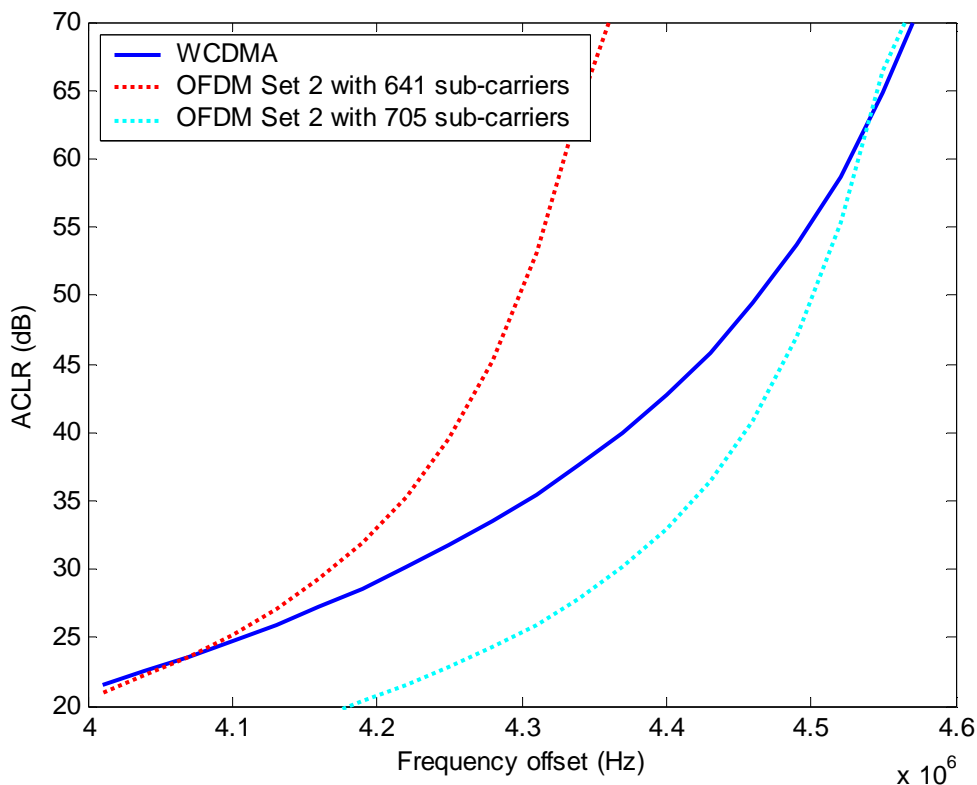
Figure 18: ACLR comparison between OFDM (Set 2) and WCDMA for different carrier offsets

6.2 Physical Layer Structure in the DL

Editor's note : Discussion of the multiplexing of user traffic on the OFDM transmissions. This includes time-division multiplexing and sub-carrier grouping. This may also include the mapping of the UTRAN logical traffic and user data channels onto the OFDM signal.

6.2.1 Physical Channels

Physical channels are defined by a specific carrier frequency, set of orthogonal subcarriers or sub-bands, time start & stop (or duration), time-frequency interleaving pattern (possibly frequency hopping pattern). Given a carrier frequency, physical channels are therefore mapped onto a specific 2-dimensional area in the time-frequency plane. Before time-frequency interleaving, each physical channel corresponds to a set of sub-bands, while after symbol interleaving, the sub-bands are distributed in a controlled manner across the overall frequency band. The time durations for specific time units for the OFDM HS-DSCH are identical to those of 3GPP, and can therefore be measured in integer multiples of WCDMA chips, where the chip rate is 3.84 MHz. The time intervals defined in this configuration are:

Radio frame:	Also called an *OFDM* frame, a radio frame is a processing duration which consists of 15 slots. The length of a radio frame corresponds to 38400 chips (10msec).
Slot:	A slot corresponds to 2560 chips.
HS-DSCH sub-frame:	A sub-frame is the basic time interval for HS-DSCH transmission and HS-DSCH-related signalling at the physical layer. The length of a sub-frame corresponds to 3 slots, i.e. 7680 chips (2msec), and is often referred to as a TTI.
OFDM symbol:	An OFDM symbol is the signal generated by one inverse FFT in the transmitter, including a cyclic prefix and suffix.

These concepts are illustrated in Figure 19. The number of OFDM symbols per TTI is L=27 for Parameter Set 1, and L=12 for Parameter Set 2 (see Section 5.2). The respective corresponding numbers of OFDM symbols per frame are therefore 135 and 60.

The OFDM signal can be conceptually generated as indicated in Figure 20. The *OFDM unit Mapping* refers to the mapping of the individual strings of QAM symbols into *OFDM units*, where such a unit is defined as a group of constellation symbols to be mapped onto a sub-band, a subset of OFDM subcarriers. The OFDM symbol duration is fixed, with a total of N subcarriers. N is equal to the FFT size, and therefore includes unused subcarriers on each extremities of the signal band. The IFFT output vector is multiplexed in the time domain, with a prefix and a suffix, into a vector identified as the OFDM symbol, with (N+p) samples per symbol, where p is equal to the total number of samples in the combination of the prefix and the suffix.
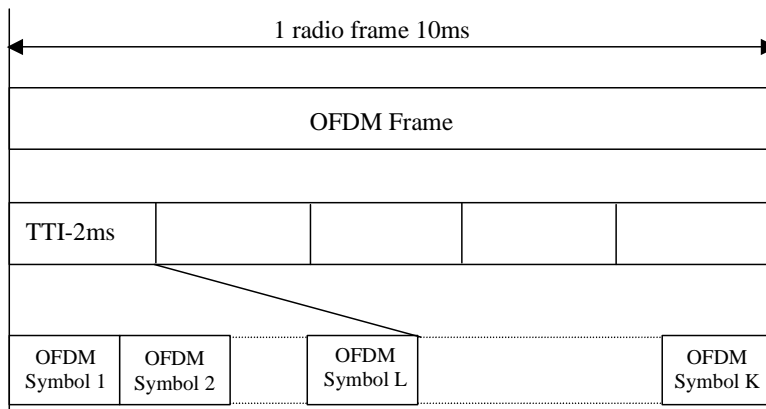
Figure 19: Frame structure for the OFDM HS-DSCH
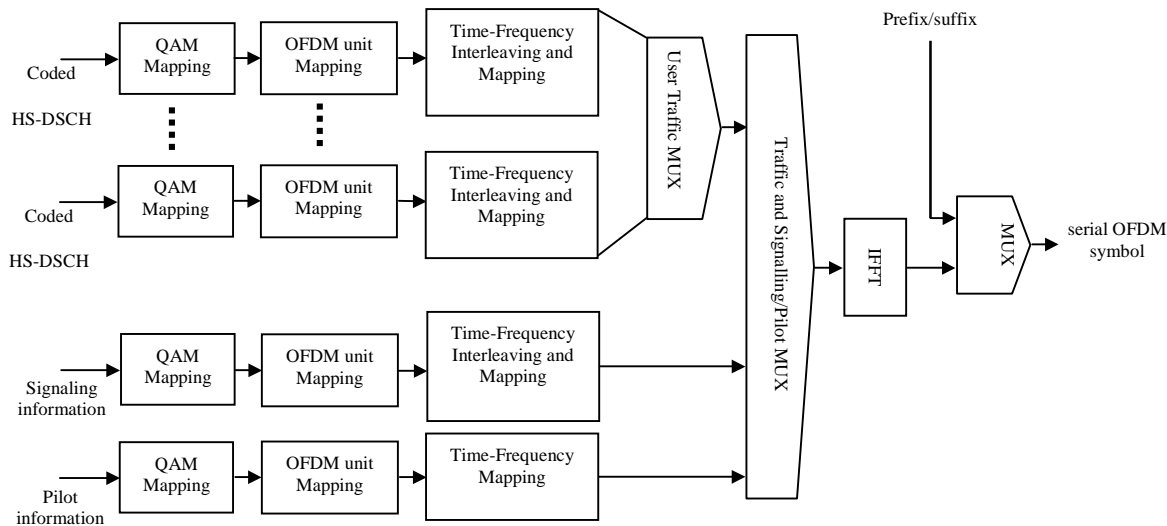
Figure 20: Conceptual representation of the generation of the OFDM signal for multiple HS-DSCHs

6.2.1.1   OFDM Physical Channel Definition

Four types of OFDM physical channels could be defined for HS-DSCH.

1)   The *OFDM-CPICH* (OFDM common pilot channel): the OFDM unit(s), within a 2 msec sub-frame, containing pilot information. This is a common channel. The pilots are inserted in the time-frequency plane and must satisfy the 2-D sampling theorem in order to enable reconstruction of the time and frequency varying channel response. The OFDM-CPICH physical channel is not interleaved.

2) The *OFDM-TPCCH* (OFDM TPC Channel): the OFDM unit(s), within a slot, containing the uplink TPC bits. This is a shared channel. The specific frequency locations used for signalling could be scattered, in order to benefit from frequency diversity. The time location could be limited to a single OFDM symbol (IFFT/FFT window) per slot, to ease its extraction by the UE. The timing of the dedicated uplink is given by the timing of the dedicated downlink in WCDMA. How to set the uplink timing in case of OFDM downlink is FFS.

3) The *OFDM-SCCHs* (OFDM shared control physical channels): the OFDM unit(s), within a 2 msec sub-frame, containing signalling information. This is a shared channel. The specific frequency locations used for signalling should be scattered, in order to benefit from frequency diversity. The time locations can be spread across the sub-frame, while limited to a small number of OFDM symbols (IFFT/FFT windows) to ease extraction of the OFDM-SCCH information by the UE (for instance, the same IFFT/FFT windows already used for the OFDM-TPCCH).

4) The *OFDM-PDSCHs* (OFDM physical downlink shared channels): the OFDM unit(s), within a 2 msec sub-frame, not used by the OFDM-CPICH, OFDM-TPCCH or OFDM-SCCH physical channels, and dedicated to carry data or higher layer signalling information.

6.2.2   Channel Coding and Multiplexing

In the process of mapping transport blocks onto physical channels, data from multiple users are multiplexed in time and frequency. Figure 21 illustrates the overall transmitter processing chain for the transport blocks of such users [4]. The reference OFDM configuration defines the final part of the transmitter processing chain: the mapping of constellation symbols onto the OFDM physical channels (grey blocks).
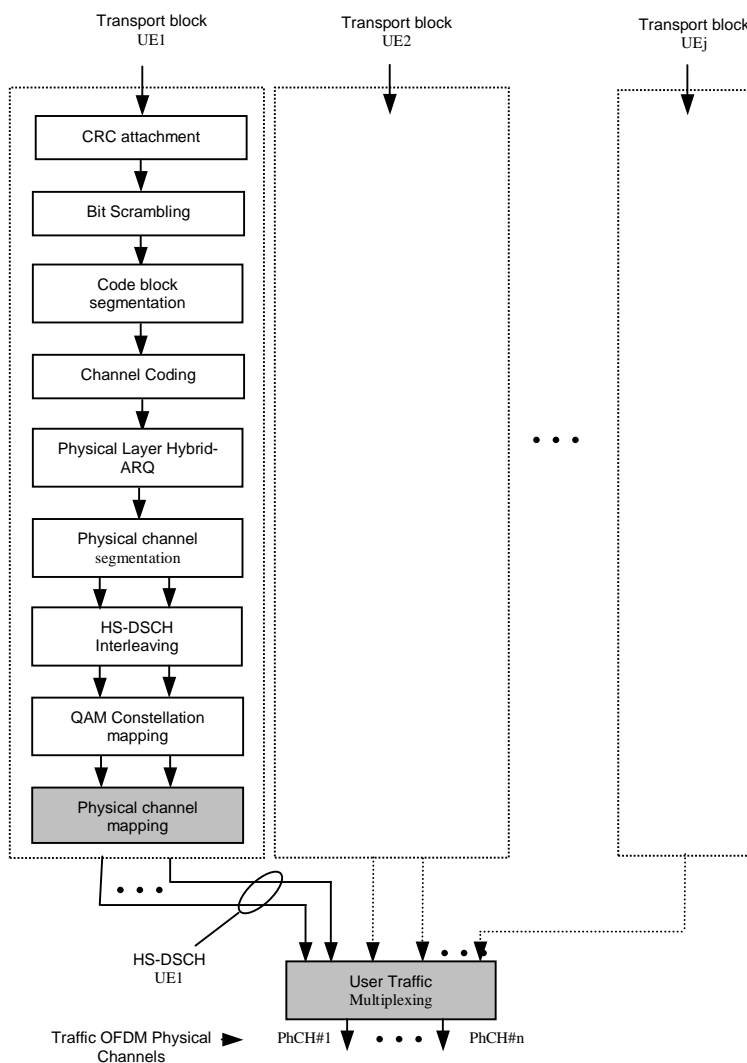
Figure 21: OFDM HS-DSCH transmitter processing chain

Data arrives at the coding unit with a maximum of one transport block every 2 msec TTI. As in HSDPA, there is one transport block of HS-DSCH type per UE [3]. Each traffic transport block is first coded with CRC attachment, then it is bit scrambled, code block segmented, channel coded, and processed by HARQ, as indicated in [3]. The output of the HARQ block is then segmented into one or more data segments, each one corresponding to a physical channel (PhCh). A UE can therefore be assigned multiple physical channels. Each PhCh is interleaved as indicated in [3], and each resulting HS-DSCH interleaved data block is mapped to a vector of symbols, taken from the selected QAM constellation.

Each QAM symbol vector is then mapped onto a number of OFDM units. Each OFDM unit is a group of constellation symbols to be mapped onto a sub-band, a subset of OFDM subcarriers. Time-frequency interleaving of OFDM units is then applied, and results in a mapping of the physical channels on the time-frequency resources.

User traffic multiplexing is finally used to multiplex the physical channels from different users, resulting in a number of *Traffic OFDM Physical Channels*.

6.2.3 Physical channel mapping

The OFDM frequency band is divided into N_B sub-bands by grouping OFDM subcarriers. Each sub-band and each OFDM symbol interval constitute together an *OFDM unit*. This means that in each OFDM symbol interval at most N_B parallel OFDM units can be transmitted.

Three different essential steps for the physical channel mapping are identified:

1. The QAM symbols, obtained in the constellation mapping, are mapped onto a number of OFDM units.
2. The OFDM unit interleaver permutes the QAM symbols in the consecutive OFDM units obtained after the previous step.
3. The time-frequency mapping of OFDM units puts each OFDM unit at a unique position in available time-frequency space. Each physical channel should have a separate, non-overlapping time-frequency mapping. The OFDM unit interleaver and time-frequency mapping constitute together a time-frequency interleaver of OFDM units.

6.2.4 User Traffic Multiplexing Solutions

The user traffic multiplexing is performed by allocating to each physical channel a separate pattern for the time-frequency (T-F) mapping of OFDM units. All the T-F mapping patterns in a cell should be orthogonal, to avoid the cross-interference between the physical channels. Choosing the T-F pattern is a tool to combat frequency selective fading and to minimise the inter-cell interference. This T-F mapping pattern can be used to support frequency scheduling.

Some possible efficient solutions, satisfying to a large extent the above requirements for both parameter sets, are described in the following sub-sections.

6.2.4.1 Solution based on a generic Costas sequence

The solution for user traffic multiplexing described in this sub-section achieves concurrently three goals: a) maximise the minimum (Lee) distance between any two points on the time-frequency grid; b) minimise the maximum normalised periodic Hamming cross-correlation between any two T-F patterns, and c) minimise the maximum side-lobe of normalised periodic Hamming auto-correlation of each T-F pattern.

The set of 15 orthogonal time-frequency mapping patterns, one for each OFDM physical channel, is derived from a single Costas sequence of length 15 [7][8]. This generic T-F pattern (TFP$_{generic}$) is shown in Figure 22, as a sequence of indices of the sub-bands used for the transmission within a TTI.
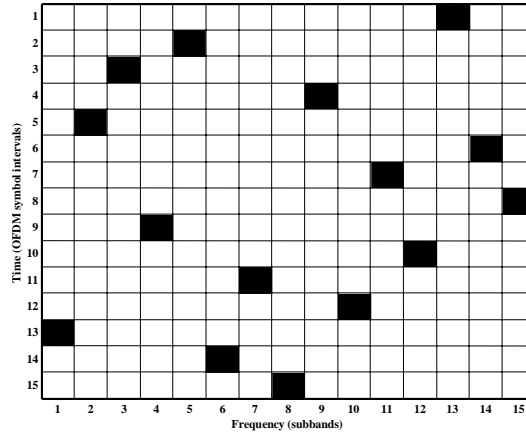
Figure 22: Generic time-frequency pattern (T4 Costas sequence of length 15)

All patterns in the set are obtained from the *first* pattern in the set by *all the different cyclic shifts in the frequency domain*.

For the parameter set 2, the first pattern is obtained by discarding the last three symbols of the generic Costas sequence, in order to obtain the patterns of length N_{OFDM} =12. For the parameter set 1, the first pattern is obtained by extending the generic Costas sequence by the reversed first 12 symbols of the same generic pattern, in order to obtain the patterns of length N_{OFDM} =27. Mathematically, it can be described as

$$\text{TFP}_0^{(\text{ParSet2})} = \text{TFP}_{\text{generic}}(1{:}12),$$

$$\text{TFP}_0^{(\text{ParSet1})} = [\text{TFP}_{\text{generic}} \quad \text{TFP}_{\text{generic}}(12{:}{-}1{:}1)].$$

For the parameter set 2, the first two T-F patterns are given by

$$\text{TFP}_0^{(\text{ParSet2})} = [13 \quad 5 \quad 3 \quad 9 \quad 2 \quad 14 \quad 11 \quad 15 \quad 4 \quad 12 \quad 7 \quad 10],$$

$$\text{TFP}_1^{(\text{ParSet2})} = [14 \quad 6 \quad 4 \quad 10 \quad 3 \quad 15 \quad 12 \quad 1 \quad 5 \quad 13 \quad 8 \quad 11].$$

For the parameter set 1, the first two T-F patterns are given by

$$\text{TFP}_0^{(\text{ParSet1})} = [13 \quad 5 \quad 3 \quad 9 \quad 2 \quad 14 \quad 11 \quad 15 \quad 4 \quad 12 \quad 7 \quad 10 \quad 1 \quad 6 \quad 8 \quad 10 \quad 7 \quad 12 \quad 4 \quad 15 \quad 11 \quad 14 \quad 2 \quad 9 \quad 3 \quad 5 \quad 13],$$

$$\text{TFP}_1^{(\text{ParSet1})} = [14 \quad 6 \quad 4 \quad 10 \quad 3 \quad 15 \quad 12 \quad 1 \quad 5 \quad 13 \quad 8 \quad 11 \quad 2 \quad 7 \quad 9 \quad 11 \quad 8 \quad 13 \quad 5 \quad 16 \quad 12 \quad 15 \quad 3 \quad 10 \quad 4 \quad 6 \quad 14].$$

Figure 1 shows an idealized situation where each OFDM unit is mapped onto the same number of contiguous sub-carriers. In practice, certain sub-carriers in certain OFDM symbol intervals will be reserved for pilots and signalling, which may lead to variation in OFDM unit size and to mapping of certain OFDM units onto the non-contiguous sub-carriers.

All the time-frequency mapping patterns in a TTI are cyclically time-shifted by a cell-specific offset, corresponding to an integer number of OFDM symbols. The time offset is changed for each TTI, according to a cell-specific multi-level pseudo-random sequence, analogous to the cell-specific scrambling code in WCDMA. The different sequences of time offsets for OFDM can be generated as different time-shifted versions of a single multi-level pseudo-random sequence, in a similar way as it is done for the scrambling codes in WCDMA. In that way, even if the two cells are synchronous in one TTI, they will very probably be asynchronous in the next TTI, resulting in a minimised cross-interference, as predicted by the correlation properties of time-frequency mapping patterns.

6.2.5 Mapping of Rel 5 HS-DSCH Signalling onto the OFDM HS-DSCH Signalling

The basic physical-channel structure for Rel 5 HS-DSCH-related associated downlink signalling, as seen from the UE point-of-view, is illustrated in Figure 1 [3]. It consists of a downlink DPCH and a number of HS-SCCHs. For each HS-DSCH sub-frame, each Shared Control Channel (HS-SCCH) carries HS-DSCH-related downlink signalling for one UE. The number of HS-SCCHs that can be monitored by a particular UE can range from one to four. A given UE has the capability to simultaneously monitor 4 HS-SCCHs, but more than four HS-SCCHs can be configured in a cell.
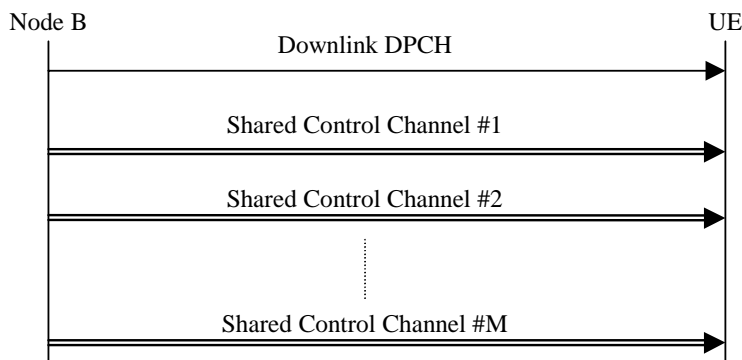
Figure 23: Basic physical-channel structure for Rel 5 HS-DSCH-related associated downlink signalling and control.

Table 1 summarizes the signalling and control parameters defined in Rel 5, which must be mapped on the Signalling or Control OFDM physical channels. One Transmit Power Control (TPC) bit per active user must be updated once per slot. The other signalling parameters are updated once per sub-frame. The TFRI format may need to be extended to allow more transport formats, depending on the final definition of the OFDM air interface. Note that the 7-bit channelisation field is not fully utilized in Release 5, and hence, could allow some extension of the transport format.

Signalling/control information	Rel 99/5 Channel	Equivalent OFDM Physical Channel	Minimum number of uncoded signalling/control bits	
Transmit power control command (TPC)	DPCCH	OFDM-TPCCH	k bits per slot	
Channelisation-code set	HS-SCCH	OFDM-SCCH	7*	per 2ms sub-frame
Modulation scheme			1*	
Transport-block size			6*	
Hybrid-ARQ process number			3	
Redundancy version			3	
New-data indicator			1	
UE identification			16	

*: The TFRI format may change, depending on transport formats allowed in the OFDM specification

Table 2: Rel 5 HS-DSCH signalling and control information mapped onto the OFDM HS-DSCH signalling and control channels. The parameter "k" indicates the number of active users in a sector.

6.2.5.1 Considerations on the Design of OFDM Pilot Channel (OFDM-CPICH)

The design optimization of an OFDM-CPICH channel would be highly dependant on the exact parameters selected for an OFDM specification. Nevertheless, some aspects, such as inter-pilot spacing in time and frequency, and relative power level of the pilot symbols, can be considered, irrespective of the specific OFDM parameters.

Figure 24 through Figure 27 show the BLER performances of OFDM HSDPA according to the various percent utilizations of pilot over frequency-time resource. The simulation assumptions are based on the annex A and summarized in Table 3. Frequency-time symbols for pilot channel are allocated by square pattern uniformly in time domain and frequency domain. Table 4 depicts the coherence bandwidth and coherence time of each channel environment used in the simulation and Table 5 shows the details about pilot allocation.

Reference OFDM physical configuration set	SET2
Modulation	16QAM
Channel coding	1/2 Turbo code
Number of channel coded bits	1920 bits
User traffic allocation pattern	Random pattern in frequency-time domain
Pilot allocation pattern	Square pattern in frequency-time domain
% utilization of the frequency-time resource for the pilot channel	0.1%, 0.5%, 1%, 2%, 5%, 10%
Interpolation method for the channel estimation	2-step linear interpolation (1st step in frequency and 2nd step in time domain)
Power for CPICH	-10 dB (10% of total maximum available transmission power)
Power for signaling channel	-10 dB (10% of total maximum available transmission power)
Time window for OFDM prefix/postfix	Triangular window
Simulation stopping condition	More than 300 erroneous blocks observed

Table 3: Simulation parameters for the evaluation of OFDM CPICH performance

Channel Type	Mobile Velocity [km/H]	Coherence BW [kHz]	Coherence Time [ms]
Pedestrian A	3	2439	83.3
Pedestrian B	3	270	83.3
Vehicular A	30	398	9
	120	398	2.2

Table 4: Coherence bandwidth/ time in the simulation channel models

% Utilization of frequency-time resource for the pilot channel [%]	Number of OFDM symbols which contain pilot symbols in a TTI	Number of subcarriers allocated to pilot symbols in an OFDM symbol	Power ratio of pilot symbol to data symbol [dB]	Freq spacing between subcarriers including pilot [kHz]	Time spacing between OFDM symbols including pilot [ms]
0.1%	2	4	20.51	1123.6	1
0.5%	2	21	13.30	214.01	1
1 %	2	42	10.29	107.01	1

2 %	2	84	7.26	53.5	1
5 %	4	106	3.27	42.4	0.5
10 %	6	141	0.26	31.88	0.33

Table 5: Pilot allocation details for the evaluation of OFDM CPICH performance

In figures, the x-axis represents the average signal to noise ratio of data plus pilot symbols. For a low mobile speed (3~30 km/hr), the performance with relatively small amout of pilot utilization (1~2%) shows better performance than that with large % pilot utilzation. Note that the pilot power of large % utilization may not be sufficient to guarantee the reliable pilot detection under the pilot energy fixed to the 10% of total transmission energy. For a high mobile speed (120 km/hr), the time spacing between OFDM pilot symbols should be smaller compared with low mobile speed case to recover fast time-varying channel. Accordingly, the performance with relatively large amout of pilot utilization (5~10%) shows better performance in high mobile speed case. It should be noted that the channel estimation was performed using the simplest 2-step linear interpolator. With an appropriate interpolator, the channel estimation error could be reduced so that the performance gap would be narrower. It should be also noted that other aspects such as inter-cell interference and base station frequency drift should be considered further for the practical design of the OFDM CPICH.
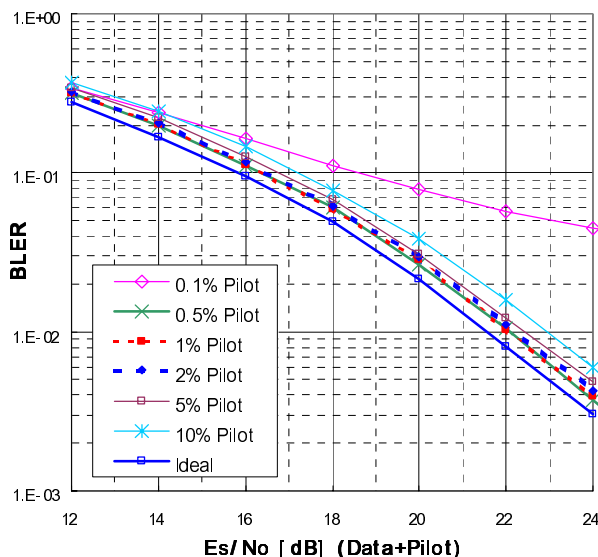
Figure 24: BLER performance of OFDM HSDPA, Pedestrian A, 3 km/hr
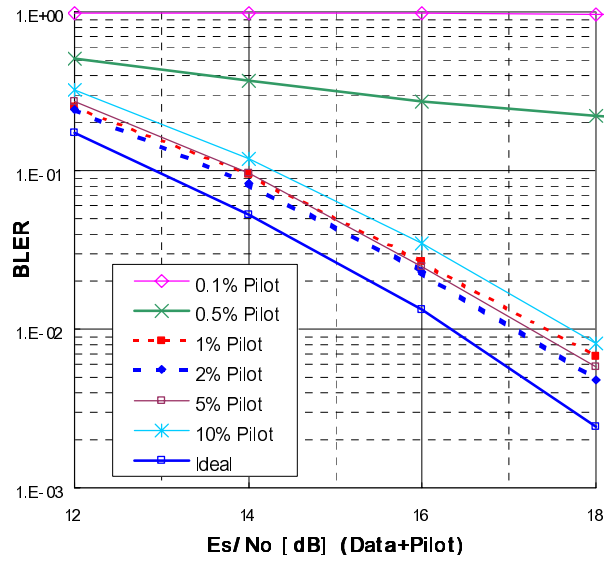
Figure 25: BLER performance of OFDM HSDPA, Pedestrian B, 3 km/hr
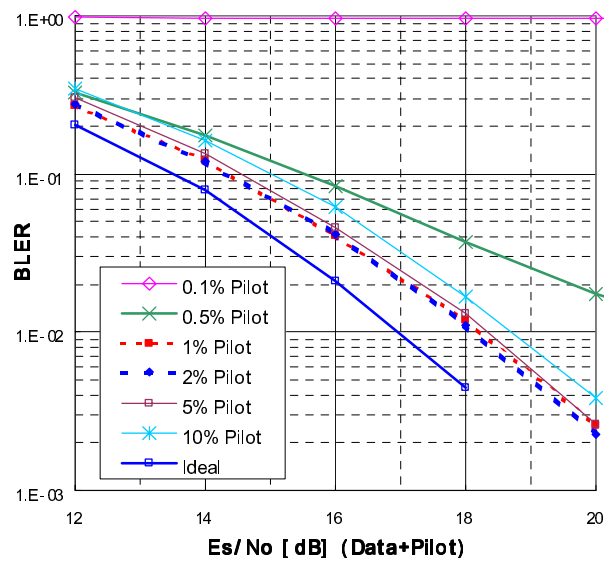
Figure 26: BLER performance of OFDM HSDPA, Vehicular A, 30 km/hr
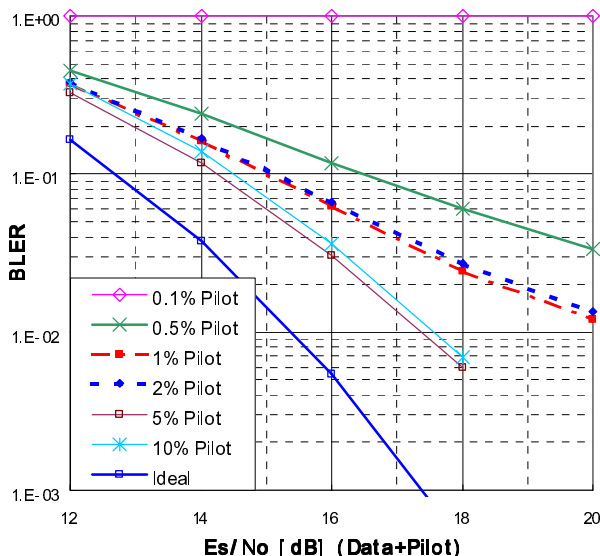
Figure 27: BLER performance of OFDM HSDPA, Vehicular A, 120 km/hr

6.2.5.2   Considerations on the Design of OFDM Signalling Channels

In the definition of the time-frequency locations of the OFDM Signalling and Control channels, the following elements could be considered (without being limited to these elements):

- At the OFDM level, the QAM symbols making up the signalling and control channels should be spread across the frequency sub-carriers to benefit from frequency diversity.
- The decoding of OFDM-SCCH channels should be more reliable than that of OFDM traffic channels, since their decoding is required for proper decoding of traffic channels.
- Given their reliability, OFDM-SCCH channels could be used by the UE to improve the channel estimation, via the re-encoding of the decoded data. If the QAM symbols making up the OFDM-SCCH channels are spread through the time-frequency plan, they can effectively reduce the required density for the OFDM-CPICH pilot symbols, or equivalently, allow an improvement in the channel estimation accuracy for the same OFDM-CPICH density.

6.3   Impacts on UL

The reference scenario described in section 5.1.1 for the comparison between OFDM-HSDPA and W-CDMA HSDPA in terms of performance is also considered here for the feasibility of introducing OFDM in UTRAN.

As depicted on figure 12, it is assumed that while OFDM may be used in the downlink to support HSDPA, the associated uplink uses W-CDMA. This means that this associated uplink may use the R99/Release 4/Release 5 W-CDMA dedicated channels or any further enhancements introduced in further releases.

Timing relationships between uplink dedicated channels and OFDM-HSDPA downlink channels as described in section 6.2 are FFS. Such timing relationships should be investigated taking into account the following aspects :

- impacts to the uplink inner loop power control
- relationships with HSDPA operation in the DL and potential system impacts
- UE/ node B complexity for handling OFDM reception and transmission in relation with the existing uplink or its enhancements

In the current specifications the timing of the uplink dedicated channel is derived from the timing of the associated downlink DPCH channel. With the introduction of OFDM under the assumptions of this Study Item, there will be no associated downlink DPCH on which to base the timing. A simple approach could be to define the uplink timing relative to a given DPCH frame offset and chip offset even if no downlink DPCH is effectively transmitted. Another alternative could be to define the uplink timing relative to the common channels.

6.4 Handover

6.4.1 Assumptions

In the following, it is assumed that coverage of the OFDM DL carrier is identical to that of the associated WCDMA cell i.e. it is assumed that there is sufficient power margin in the downlink to cope with the pathloss difference between different bands (if OFDM and WCDMA are deployed in different bands) and also potential difference due to the use of OFDM instead of WCDMA. Therefore no particular assumption is made in terms of frequency bands for both WCDMA and OFDM i.e. the following is meant to cover all deployment scenarios:

- WCDMA UL in core band
  WCDMA DL in core band

  OFDM in core band

- WCDMA UL in core band
  WCDMA DL in core band

  OFDM in new band

- WCDMA UL in new band
  WCDMA DL in new band

  OFDM in new band

- WCDMA in new band
  WCDMA in new band

  OFDM in core band

In the framework of the Study Item, OFDM is used in conjunction with HSDPA channels. This has a number of implications:

- Access procedures as well as radio bearer setup are performed on the WCDMA carrier. Subsequently a reconfiguration takes place to move the UE from the WCDMA carrier to the OFDM carrier and configure HS-SCCH and HS-PDSCH reception in the UE.
- When a conversational service needs to be setup, a handover towards the WCDMA carrier is necessary. This is based solely on request for conversational services from the CN and does not necessitate the UE to perform any kind of measurements. The physical channel and TFCS are reconfigured on the WCDMA carrier to support the new service. If WCDMA is deployed in the core band, this procedure is already supported by the signaling. If WCDMA is deployed in an additional set of spectrum, no other signaling is needed other than that necessary to indicate to the UE to which band the physical channel belongs.
- Only handover is considered in the following: cell selection/reselection to or from the OFDM carrier is not described as the assumption is that the UE is in CELL_DCH state (there is a dedicated channel setup in the UL).
- Mobility procedures will follow what has been defined in release 5 specifications to support the "HS-DSCH serving cell change".

Use of compressed mode

It is assumed that compressed mode is not used in the downlink as there is no associated downlink DPCH as in release 5 HSDPA. However an equivalent of "measurement occasions" may be defined to allow the creation of transmission gaps in the downlink. These gaps are idle periods when the UE is not required to receive any data and is therefore able to measure on another frequency if needed. A possible way to do this could be to let the MAC-hs scheduler handle the creation of idle periods according to parameters signaled by the RNC, similarly to FACH measurement occasions in R99. The UE would also be informed via higher layer signaling of the position of the transmission gaps. The impact of such gaps on the packet delay and throughput needs to be investigated to ensure that the creation of such downlink gaps do not increase the scheduling delay for the UE unnecessarily. The need for such gaps is dependant on the UE capability like other R99 measurements.

Compressed mode maybe needed in the UL depending on UE implementation and spectrum arrangements i.e. separation between the DL OFDM carrier and the W-CDMA UL carrier. The need for such gaps is dependant on the UE capability and also to frequency arrangements i.e. the separation between the OFDM DL carrier and the WCDMA UL carrier matters in terms of UE complexity.

UE aspects

In the RAN4 study on " feasibility study considering the viable deployment of UTRA in additional and diverse spectrum arrangements" RAN4 have demonstrated the possibility of implementing multiple band pairing options using variable duplex technology, it is assumed that the conclusion is equally applicable to the reception of downlink OFDM however no assumption is made regarding mandatory support of Variable Duplex Technology.

In the following only the HS-DSCH serving cell changes either on OFDM or WCDMA are considered. The term "OFDM HS-DSCH serving cell" designates a mobility case where the UE changes HS-DSCH serving cell and the HS-DSCH resources from the serving cell are mapped onto OFDM. It should be noted that the OFDM carriers is not considered as a cell itself, but comes as an addition to a W-CDMA cell.

6.4.2 Serving HS-DSCH cell change

6.4.2.1 Mobility between OFDM HS-DSCH serving cells

In this scenario, the UE reaches the coverage limit of the source OFDM HS-DSCH serving cell and needs to be handed over to a neighbouring OFDM HS-DSCH serving cell.

At least one UE measurement equivalent to CPICH RSCP or CPICH Ec/Ior is necessary for the UTRAN to be able to track the UE leaving the coverage area of one OFDM carrier and entering that of a neighbouring one.

To support blind HS-DSCH serving cell change, it is sufficient for the UE to measure and report this measurement for the current serving OFDM HS-DSCH serving cell.

For non blind handover, the UE will also need to measure and report neighbouring OFDM HS-DSCH serving cells. Measurement occasions may be needed depending on UE implementation when the source and target OFDM HS-DSCH serving cells are on separate carrier frequencies.

This measurement could be performed on the OFDM-CPICH described in section 6.2.1.1. To distinguish between OFDM-CPICH channels from different cells, orthogonal pilot patterns could used, the UE would be informed via higher layer signaling of the pattern for the OFDM-CPICH it will measure. The impact of the OFDM-CPICH discontinuity on the accuracy of this measurement is FFS. Methods for searching among these different patterns have not been studied. E.g., cell search and synchronization could be obtained from the associated WCDMA cell.

Alternatively, this type of mobility could be managed only by existing CPICH measurements based on the assumption that OFDM and W-CDMA carrier have an identical coverage.

6.4.2.2 Mobility from an OFDM serving HS-DSCH cell to a WCDMA HS-DSCH serving cell

In this scenario, the UE reaches the coverage limit of an OFDM HS-DSCH serving cell and needs to be handed over to a WCDMA HS-DSCH serving cell. This happens e.g when reaching the deployment limit of OFDM within an operator's network or when a conversational service needs to be setup for the UE.

In this case, the source and target serving cells maybe on separate carrier frequencies, possibly different frequency bands depending on the deployment scenario.

The UE needs to measure the serving OFDM HS-DSCH serving cell for the network to be able to identify that the UE is leaving the coverage area of the OFDM HS-DSCH serving cell. This also applies to the case when a conversational service needs to be setup for the UE.

In case of blind HS-DSCH serving cell change, this measurement will be sufficient.

In the general case, the UE will also need to perform existing WCDMA measurements for the UTRAN to identify the best target cell for this UE. For such measurements, the scheduler may need to create some gaps in the data transmission to the UE and depending on UE capabilities compressed mode may be needed in the uplink. This is

deemed feasible from a UE implementation point-of view as the UE is not required to simultaneously receive OFDM and WCDMA but it has the capability of receiving either of them.

Alternatively, this type of mobility could be managed only by existing CPICH measurements based on the assumption that OFDM and W-CDMA carrier have an identical coverage.

6.4.2.3 Mobility from a W-CDMA HS-DSCH serving cell to an OFDM serving cell

In this scenario, the UE reaches the coverage limit of a W-CDMA HS-DSCH serving cell and needs to be handed over to an OFDM HS-DSCH serving cell. This happens e.g when entering OFDM coverage within an operator's network.

In this case, the source and target serving cells are on different frequencies, possibly different frequency bands depending on the deployment scenario.

The UE needs to measure the serving WCDMA HS-DSCH serving cell for the network to be able to identify that the UE is leaving the coverage area of the WCDMA HS-DSCH serving cell.

In case of blind HS-DSCH serving cell change, this measurement will be sufficient.

In the general case, the UE will also need to perform measurements on the OFDM-CPICH for the UTRAN to identify the best target cell for this UE. For such measurements, the scheduler may need to create some gaps in the data transmission to the UE and depending on UE capabilities compressed mode may be needed in the UL/DL. This is deemed feasible from a UE implementation point-of view as the UE is not required to simultaneously receive OFDM and WCDMA but it has the capability of receiving either of them.

Alternatively, this type of mobility could be managed only by existing CPICH measurements based on the assumption that OFDM and W-CDMA carrier have an identical coverage.

6.4.3 Impact on radio resource management in UTRAN

Introduction of OFDM in UTRAN would impact radio resource management in the network regarding the following aspects

- Call Admission Control /Management: traffic needs to be split between OFDM and WCDMA
- Resource management for HSDPA: the scheduler for the OFDM carrier needs to consider the time-frequency dimension instead of the time-code dimension
- Mobility procedures : UTRAN needs to manage a new type of measurement as described in section 6.2. Alternatively, if mobility is solely based on W-CDMA CPICH measurements management of a new type of measurements is not needed and the corresponding simplifications can be applied to UE and UTRAN implementations.. This alternative is deemed valid due to the assumption of identical W-CDMA and OFDM coverage. However it implies the definition of a specific timing relationship between OFDM-CPICH and C-PICH of the W-CDMA cell.

The exact amount of modifications to radio resource management required to support the introduction of OFDM in existing RNC products is implementation dependant. It is not further discussed in this document as it covers an area outside the specifications scope.

6.5 Synchronisation

6.5.1 UE Synchronization

Among several methods, frequency and time synchronization methods presented in this section might be used.

6.5.1.1 Frequency synchronization and tracking

Let F_0 stands for the frequency carrier of the transmitted signal. Frequency synchronization consists in finding this value at the reception side. Because of impairments due to the fact that oscillators at the transmission and the reception side are never completely identical, even if the initial carrier frequency value was exactly found, a shift may occurs which must be corrected. This shift is usually supposed to be slow in time.

Frequency tracking can be done by using a classical Automatic Frequency Control (AFC) This unit detects the frequency changes between two successive pilot symbols. The AFC is used in WCDMA system as well. In order to better tracking the frequency shift in case of OFDM, the AFC should be done using consecutive pilots located on the same sub-carrier.

6.5.1.2 Time synchronization and tracking

Let T_0 stands for the initial transmitting time and T_c stands for the samples period. Time synchronization consists on finding these two values.

T_c value is supposed to be known since it corresponds to a system parameter. Due to several impairments, a shift in T_c value may occur, a tracking mechanism must be applied.

The most general method for time synchronization is done by fulfilling an auto-correlation over the received signal with a length equal to the cyclic prefix length. Since the cyclic prefix is a copy of the last part of the OFDM symbol, the autocorrelation will present a peak when it is done between the cyclic prefix (which is located at the beginning of the OFDM symbol) and the last part of the same OFDM symbol of the same length. This allows the detection of the beginning of the OFDM symbol.

Time synchronization tracking is done by the same technique. But in this case, there is no more need to fulfill correlation over the whole OFDM symbol. Only a correlation between the cyclic prefix and the last part of the OFDM symbol of the same length is required. Moreover, this correlation can be done over a range of few points around the starting point.

6.5.2 Synchronization scenarios

Several assumptions about the cooperation between WCDMA and OFDM system may be considered. Synchronization complexity is not the same for these cases. For each of the following cases, the required synchronization operations are presented (in all cases, the OFDM carrier frequency is supposed to be known at the receiver prior to signal reception):

1. WCDMA-OFDM independent clock
   Frequency synchronization is reduced to frequency tracking. This may be fulfilled by using an Automatic Frequency Control (AFC) which estimates the frequency shift between successive received pilot symbols.

   Time synchronization and tracking have to be done with the OFDM signal only. This can be done according to the method presented in section 6.5.1.2.

2. WCDMA-OFDM shared clock
   The OFDM link will be controlled by the UTRAN system. The same clock is used for both systems. Only one signal is received at a time.

   If the OFDM transmission is very short (a few of TTI's), the frequency drift can be considered small enough to be tracked only by the WCDMA link. If the OFDM transmission period is longer than a certain threshold, frequency tracking synchronization might be required. In that case, an AFC can use the OFDM signal in order to track the frequency drift.

   In terms of time synchronisation, the matching between both systems is done on a basis of a TTI period. One possible method to perform time synchronisation is to consider that the difference between OFDM-TTI starting time and WCDMA reference time is known. The WCDMA reference time may be the beginning of WCDMA-frame, WCDMA-sub-frame or WCDMA-slot. Time synchronization tracking can be done by using the guard interval according to the method presented in section 6.5.1.2.

6.6 Frequency re-use and Inter-cell Interference

6.6.1   Frequency Re-use

The assumption regarding the frequency re-use for the OFDM study has been that the same 5MHz carrier can be re-used in each cell, which is often referred to a full frequency re-use, or frequency re-use factor of 1. The main benefit of such a frequency re-use is mainly ease of deployment, given that no frequency planning is required. In the case of the introduction of OFDM in UTRAN, it would be also desirable to maintain this property, which is already available with WCDMA.

Note however that using the same 5MHz carrier in each cell does not necessarily imply that all of the OFDM sub-carriers would be re-used equally in each cell. One could consider several methods based on the orthogonality of OFDM sub-carriers (even in systems that are not time-synchronised) to improve the coverage. The feasibility, benefits and costs of such methods are FFS.

6.6.2   Inter-cell Interference

Given a frequency re-use factor of 1, the system becomes interference-limited, and the interference perceived by the UE from the different cells might not be perfectly white, as assumed for most of the simulations. First, the interfering signals undergo time dispersion, and hence, do not have a flat spectrum. Furthermore, if the OFDM units are not all being used in the interfering cells, the resulting spectrum from each of these partially-load interfering cells will contain gaps. It is therefore likely that the total interference spectrum observed by the UE would not be flat, and hence, it might not be accurately modelled using white noise.

The impact of realistic inter-cell interference on performance has therefore been evaluated using the Exponential Effective SIR Mapping (EESM). The results are presented in Annex A.2 for PedA and PedB. The following conclusions might be drawn from these results:

- As expected, the performance is improving when the number of OFDM units used in the interfering cells is reduced (as in WCDMA). Hence, the fully loaded case can be considered as a worse-case.
- The throughput obtained with the realistic interference profile is larger or equal to that obtained for interference modeled as AWGN with the same power. Hence, the AWGN assumption is conservative.

6.7   Analysis of User Equipment Complexity

6.7.1   OFDM UE Receiver Functionalities

This section addresses the additional UE functionality needed to support downlink OFDM transmission and its corresponding impact on the UE complexity. The critical UE functionality needed to support downlink OFDM transmission includes:

- RF functionality related to the reception of an OFDM signal
- Functionality for cell search and corresponding measurements (for handover)
- Functionality for time and frequency synchronisation to an OFDM signal
- Functionality for data demodulation of an OFDM signal, including (e.g.) time-domain-to-frequency-domain translation ("FFT operation"), channel estimation, and channel equalisation

The complexity associated with each of these functions is discussed in more details below. It should noted that the list above may not be exhaustive. Furthermore, the complete detailed set of functionalities required to support OFDM would depend on the outcome of a future specification phase. Also, it is important to note that the complexity numbers in this section are provided as examples. The actual complexity may vary according to design and implementation choices.

6.7.2   RF Functionality

When considering the reception of the OFDM signal by the W-CDMA front end receiver, one possible architecture of the Radio Functionality can be depicted in Figure 28.
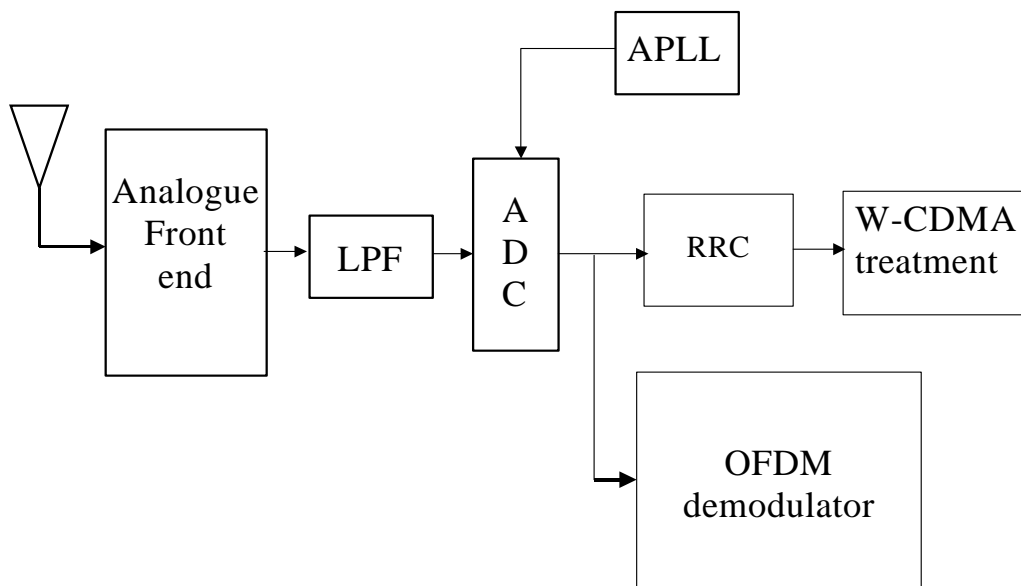
Figure 28: W-CDMA / OFDM radio receiver chain

The Analogue Front End module transposes the signal from carrier frequency into the base band. Since no modulation-specific operations are required, it can be used for OFDM signal.

The frequency bandwidth of the W-CDMA designed RF Low Pass Filter (LPF) is approximately 5MHz and may fall down to 3.84MHz in the worst case. This may distort the OFDM signal, with bandwidth of 4.5 MHz, especially on the frequency band borders. Since the OFDM transforms the wide selective frequency band into a set of narrow unselective bands, thus the W-CDMA Low Pass Filter impairments on the OFDM signal are assimilated to the propagation channel variation and can be compensated by the OFDM equalizer, given a reasonable resolution of the ADC (12 bits, no AGC was used), with no additional complexity. Therefore, when using RF architecture as presented in Figure 1 (12 bits ADC with no AGC), and in case of un-simultaneous W-CDMA-OFDM reception, and when the OFDM carrier frequency is within the W-CDMA specified frequency band, then the same RF module can be used in both modes. Other architectures and ADC resolutions have not been considered.

6.7.3   Cell Search and Measurements

Editor's note: This section should address the functionalities related to the cell search and measurements required for handover.

6.7.4   Synchronisation

Editor's note: This section should address the functionalities related to the OFDM carrier's time and frequency synchronisation.

6.7.5   Data demodulation

Data demodulation for the downlink OFDM signal can be broken into three blocks: (1) time-domain-to-frequency-domain translation (i.e. the FFT), (2) channel estimation, and (3) channel equalization. These three blocks and their relationship are shown in Figure 29 below. Each block will be considered in turn in the following sections.
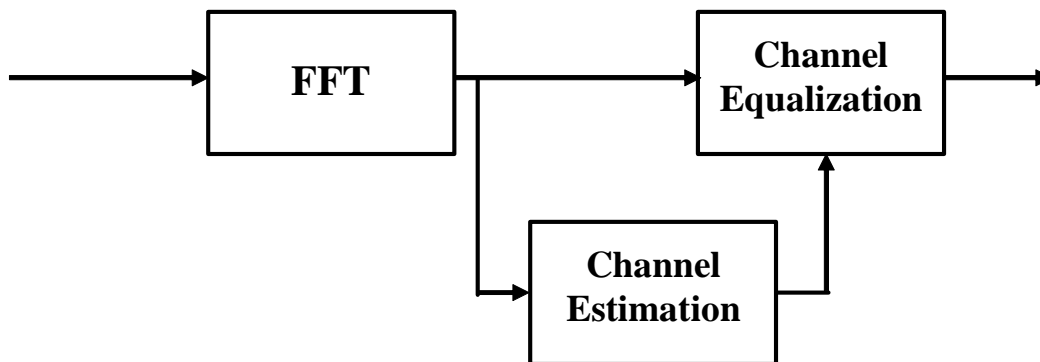
Figure 29: OFDM Data Demodulation Block Diagram

6.7.5.1 Time-Domain-to-Frequency-Domain Translation (i.e. FFT) Complexity

The FFT operation can be implemented with the following commonly used architecture for demodulating OFDM systems (see Figure 30).
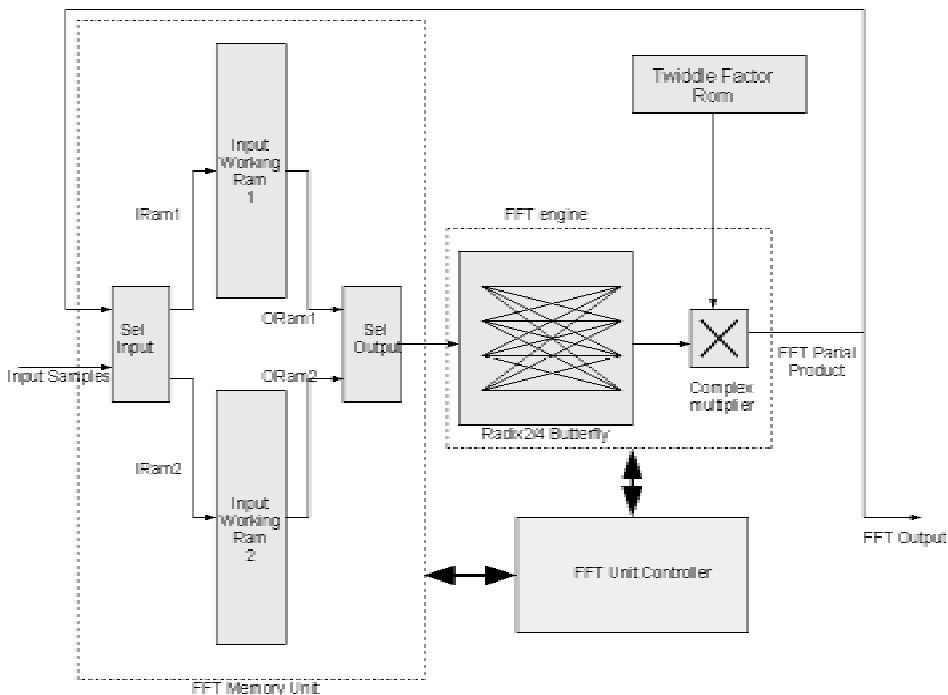
Figure 30: FFT Processor Block Diagram

The key components of this FFT processor are:

- **FFT Memory unit :** Memory is needed in order to be able to store the incoming OFDM symbols while processing the available OFDM symbol. The input samples are usually coded with 12 to 16 bits.

- **Twiddle_Factor_Rom:** The Fourier Transform operation done on a N_{FFT}-point is given by the expression:

$$X(k) = \sum_{n=0}^{N_{FFT}-1} x(n) * W_{N_{FFT}}^{nk}$$

where the terms $W_{N_{FFT}}^{nk}$, called twiddle factors, are given by $W_{N_{FFT}}^{nk} = \exp\left(\dfrac{-2j\pi nk}{N_{FFT}}\right)$, $\qquad j = \sqrt{-1}$.

The twiddle factors are usually coded on a number of bits ranging from 13 to 16 bits. The ROM size can be reduced by using symmetrical properties and the fact that in some cases, the twiddle factor is just equal to 1, -1, j or –j.

- **Radix 2/4 Butterfly and complex multiplier:** The FFT algorithms consist in decomposing the N_{FFT}-point DFT (Discrete Fourier Transform) into N_{FFT} / 2 two-point DFTs (radix-2) or N_{FFT} / 4 four-point DFTs (radix-4), which are then recombined recursively until reaching the result of the N_{FFT}-point DFT. A radix-2 butterfly is illustrated in Figure 3, and a radix-4 butterfly is illustrated in Figure 4.
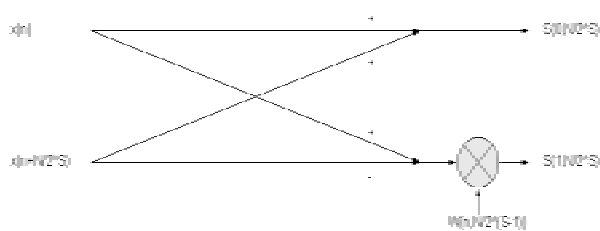
Figure 31: Radix-2 butterfly structure   **Figure 32: Radix-4 butterfly structure**
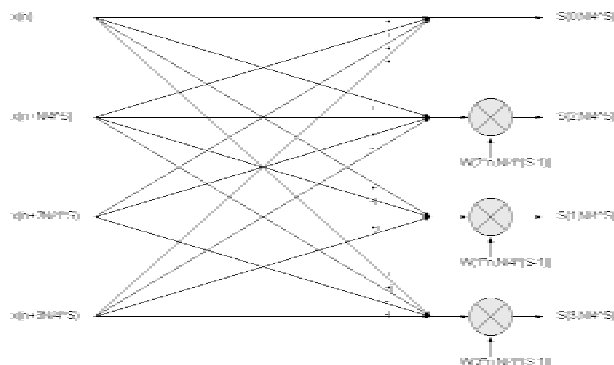
The most straightforward implementation for the 512-point FFT of OFDM parameter set 1 is with a radix-2 FFT. Each butterfly in a radix-2 FFT requires 1 complex multiply, 4 real additions, and 1 table look-up (with a complex value returned per table look-up). This count does not take into account the fact that some of the twiddle factors lead to trivial multiplications (i.e. multiply by +1, or –j). There are a total of $(N_{FFT}$ / 2) $\log_2 N_{FFT}$ butterflies, which for a 512-point FFT equals 2304 butterflies. The FFTs are performed at the OFDM symbol rate, $1/T_s$.

There are other slightly more efficient 512-point FFT implementations possible. These alternatives do not make a large difference to the complexity estimates. The most obvious alternative is a mixed-radix FFT with a combination of radix-2 and radix-4 FFT butterflies. Each radix-2 butterfly requires 1 complex multiply, 4 real additions, and 1 table look-up, and there are $(N_{FFT}$ / 2) such radix-2 butterflies. Each radix-4 butterfly requires 3 complex multiplies, 16 real additions, and 3 table look-ups, and there are a total of $(N_{FFT}$ / 4) $\log_4(N_{FFT}$ / 2) radix-4 butterflies. Once again, the FFTs are performed at the OFDM symbol rate, $1/T_s$.

For the 1024-point FFT required for parameter set 2, a radix-4 FFT can be used. Each butterfly in a radix-4 FFT requires 3 complex multiplies, 22 real additions, and 3 table look-ups (with a complex value returned per table look-up). This count does not take into account the fact that some of the twiddle factors lead to trivial multiplications (i.e. multiply by +1, or –j). There are a total of $(N_{FFT}$ / 4) $\log_4 N_{FFT}$ butterflies, which for a 1024-point FFT equals 1280 butterflies. The FFTs are performed at the OFDM symbol rate, $1/T_s$.

Note that each complex multiplication can be done as follows:

$$(a+ib)*(c+id) = \left[a*(c+d) - (a+b)*d\right] + i\left[a*(c+d) - (a-b)*c\right]$$

and so, by storing the quantity $a*(c+d)$ a complex multiplication requires 5 real additions and 3 real multiplications.

The FFT complexity main features are summarized below for both OFDM reference sets:

For set 1, with the 512-point FFT and a radix-2 architecture:

- a 65 MHz clock rate guarantees real time processing,

- the number of real multiplies per second is 93.312 million and the number of real additions per second is 279.936 million,

- for input samples of (12..16) bits the required FFT RAM memory is (24..33) Kbits, and the twiddle factor ROM memory is (3..4) Kbits, and

- the complex multiplier gate count is (6..12) K.

For set 2, with the 1024-point FFT, and a radix-4 architecture:

- a 39 MHz clock rate guarantees real time processing,

- the number of real multiplies per second is 69.12 million and the number of real additions per second is 238.08 million,

- for input samples of (12..16) bits the required FFT RAM memory is (49..66) Kbits, and the twiddle factor ROM memory is (6..8) Kbits, and

- the complex multiplier gate count is (6..12) K.

Note that the FFT complexity figures given above have been calculated assuming a radix-2 implementation for parameter set 1 and a radix-4 implementation for parameter set 2. However, other possibilities exist that enable trading off speed for code and memory size. For example, 512-point FFT cores are available which employ a mixed radix-4/2 architecture and require less processing speed than the radix-2 architecture, at the cost of extra control code and memory.

6.7.5.2 Channel Estimation

Since the pilot symbols are transmitted in specific time/frequency locations, channel estimation is generally done by interpolating among these pilots. The complexity depends on the interpolation method.

The simplest method without additional complexity is to simply repeat the channel value of the nearest pilot. This may be sufficient when the channel is relatively constant between two consecutive pilots.

Another straightforward method is to perform 2-D linear interpolation. For example, if the 4 nearest pilots are linearly combined with real coefficients to determine the channel estimate, there is a requirement for 8 real multiplies and 6 real additions per data sub-carrier. The number of data sub-carriers is equal to the number of useful sub-carriers minus the number of pilots. So for instance, if 10% of the sub-carriers are pilots then there are 269 data sub-carriers per OFDM symbol, and the OFDM symbol rate is 13500 symbols per second for OFDM parameter set 1. For parameter set 2, there would be 635 data sub-carriers (with 10% pilot) per OFDM symbol and the OFDM symbol rate is 6000 symbols per second. A single real MAC unit would need to operate at 29 MHz and 30 MHz for parameter set 1 and 2 respectively. Other, more efficient, methods may exist to perform the 2-D linear interpolation.

A more complex interpolating method is based on projection over some orthogonal basis of an arbitrarily chosen dimension. The advantage of this method is its flexibility, with the basis dimension chosen to cope with the rate of change of the channel conditions (higher dimension for higher channel variability).

6.7.5.3 Channel Equalization

Let c_i stand for the channel coefficient, y_i the received (demodulated) symbol and $\tilde{y}_i$ the equalizer output.

Single symbol equalization can be done by one of several methods:

- Phase Compensation (PC) : $\tilde{y}_i = y_i * angl(c_i)$

- Maximum Ratio Combiner (MRC): $\tilde{y}_i = y_i * conj(c_i)$

- Zero Forcing : $\tilde{y}_i = y_i / c_i = y_i * conj(c_i) / |c_i|^2$

- MMSE : $\tilde{y}_i = y_i * conj(c_i) / (|c_i|^2 + \sigma_N^2)$, where σ_N^2 is the Additive White Gaussian Noise variance.

Obviously, these methods are not of equal complexity and so the choice of method depends on the receiver realization, the mapping constellation and the required performance. Note that these operations are also applicable to HSDPA.

So, for instance, for channel equalization with a maximum ratio combiner each of the useful data sub-carriers is multiplied by the conjugate of the complex channel gain corresponding to that carrier. In this case, there are N_u x $(1/T_s)$ complex multiplies per second with 3 real multiplies and 5 real additions required per complex multiply. This formula applies to both parameter sets. For example, if 10% of the sub-carriers are assumed to carry pilot signals, then a single complex multiplier unit would need to operate at approximately 4.25 MHz for both parameter set 1 and 2.

6.8 Analysis of Node B impacts

6.8.1 OFDM Node B Transmitter Functionalities

This section addresses the additional Node B functionality needed to support downlink OFDM transmission and its corresponding impact on the Node B complexity. The critical Node B functionality needed to support downlink OFDM transmission includes:

- Functionality for data modulation of an OFDM signal, including (e.g.) frequency-domain-to-time-domain translation ("IFFT operation")
- RF functionality related to the transmission of an OFDM signal

The complexity associated with each of these functions is discussed in more details below. It should be noted that the list above may not be exhaustive. Furthermore, the complete detailed set of functionalities required to support OFDM would depend on the outcome of a future specification phase. Also, it is important to note that the complexity numbers in this section are provided as examples. The actual complexity may vary according to design and implementation choices.

6.8.2 Data Modulation

It is assumed that the first steps of the HSDPA HS-DSCH processing chain could be also used for OFDM (i.e. same CCTrCh encoding, etc.), before QAM symbols are mapped to OFDM-specific physical channels. The following steps of the data modulation processing chain are OFDM-specific, and thus, would need to be added to the Node B functionality in the event of the introduction of OFDM in UTRAN. The OFDM data processing chain is illustrated in Figure 33.
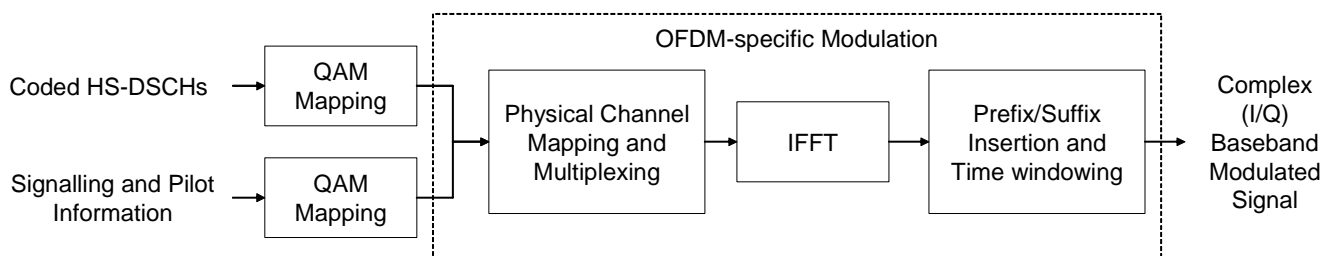
Figure 33: OFDM Data Modulation

6.8.2.1 OFDM Physical Channel Mapping and Multiplexing

The mapping of transport channels to OFDM physical channels, as well as the multiplexing of the physical channels on the OFDM T-F grid, are discussed further in Section 6.2. The complexity of this process would depend on the OFDM specification. For instance, if a solution based on a Costas sequence is used (as described in Section 6.2.4.1), the T-F

patterns are limited to 27 or 12 distinct values, depending on the parameter set, and cyclic shifts of these basic patterns in the frequency domain. These basic T-F patterns could therefore be stored in lookup tables. For T-F patterns with longer periods, some on-the-fly computations might be required to lower memory requirements. The inclusion of an OFDM-specific QAM symbol interleaver would also require additional complexity.

6.8.2.2 Frequency-Domain-to-Time-Domain Translation (i.e. IFFT)

Once mapped to the OFDM sub-carriers, the QAM symbols in each OFDM symbols are typically padded with inactive sub-carriers on each side of the spectrum (as discussed in Section 4.1.8), and transformed to a time-domain signal via an Inverse Fast Fourier Transform (IFFT). The complexity of the IFFT is comparable to that of the FFT, which is discussed in Section 6.7.5.1.

6.8.2.3 Prefix Insertion and Time Windowing

As discussed in Section 4.1.4, a cyclic prefix is usually added prior to each useful OFDM symbol (to reduce the inter-symbol interference). This prefix insertion can also be associated with a time-windowing of the OFDM symbols, as discussed in Section 6, to improve the spectral properties of the OFDM signal. Note that time-windowing could also be accompanied with filtering, or replaced by filtering. The time windowing approach is however typically less complex than the introduction of a filter.

6.8.3 RF Functionality

 The OFDM complex baseband digital signal obtained after data modulation has to be converted to the analog domain and up-converted to RF, before being amplified to the proper level and fed to the antenna. This process is illustrated in Figure 34.
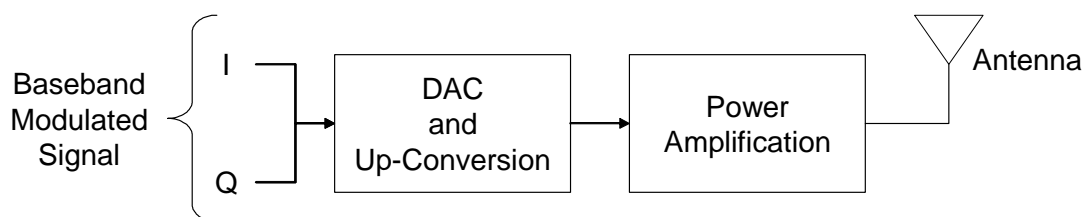
Figure 34: Node B RF Functionality

6.8.3.1 Digital-to-Analog Conversion and Up-Conversion

The Digital-to-Analog Conversion (DAC) is often combined in part with the up-conversion through the use of Digital Up-Conversion (DUC). In this case, the signal is first digitally up-converted to an Intermediate Frequency (IF), then converted to the analog domain, and finally up-converted from IF to RF with analog mixers. This possible processing chain is illustrated in Figure 35. Note that in some cases, it is possible to bypass the IF and do the up-conversion to RF digitally. This however requires very high speed DAC (in the order of twice the RF frequency), and is unlikely to be the preferred architecture for current UMTS frequencies and potential UMTS extension bands. This analysis is therefore limited to the case of DUC with an analog IF-to-RF up-conversion.
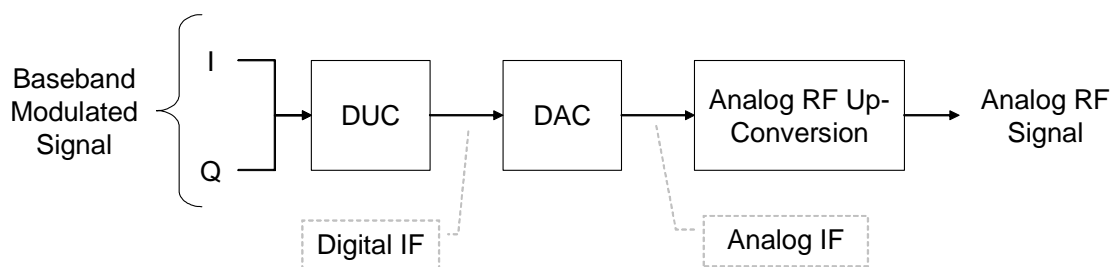
Figure 35: Architecture with Digital Up-Conversion (DUC) to IF

In this case, the DUC takes the baseband digital signal and brings it to IF via digital mixers. With OFDM parameter set 1, given that the OFDM sampling frequency is 2Fc, the same DUC and DAC modules might be used for both OFDM and WCDMA. In the case where the sampling frequencies are different (e.g. with set 2), different scenarios are possible:

- A specific DUC and DAC can be used for OFDM (i.e. not share between OFDM and WCDMA).
- The OFDM signal is re-sampled to match the WCDMA sampling rate prior to the DUC.
- A programmable DUC (i.e. with variable digital mixers) and a DAC with variable input sampling frequency can be shared by OFDM and WCDMA.

Other architectures are also possible for the DAC and up-conversion. For instance, the I and Q signals can be converted to the analog domain at baseband and then up-converted to RF (with or without an IF). This architecture is illustrated in Figure 36.
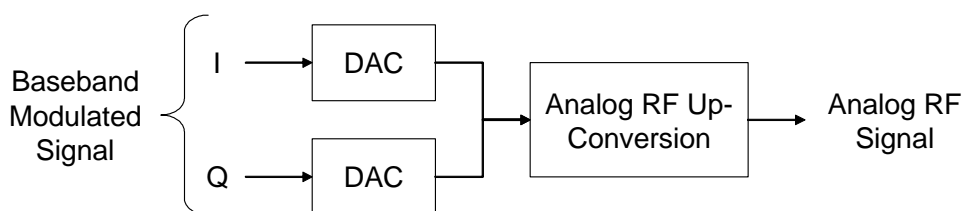
Figure 36: Architecture with Analog Up-Conversion

In the case of analog up-conversion, the I/Q DACs might be shared if the sampling frequencies are similar for OFDM and WCDMA (e.g. 2Fc). Again, if the sampling frequencies are different, different scenarios are possible:

- Separate DACs can be used for OFDM and WCDMA.
- The OFDM signal can be re-sampled to match the WCDMA sampling rate.
- The DAC input clock frequency can be simply adapted to the input sampling frequency.

In all cases, it is assumed that the analog component of the up-conversion process can be shared by OFDM and WCDMA. The actual impact of filters and impairments on OFDM might vary with the implementation.

6.8.3.2 Amplification

A Power Amplifier (PA) is required to bring the signal power to an acceptable level for the antenna transmission. Typically, a PA acts in a linear fashion over a range of input/output power, and saturates at a maximum power P_{max}. This is illustrated in Figure 37. The sharpness of the transition from the linear range to the saturation range depends on the PA design. Modern PA designs tend to maximise the linear range, resulting in a rather sharp transition to saturation.
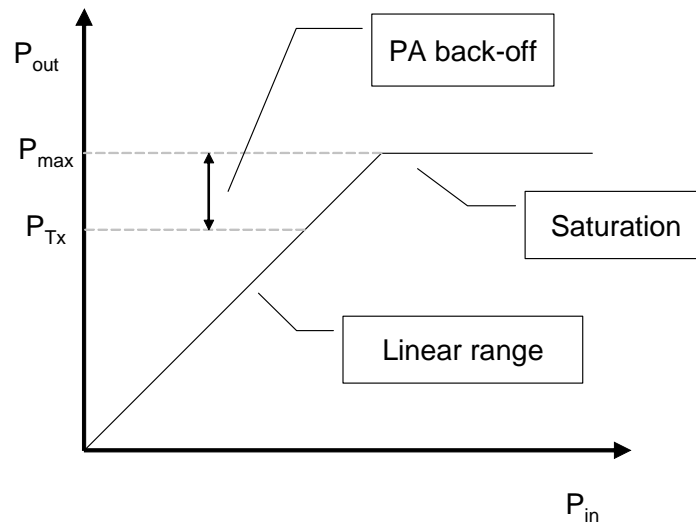
Figure 37: Power Amplifier (PA) Model

If the signal reaches this non-linear transition, high-power out-of-band emissions are created. The input power is therefore backed off from the maximum power to allow peaks in the amplitude of the signal to be limited to the linear range. The amount of power that needs to be subtracted from the maximum power depends on the signal's Peak-to-Average Ratio (PAR). For a given desired transmit power, a signal with a larger PAR will require a more powerful PA, which might increase significantly the cost of a Node B. It is therefore important to compare the PAR of an OFDM signal to that of a WCDMA signal to assess the impact on the Node B.

6.8.3.2.1   Peak-to-Average Ratio (PAR)

The PAR characteristic of an OFDM signal is compared to that of WCDMA in Figure 38. The WCDMA PAR curve is reproduced from [10]. It was obtained for Test Model 5 with 8 HS-DPSCHs, using a random bit sequence. A similar curve has been obtained for OFDM parameter sets 1 and 2. The resource assignments used for the analysis are detailed in Table 6 and Table 7, for parameter sets 1 and 2 respectively. In all cases, the signals are over-sampled to capture the peaks correctly.
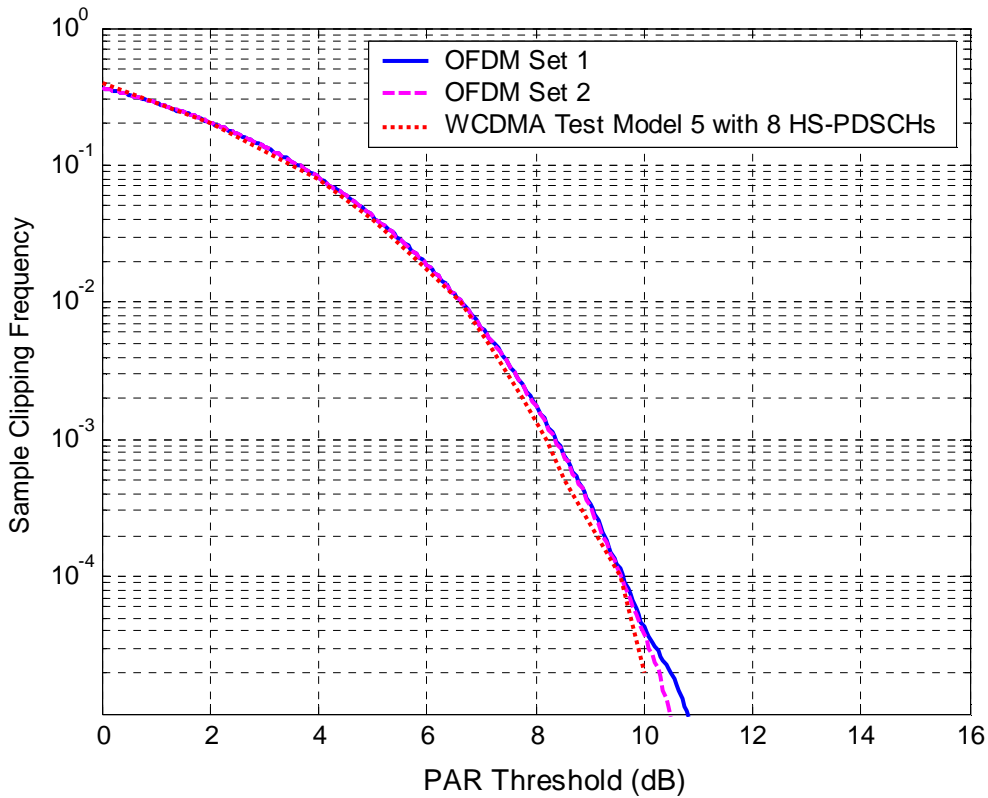
Figure 38: PAR for OFDM and WCDMA (without PAR reduction)

Physical Channels	T-F Resource	Power	Modulation
OFDM-PDSCHs	90%	80%	QAM16
OFDM-CPICH	5%	10%	QPSK
Other Control Channels	5%	10%	QPSK

Table 6: Resource Assignment for OFDM Parameter Set 1

Physical Channels	T-F Resource	Power	Modulation
OFDM-PDSCHs	85%	80%	QAM16
OFDM-CPICH	5%	10%	QPSK
Other Control Channels	10%	10%	QPSK

Table 7: : Resource Assignment for OFDM Parameter Set 2

These PAR curves indicate the probability of clipping a sample for a given PAR threshold. For instance, 0.01% (10^{-4}) of the samples would be clipped if a PAR threshold was set to about 9.5dB, for both OFDM parameter sets and WCDMA. Therefore, when no form of signal PAR reduction is used, the PAR of an OFDM signal would be similar to that of a WCDMA signal.

6.9 Impact to L2 and L3 protocols

6.9.1 Protocol Model

In the framework of this Study Item, OFDM is introduced as a separate carrier to carry HSDPA traffic only. The protocol model is kept unchanged in the UE and the UTRAN compared to the release 5 architecture described in 25.301 and 25.401.

The OFDM carrier is not considered as a cell itself as it does not carry any common channels. Therefore no further modification is required to support this type of deployment than what would be required to support multi-carrier cells.

6.9.2 RRC impacts

Introduction of OFDM in UTRAN to support an OFDM-HS-DSCH at the physical layer implies the definition of new physical channels as described in section 6.2. It will have an impact on the RRC protocol 25.331.

To support these new physical channel(s) RRC procedures for radio bearer setup, reconfiguration, transport channel and physical channel reconfiguration will require some modifications. These modifications would mainly consist in adding new information elements to characterize the physical channels which are mapped onto the OFDM carrier.

Additionally, to support the mobility procedures as described in section 6.4, measurements procedures would require some modifications to allow the configuration and reporting of OFDM-CPICH measurements. This could be done e.g. by updating the inter-frequency measurements methods.

6.9.3 Iub/Iur impacts

Introduction of OFDM in UTRAN is not expected to have any impact on the frame protocol but it will have an impact on RNSAP and NBAP protocols.

According to the scenario described in section 5.1, a cell supporting OFDM will be a multi-carrier cell. This implies some modifications to the common procedures of cell setup and reconfiguration. However some of these modifications are independent from the nature of the modulation i.e. introducing W-CDMA only multi-carrier cells would also require some modifications to these procedures.

Additionally, introducing OFDM in UTRAN would impact the NBAP/RNSAP procedures for setup, addition, reconfiguration and deletion of related radio links as well as HSDPA related common procedures i.e. physical shared channel reconfiguration and common measurements procedures.

7 Conclusion

Within the scope of the Study Item defined by RAN on" Analysis of OFDM for UTRAN Enhancement", RAN1 has carried out a study of the feasibility, complexity impact, and potential performance benefit vs. HSDPA release 5 of introducing OFDM modulation as an additional transmission mode for the UTRAN FDD downlink. More specifically, the following key aspects have been studied by RAN1:

- Spectrum compatibility
- Frequency Re-use
- Physical channel structure
- Synchronisation
- Impacts on the UE and Node B
- Impacts on the UL
- Impacts on L2 and L3 protocols
- Performance comparison between OFDM and HSDPA as of release 5

As agreed in the RAN Plenary and also stated in the Study Item description, the analysis has been based on a basic OFDM scheme (often referred to as "textbook" OFDM). More elaborate schemes, including e.g. MIMO and advanced modulation schemes, have not been considered to any substantial extent.

As further agreed in the RAN Plenary and also stated in the Study Item description, the study has focused on an OFDM-based Layer 1 with 5MHz transmission bandwidth in a high-speed-packet-data-only cell. The services to upper layers i.e. Transport-channels structure, measurements, etc. have been basically kept the same as release 5 in order to minimise impacts and ease the comparison. The performance metrics used are the aggregated cell throughput, the packet throughput and the packet delay.

The following conclusions are drawn by RAN1:

In terms of feasibility of introducing OFDM:

For the aspects considered in the Study Item, there are no indications that the introduction of OFDM in UTRAN is not feasible for the downlink. Further study is required to fully characterize some aspects (e.g. channel estimation, radio resource management aspects, inter-cell interference etc).

In terms of performance benefits of introducing OFDM:

For the performance comparison, two different receiver structures have been considered in case of HSDPA release 5:

- a "normal" RAKE receiver
- a receiver utilizing more "advanced" MMSE chip-level equalizer.

Ideal channel estimation has been assumed for the system-level performance evaluation. Performance with more realistic channel estimation has been investigated at the link level.

The studies carried out within the study item indicates that the basic OFDM scheme offers the possibility for improved performance, compared to HSDPA release 5 with a Rake receiver, for channels with significant time dispersion. This performance advantage decreases for channels with less time dispersion. However, by the introduction of more advanced receiver structure, there is no significant performance difference between HSDPA release 5 and the performance of the OFDM.

In terms of complexity impact of introducing OFDM:

The introduction of OFDM will have an incremental complexity impact on (multi-mode) UE complexity. Introducing OFDM on the network side will also require modifications to existing Node B design. The exact amount of modifications and the corresponding effort has not been concluded on and may also be manufacturer dependent.
It should be noted that the considered advanced receiver structure for HSDPA release 5 is more complex than the corresponding detector for OFDM. The overall terminal complexity impact from introducing OFDM also depends on whether or not it can be assumed that advanced receivers will anyway be introduced in the UE. Note that work on improved receivers and the specification of related performance requirements is already underway within RAN4 within the Work Item "Improved receiver performance requirements for HSDPA".

Annex A:
Simulation Assumptions and Results

A.1 Link Simulation Assumptions

Some specific link-level assumptions are listed in this section. In terms of physical layer operations that are not covered specifically here, the specifications described in **[2]** and **[3]** are followed. Information on channel power levels is also included in **Table 16**.

The following design aspects should be documented explicitly by any company presenting link-level simulation results.

- Any deviation from the standard set of parameters specified within this section. (OFDM & WCDMA)
- The criterion used to stop the simulation (or another appropriate measure for the reliability of the presented link-performance curves. (OFDM & WCDMA)
- How data symbols are mapped onto the TF (Time-Frequency) grid. (OFDM only)
- How pilot/signalling symbols are mapped onto the TF grid. (OFDM only)

A.1.1 Link Level Simulation Assumptions for OFDM

Table 8 provides a list of the link-level simulation assumptions that are relevant to the OFDM evaluation case. Here, it has been necessary to define an OFDM structure that is compatible with the HSDPA physical layer design.

Parameter	Explanation/Assumption	Comments
Carrier frequency	2 GHz	
Residual Frequency Offset Correction Error	TBD	
Fast fading model	Jakes model	
HSDPA slot length (TTI)	2 msec	
OFDM-CPICH power	Up to -10 dB (up to 10% of total maximum available transmission power, as averaged across each TTI)	The OFDM-CPICH power remains fixed, regardless of the number of data channels in use.
Power for other common channels	Up to -10 dB (up to 10% of total maximum available transmission power, as averaged across each TTI)	The other channel power remains fixed, regardless of the number of data channels in use.
Power for HSDPA data transmission	Maximum of 80% of total maximum available transmission power, as averaged across each TTI	The total HSDPA data transmission power will depend on the number of data channels in use.
Channel estimation	Ideal	Ideal channel information is assumed to be available at the receiver. Perfect timing and frequency estimation is also assumed. Real channel estimation from pilot subcarriers.

	Real	
MIMO configuration *NT:NR*	1:1	
Channel width	5 MHz	
Number of subcarriers	See Table 1	
OFDM sampling frequency	See Table 1	
FFT size	See Table 1	
Subcarrier MCS levels	All data subcarriers carry equal-weight data with the same modulation and code rate.	Assume one user per TTI
Bit interleaving	Uses 2nd interleaving defined in **[4]**.	
Rate matching	Performed to make the number of coding blocks compatible with the radio frame size.	Refer to Section 5.5.2 of [4]

Table 8: Down link OFDM link-level simulation assumptions

A.1.1.1 Time Windowing

Triangular time windowing on each OFDM symbol (as shown in Figure 39, with parameter values given in Table 9, and also as described earlier in Section 6.1.1) should be used at the transmitter to shape the OFDM signal spectrum in order to comply with the out-of-band spectral emission requirements given in [6]. The time windows for successive OFDM symbols are overlapped, so that the overall OFDM sampling rate remains unchanged. Other time window designs may be used, but it will then be necessary to demonstrate that the resulting OFDM signal spectrum also satisfies the spectral emission mask.
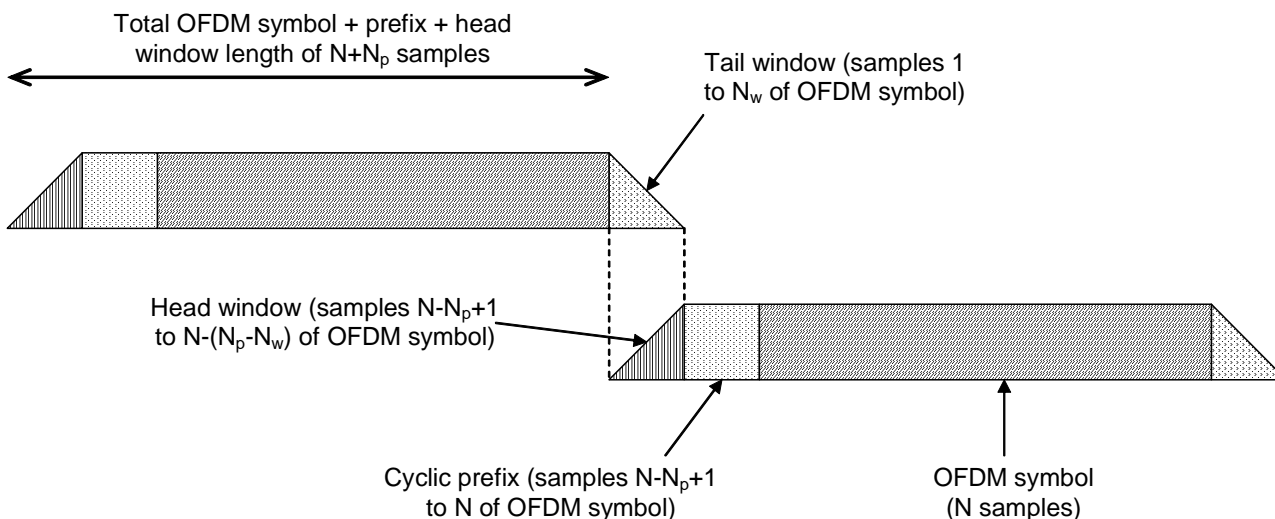
Figure 39: Triangular time-windowing with successive OFDM symbols

Parameter	OFDM Parameter Set 1	OFDM Parameter Set 2
FFT size (N)	512	1024
Cyclic prefix length (N_p)	56/57	64
Time window length (N_w)	20	32

Table 9: Time windowing parameters for OFDM parameter sets 1 and 2

A.1.2 Link Level Simulation Assumptions for WCDMA

Table 10 provides a list of the link-level simulation assumptions that are relevant to the WCDMA evaluation case. These are consistent with the HSDPA design presented in **[3]**. Other aspects of the WCDMA HSDPA link level simulator are directly taken from **[3]** and **[4]**.

Parameter	Explanation/Assumption	Comments
Carrier frequency	2 GHz	
Fast fading model	Jakes model	
HSDPA slot length (TTI)	2 msec	
CPICH power	-10 dB (10% of total maximum available transmission power)	The CPICH power remains fixed, regardless of the number of data channels in use.
Power for other common channels	-10 dB (10% of total maximum available transmission power)	The other channel power remains fixed, regardless of the number of data channels in use.
Power for HSDPA data transmission	Maximum of 80% of total maximum available transmission power	The total HSDPA data transmission power will depend on the number of data channels in use.
Channel estimation	Ideal Real	Ideal channel information is assumed to be available at the receiver. Perfect timing and frequency estimation is also assumed. Real channel estimation from pilot subcarriers
MIMO configuration *NT:NR*	1:1 used	
Chip-rate	3.84 Mcps	
Spreading factor	16	
Channel width	5 MHz	

Table 10: Down link WCDMA link-level simulation assumptions

A.1.3 Link Level Simulation Scenarios

Table 11 provides a list of the specific simulation cases that will need to be evaluated. For each of the channel models, a fading rate (corresponding to the UE velocity in km/h) is also given. The channel models are described in more detail earlier in **Table 21**.

Parameter	Cases	Comments
Channel model and fade rate	Ch-100, 30 km/h	Single path
	Ch-100, 120 km/h	Single path
	Ch-104, 30 km/h	ITU Vehicular A
	Ch-104, 120 km/h	ITU Vehicular A
	Ch-102, 3 km/h	ITU Pedestrian A
	Ch-103 3 km/h	ITU Pedestrian B
Modulation	QPSK, 16QAM, 64QAM	64QAM is optional
Code rate	1/3, 1/2, 2/3 , 3/4, 4/5	
User Geometry Values	The following G factors to be considered as realistic – (1) 0 dB to ensure good service availability (2) 10 dB to test AMC performance in typical low interference scenarios	It is to be noted that available C/I is limited by the geometry factor. The utilised geometry distribution should respect the geometry distribution derived from the system level assumptions in A.3.3.

Table 11: Down link link-level simulation scenarios

Table 12 through Table 14 provide appropriate information bit payload and code block segmentation values (calculated according to TS25.212 [4]) for example test cases assuming 5, 10, and 15 WCDMA or OFDM data units allocated to a single user within a 2 ms TTI. Other numbers of data units per user may also be evaluated if so desired.

Modulation	Code Rate	Information Bit Payload	24-bit CRC Addition	Code Block Segmentation	R=1/3 Turbo Encoding	Rate Matching
QPSK	1/3	1600	1624	1×1624	4884	4800
QPSK	1/2	2400	2424	1×2424	7284	4800
QPSK	2/3	3200	3224	1×3224	9684	4800
QPSK	3/4	3600	3624	1×3624	10884	4800
QPSK	4/5	3840	3864	1×3864	11604	4800
16QAM	1/3	3200	3224	1×3224	9684	9600
16QAM	1/2	4800	4824	1×4824	14484	9600
16QAM	2/3	6400	6424	2×3212	19296	9600
16QAM	3/4	7200	7224	2×3612	21696	9600
16QAM	4/5	7680	7704	2×3852	23136	9600

Table 12: Information bit payload and code block sizes for each transport format assuming 5 WCDMA or OFDM data units allocated to a single user per 2 ms TTI

Modulation	Code Rate	Information Bit Payload	24-bit CRC Addition	Code Block Segmentation	R=1/3 Turbo Encoding	Rate Matching
QPSK	1/3	3200	3224	1×3224	9684	9600

QPSK	1/2	4800	4824	1×4824	14484	9600
QPSK	2/3	6400	6424	2×3212	19296	9600
QPSK	3/4	7200	7224	2×3612	21696	9600
QPSK	4/5	7680	7704	2×3852	23136	9600
16QAM	1/3	6400	6424	2×3212	19296	19200
16QAM	1/2	9600	9624	2×4812	28896	19200
16QAM	2/3	12801	12825	3×4275	38611	19200
16QAM	3/4	14400	14424	3×4808	43308	19200
16QAM	4/5	15360	15384	4×3846	46200	19200

Table 13: Information bit payload and code block sizes for each transport format assuming 10 WCDMA or OFDM data units allocated to a single user per 2 ms TTI

Modulation	Code Rate	Information Bit Payload	24-bit CRC Addition	Code Block Segmentation	R=1/3 Turbo Encoding	Rate Matching
QPSK	1/3	4800	4824	1×4824	14484	14400
QPSK	1/2	7200	7224	2×3612	21696	14400
QPSK	2/3	9600	9624	2×4812	28896	14400
QPSK	3/4	10800	10824	3×3608	32508	14400
QPSK	4/5	11520	11544	3×3848	34668	14400
16QAM	1/3	9600	9624	2×4812	28896	28800
16QAM	1/2	14400	14424	3×4808	43308	28800
16QAM	2/3	19200	19224	4×4806	57720	28800
16QAM	3/4	21601	21625	5×4325	64935	28800
16QAM	4/5	23041	23065	5×4613	69255	28800

Table 14: Information bit payload and code block sizes for each transport format assuming 15 WCDMA or OFDM data units allocated to a single user per 2 ms TTI

To reduce computational expense for simulations, the following link modes are considered to be core transport formats for purposes such as simulator calibration, evaluation of various designs and algorithms (e.g. pilot patterns, channel estimators, etc):

- QPSK R=1/3
- QPSK R=2/3
- QPSK R=4/5
- 16QAM R=1/2
- 16QAM R=3/4

These five transport formats should, as a minimum, each be simulated for these types of evaluation situations; additional transport formats may also be simulated if so desired.

A.2 Link Simulation Results

A.2.1 Link-Level Performance with Realistic Performance Using EESM Modelling

The simulation assumptions used to generate the results presented in this section are summarised in Table 15.

Parameter	Value
System configuration:	See A.3

Cell layout, path loss, antenna profile, shadowing, etc.	
Site to site distance	2.8km
Number of drops	100
Number of UEs per drop	100
OFDM parameters	Set 2
OFDM units	15 units of 480 symbols per sub-frame, 85% of the time-frequency resource
OFDM traffic multiplexing	Based on Costas sequence (see 6.2.4)
OFDM-CPICH	5% of the time-frequency resource, 10% of total power
OFDM signalling and other common channels	10% of the time-frequency resource, 10% of power
Channel experienced from the serving cell	Pedestrian A or B
Channel experienced from the interfering cells	Pedestrian B
EESM beta values	See A.4.6.1
Sub-frame alignment from the different cells perceived by UE	Uniformly distributed in [0,2] ms

Table 15: Simulation assumptions

Simulation results are presented in Figure 40 and Figure 41 for Pedestrian A and B channel models, respectively. The results are illustrated as the average throughput achievable for a given geometry. The throughput obtained using realistic interference is also compared to that obtained for interference modelled as AWGN with the same power.
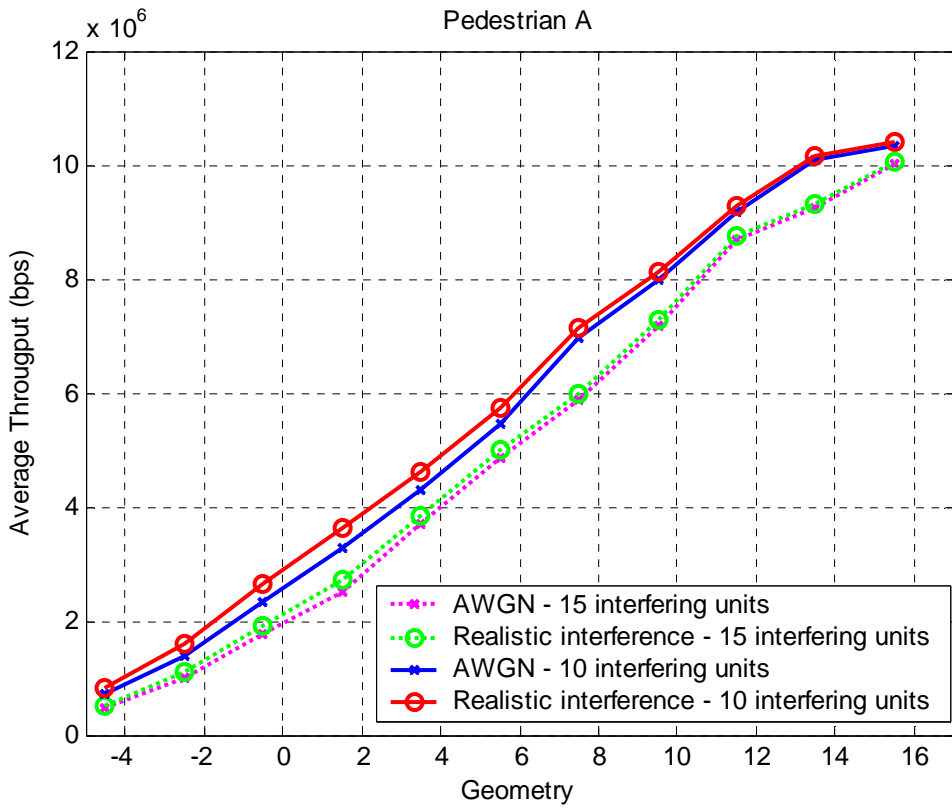
Figure 40: Link-Level Performance in Pedestrian A
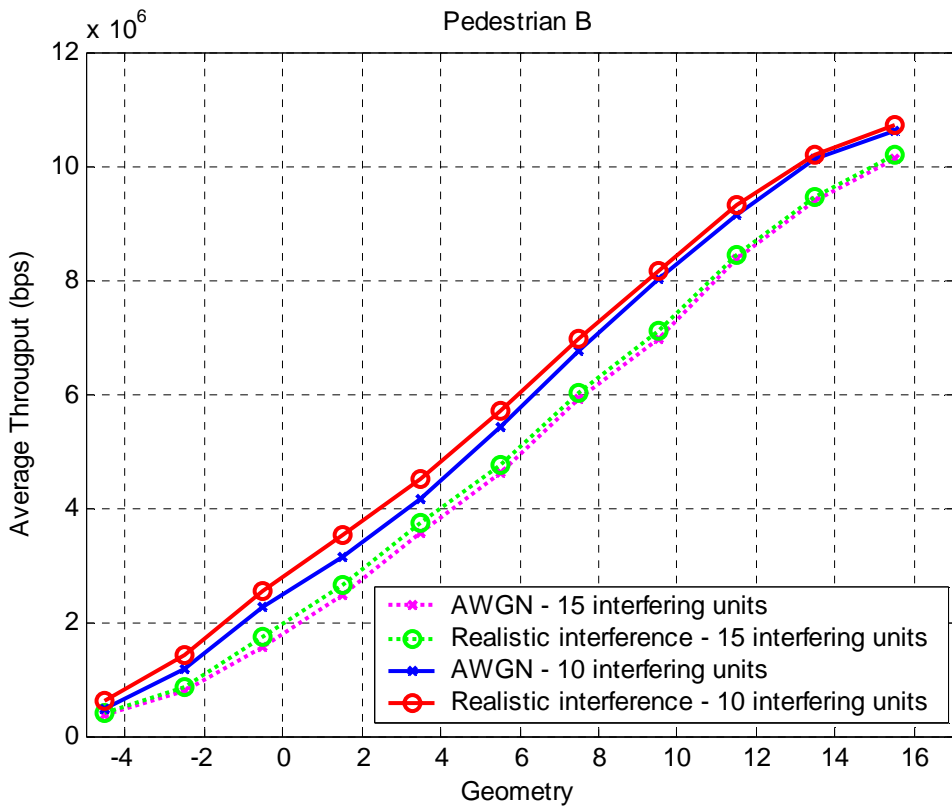
Figure 41: Link-Level Performance in Pedestrian B

A.3   System Simulation Assumptions

A.3.1   Antenna Pattern

The antenna pattern used for each sector, is specified as :

$$A(\theta) = -\min\left[12\left(\frac{\theta}{\theta_{3\,dB}}\right)^2, A_m\right], \quad \text{where} \quad -180 \le \theta \le 180,$$

where min[ ] is the minimum function, θ_{3dB} is the 3dB beamwidth (corresponding to θ_{3dB} = 70 degrees) , and A_m= 20 dB is the maximum attenuation.

A.3.2   Antenna Orientation

The antenna bearing is defined as the angle between the main antenna lobe center and a line directed due east given in degrees. The bearing angle increases in a clockwise direction. Figure 42 shows an example of the 3-sector 120-degree center cell site, with Sector 1 bearing angle of 330 degrees. Figure 43 shows the orientation of the center cell (target cell) hexagon and its three sectors corresponding to the antenna bearing orientation proposed for the simulations. The main antenna lobe center directions each point to the sides of the hexagon. The main antenna lobe center directions of the 18 surrounding cells shall be parallel to those of the center cell. Figure 43 also shows the orientation of the cells and sectors in the two tiers of cells surrounding the central cell.
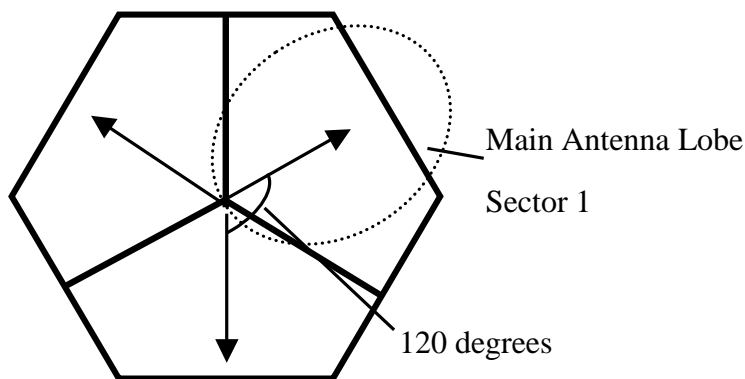
Figure 42: Centre cell antenna bearing orientation diagram
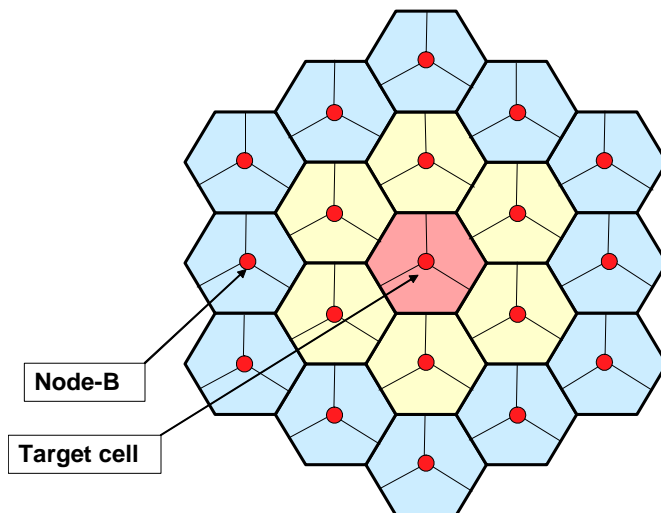
Figure 43: Configuration of adjacent tiers of neighbouring cells, sectors, and Node-Bs

A.3.3 Common System Level Simulation Assumptions

The assumptions used in the system-level simulations are listed in Table 16 and are primarily taken from [1].

Parameter	Explanation/Assumption	Comments
Cellular layout	Hexagonal grid, 3-sector sites	See Figure 43
Antenna horizontal pattern	70 deg (-3 dB) with 20 dB front-to-back ratio	
Site to site distance	2800 m	Or 1000 m
Propagation model	$L = 128.1 + 37.6 \, Log_{10}(R)$	R in kilometers
CPICH power	-10 dB	
Other common channels	-10 dB	
Power allocated to HSDPA transmission, including associated signalling	Max. 80 % of total cell power	
Slow fading	As modelled in UMTS 30.03, B 1.4.1.4	
Standard deviation of slow fading	8 dB	
Correlation between sectors	1.0	
Correlation between sites	0.5	
Correlation distance of slow fading	50 m	
Carrier frequency	2000 MHz	
BS antenna gain	14 dB	
UE antenna gain	0 dBi	
UE noise figure	9 dB	

Thermal noise density	-174 dBm/Hz	
Max. # of retransmissions	3	Retransmissions by fast HARQ. Does not include the initial transmission. Programmable
Fast HARQ scheme	Chase combining or incremental redundancy	
Scheduling algorithm	TBD	
BS total Tx power	Up to 44 dBm	
Specific fast fading model	Jakes spectrum	
HSDPA slot length	2 msec	
MCS feedback delay	2 TTIs	This implies that after a channel measurement is made, it requires two additional TTIs before it can be used at the Node B. For example, a channel measurement made during TTI 1 would be transmitted to the Node B and processed during TTIs 2 and 3, and could be used to select the MCS level for TTI 4.
UE spatial distribution	Uniform random spatial distribution over elementary single cell hexagonal central Node-B	
MIMO configuration *NT:NR*	1:1	
Channel width	5 MHz	
Frequency Re-use	1	

Table 16 Down-link system-level simulation assumptions

A.3.4   Traffic Sources

Three different traffic types are suggested for evaluation purposes.

A.3.4.1 HTTP Traffic Model Characteristics
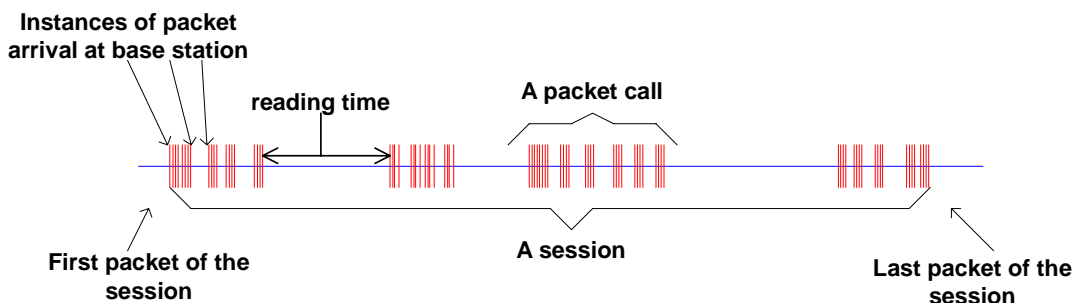
Figure 44: Packet Trace of a Typical Web Browsing Session

Figure 44 shows the packet trace of a typical web browsing session. The session is divided into ON/OFF periods representing web-page downloads and the intermediate reading times, where the web-page downloads are referred to as packet calls. These ON and OFF periods are a result of human interaction where the packet call represents a user's request for information and the reading time identifies the time required to digest the web-page.

As is well known, web-browsing traffic is self-similar. In other words, the traffic exhibits similar statistics on different timescales. Therefore, a packet call, like a packet session, is divided into ON/OFF periods as in Figure 44. Unlike a packet session, the ON/OFF periods within a packet call are attributed to machine interaction rather than human interaction. A web-browser will begin serving a user's request by fetching the initial HTML page using an HTTP GET request. The retrieval of the initial page and each of the constituent *objects* is represented by ON period within the packet call while the parsing time and protocol overhead are represented by the OFF periods within a packet call. For simplicity, the term "page" will be used in this paper to refer to each packet call ON period.
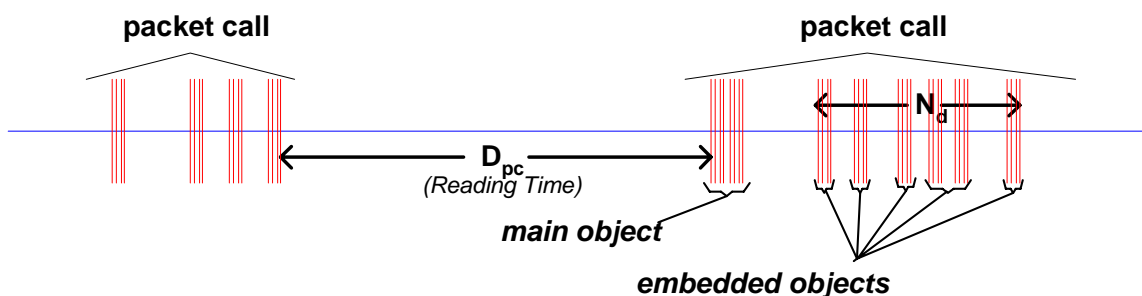
Figure 45: Contents in a Packet Call

The parameters for the web browsing traffic are as follows:

- S_M: Size of the main object in a page

- S_E: Size of an embedded object in a page

- N_d: Number of embedded objects in a page

- D_{pc}: Reading time

- T_p: Parsing time for the main page

HTTP/1.1 persistent mode transfer is used to download the objects, which are located at the same server and the objects are transferred serially over a single TCP connection as modelled in[5]. The distributions of the parameters for the web browsing traffic model are described in Table 17. Based on observed packet size distributions, 76% of the HTTP packet calls should use an MTU of 1500 bytes, with the remaining 24% of the HTTP packet calls using an MTU of 576 bytes. These two potential packet sizes also include a 40 byte IP packet header (thereby resulting in useful data payloads of 1460 and 536 bytes, respectively), and this header overhead for the appropriate number of packets must be added to the object data sizes calculated from the probabilistic distributions in Table 17.

Component	Distribution	Parameters	PDF
Main object size (S_M)	Truncated Lognormal	Mean = 10710 bytes Std. dev. = 25032 bytes Minimum = 100 bytes Maximum = 2 Mbytes	$f_x = \dfrac{1}{\sqrt{2\pi}\sigma x}\exp\left[\dfrac{-(\ln x - \mu)^2}{2\sigma^2}\right], x \geq 0$ $\sigma = 1.37, \mu = 8.35$
Embedded object size (S_E)	Truncated Lognormal	Mean = 7758 bytes Std. dev. = 126168 bytes Minimum = 50 bytes Maximum = 2 Mbytes	$f_x = \dfrac{1}{\sqrt{2\pi}\sigma x}\exp\left[\dfrac{-(\ln x - \mu)^2}{2\sigma^2}\right], x \geq 0$ $\sigma = 2.36, \mu = 6.17$
Number of embedded objects per page (N_d)	Truncated Pareto	Mean = 5.64 Max. = 53	$f_x = \dfrac{\alpha k^\alpha}{x^{\alpha+1}}, k \leq x < m$ $f_x = \left(\dfrac{k}{m}\right)^\alpha, x = m$ $\alpha = 1.1, k = 2, m = 55$ Note: Subtract k from the generated random value to obtain N_d
Reading time (D_{pc})	Exponential	Mean = 30 sec	$f_x = \lambda e^{-\lambda x}, x \geq 0$ $\lambda = 0.033$
Parsing time (T_p)	Exponential	Mean = 0.13 sec	$f_x = \lambda e^{-\lambda x}, x \geq 0$ $\lambda = 7.69$

Table 17: HTTP Traffic Model Parameters

A.3.4.2   FTP Traffic Model Characteristics

In FTP applications, a session consists of a sequence of file transfers, separated by *reading times*. The two main parameters of an FTP session are:

1.   S : the size of a file to be transferred

2. D_{pc}: reading time, i.e., the time interval between end of download of the previous file and the user request for the next file.

The underlying transport protocol for FTP is TCP. The model of TCP connection described in [5]will be used to model the FTP traffic. The packet trace of an FTP session is shown in Figure 46.

Packet calls

Packets of file 1   Packets of file 2   Packets of file 3
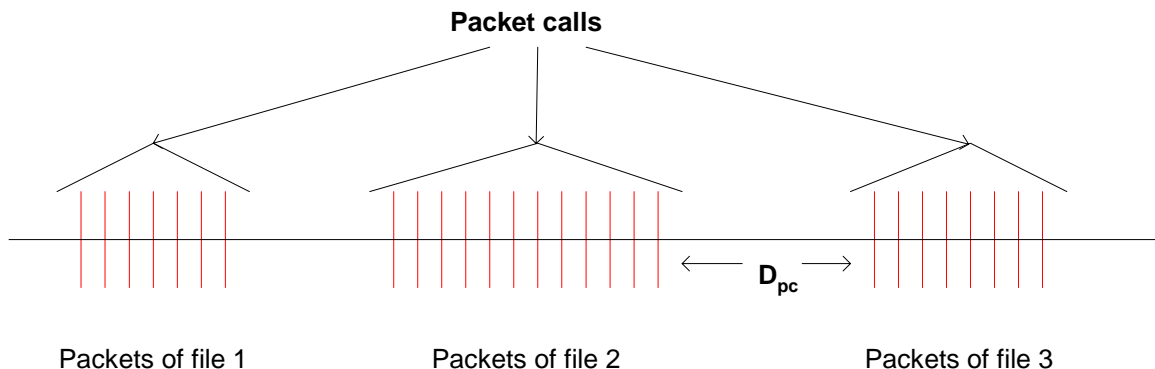
Figure 46: Packet Trace in a Typical FTP Session

The parameters for the FTP application sessions are described in Table 18.

Component	Distribution	Parameters	PDF
File size (S)	Truncated Lognormal	Mean = 2Mbytes Std. Dev. = 0.722 Mbytes Maximum = 5 Mbytes	$f_x = \dfrac{1}{\sqrt{2\pi}\sigma x}\exp\left[\dfrac{-(\ln x - \mu)^2}{2\sigma^2}\right], x \ge 0$ $\sigma = 0.35, \mu = 14.45$
Reading time (D_{pc})	Exponential	Mean = 180 sec.	$f_x = \lambda_e^{-\lambda x}, x \ge 0$ $\lambda = 0.006$

Table 18: FTP Traffic Model Parameters

Based on the results on packet size distribution, 76% of the files are transferred using and MTU of 1500 bytes and 24% of the files are transferred using an MTU of 576 bytes. Note that these two packet sizes also include a 40 byte IP packet header (thereby resulting in useful data payloads of 1460 and 536 bytes, respectively) and this header overhead for the appropriate number of packets must be added to the file sizes calculated from the probabilistic distributions in Table 18. For each file transfer a new TCP connection is used whose initial congestion window size is 1 segment (i.e. MTU).

A.3.4.3   NRTV (Near Real Time Video) Traffic Model Characteristics

This section describes a model for streaming video traffic on the forward link. Figure 47 describes the steady state of video streaming traffic from the network, as seen by the base station. Latency at call startup is not considered in this steady-state model.
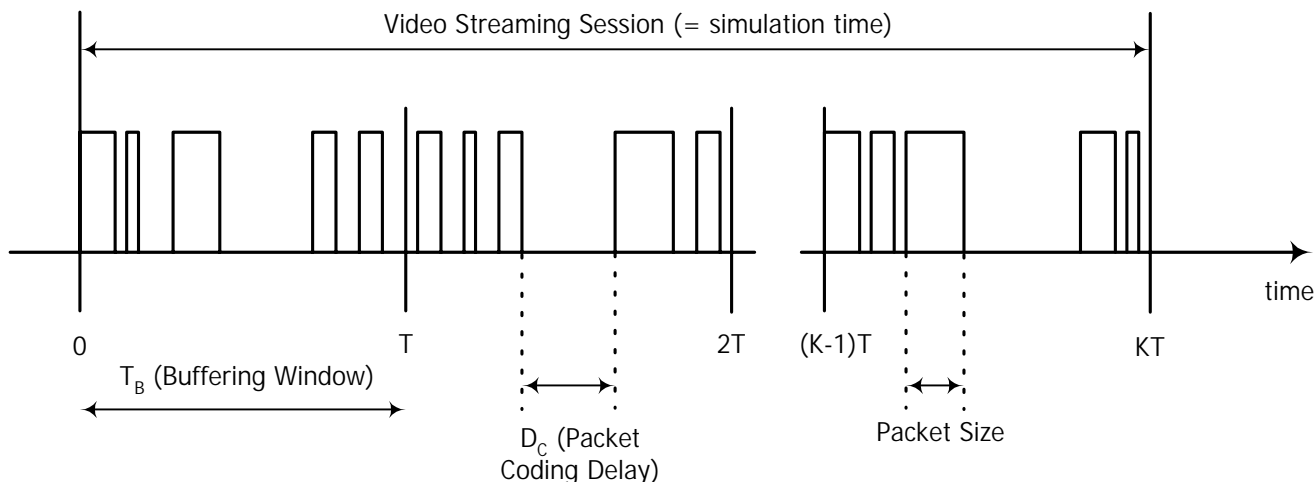
Figure 47: Video Streaming Traffic Model

A video streaming session is defined as the entire video streaming call time, which is equal to the simulation time for this model. Each frame of video data arrives at a regular interval T determined by the number of frames per second (fps). Each frame is decomposed into a fixed number of slices, each transmitted as a single packet. The size of these packets/slices is distributed as a truncated Pareto distribution. Encoding delay, Dc, at the video encoder introduces delay intervals between the packets of a frame. These intervals are modelled by a truncated Pareto distribution.

The parameter T_B is the length (in seconds) of de-jitter buffer window in the mobile station, and is used to guarantee a continuous display of video streaming data. This parameter is not relevant for generating the traffic distribution, but it is useful for identifying periods when the real-time constraint of this service is not met. At the beginning of the simulation, it is assumed that the mobile station de-jitter buffer is full with (T_B x source video data rate) bits of data. Over the simulation time, data is "leaked" out of this buffer at the source video data rate and "filled" as forward link traffic reaches the mobile station. As a performance criterion, the mobile station can record the length of time, if any, during which the de-jitter buffer runs dry. The de-jitter buffer window for the video streaming service is 5 seconds.

Using a source video rate of 64 kbps, the video traffic model parameters are defined in Table 19.

Information types	Inter-arrival time between the beginning of each frame	Number of packets (slices) in a frame	Packet (slice) size	Inter-arrival time between packets (slices) in a frame
Distribution	Deterministic (Based on 10fps)	Deterministic	Truncated Pareto (Mean= 50bytes, Max= 250bytes)	Truncated Pareto (Mean= 6ms, Max= 12.5ms)
Distribution Parameters	100ms	8	K = 40 bytes $\alpha = 1.2$	K = 2.5ms $\alpha = 1.2$

Table 19: Video Streaming Traffic Model Parameters.

Only system-level simulations with homogenous traffic mixes are to be conducted. That is, for a particular simulation, all users will either have all FTP traffic, all HTTP traffic, or all NRTV traffic. There is no mixing of different traffic types within a single simulation.

A.3.5 Performance Metrics

This section describes the performance statistics that are generated as an output from the system-level simulations. In each case, a performance curve given as a function of the number of users per sector is generated.

A.3.5.1 Output Metrics for Data Services

The following statistics related to data traffics should be generated and included in the evaluation report for each scheme. A frame as used below is also referred to as a transport block and consists of information bits, CRC, and tail bits.

1. **Average cell throughput [kbps/cell]** is used to study the network throughput performance, and is measured as

$$R = \frac{b}{k \cdot T}$$

   where b is the total number of correctly received data bits in all data UEs in the simulated system over the whole simulated time, k is the number of cells in the simulation and T is the simulated time. In the case of only evaluating the center cell site, k is the number of sectors.

2. **Average packet call throughput [kbps]** for user i is defined as

$$R_{pktcall}(i) = \frac{\sum_{k} \text{good bits in packet call } k \text{ of user } i}{\sum_{k} \left(t_{end\_k} - t_{arrival\_k}\right)}$$

   where $k =$ denotes the kth packet call from a group of K packet calls where the K packet calls can be for a given user i, $t_{arrival\_k} =$ first packet of packet call k arrives in queue, and $t_{end\_k} =$ last packet of packet k is received by the UE. Note for uncompleted packet calls, t_{end_k} is set to simulation end time. The mean, standard deviation, and distribution of this statistic are to be provided.

3. **The packet service session FER** is calculated for all the packet service sessions. A packet service session FER is defined as the ratio

$$FER_{session} = \frac{n_{erroneous\_frames}}{n_{frames}},$$

   where $n_{erroneous\_frames}$ is the total number of erroneous frames in the packet service session and n_{frames} is the total number of frames in the packet service session. These individual packet service session FERs from all packet service sessions form the distribution for this statistic. The mean, standard deviation, and the distribution of this statistic are to be provided.

   A Definition of a Packet Service Session: A Packet Service Session contains one or several packet calls depending on the application. Packet service session starts when the transmission of the first packet of the first packet call of a given service begins and ends when the last packet of the last packet call of that service has been transmitted. (One packet call contains one or several packets.) Note, that FER statistics are only collected from those frames during which UE is receiving data.

4. **The residual FER** is calculated for each user for each packet service session. A packet service session residual FER is defined by the ratio

$$FER_{residual} = \frac{n_{dropped\_frames}}{n_{frames}},$$

where $n_{dropped\_frames}$ is the total number of dropped frames in the packet service session and n_{frames} is the total number of frames in the packet service session. A dropped frame is one in which the maximum ARQ or HARQ re-transmissions have been exhausted without the frame being successfully decoded. It does not include the RLC initiated re-transmissions. The mean, standard deviation, and distribution of this statistic over all the packet service sessions in the simulation are to be provided.

5. **The averaged packet delay per sector** is defined as the ratio of the accumulated delay for all packets for all UEs received by the sector and the total number of packets. The delay for an individual packet is defined as the time between when the packet enters the queue at transmitter and the time when the packet is received successively by the UE. If a packet is not successfully delivered by the end of a run, its ending time is the end of the run.

6. **System Outage**

A user is in outage if more than a given percentage of packets (blocks) experience a delay of greater than a certain time. The system is considered to be in outage if any individual users are in outage.

A.3.6 Channel Models and Interference

A.3.6.1 Channel Models

In this context, a channel model corresponds to a specific number of paths, a power profile giving the relative powers of these multiple paths (ITU multi-path models), and Doppler frequencies to specify the fade rate.

The channel models (from 1 to 6) are randomly assigned to the various users according to the probability distribution listed in Table 20. The channel model assigned to a specific user remains fixed over the duration of a simulation drop.

Channel Model	Multi-path Model	# of Paths	Speed (km/h)	Fading	Assignment Probability
Model 1	Ch-100	1	30	Jakes	0.1
Model 2	Ch-100	1	120	Jakes	0.1
Model 3	Ch-104	6	30	Jakes	0.1
Model 4	Ch-104	6	120	Jakes	0.1
Model 5	Ch-102	4	3	Jakes	0.3
Model 6	Ch-103	6	3	Jakes	0.3

Table 20: Channel Models and associated assignment probability distribution

The channel models, UE speeds (for fading rates), and assignment probabilities listed in Table 20 are adapted from [1]. Note that a separate link-level simulation must be performed for each specific channel model and UE velocity combination. Hence, there is a desire to minimize the number of different possible channel model combinations, while ensuring that an accurate modelling of reality is also made. The assignment probabilities in Table 20 were selected to

agree with the corresponding probabilities in [1], while reducing the number of different distinct fading velocities in order to reduce the number of link level simulations that must be performed.

The normalized power profiles for the different channel models such as flat fading: Ch-100, ITU vehicular-A: Ch-104, ITU pedestrian-A: Ch-102, and ITU pedestrian-B: Ch-103 are given in Table 21. For the channel models that correspond to the standard ITU channel models, the relative ratios of the path powers are the same, but the absolute power values have been normalized so that they sum to 0 dB (unit energy) for each given channel model.

Channel Model	Path 1 (dB)	Path 2 (dB)	Path 3 (dB)	Path 4 (dB)	Path 5 (dB)	Path 6 (dB)	Rake Fingers
Flat Fading Ch-100	0	–	–	–	–	–	1
ITU Vec. A Ch-104	-3.14	-4.14	-12.14	-13.14	-18.14	-23.14	1,2,3,4,5,6
ITU Ped. A Ch-102	-0.51	-10.21	-19.71	-23.31	–	–	1,2,3,4
ITU Ped. B Ch-103	-3.92	-4.82	-8.82	-11.92	-11.72	-27.82	1,2,3,4,5,6

Table 21: Normalized power profiles for multi-path channel models

The Rake finger column in the above table indicates the paths to which WCDMA Rake fingers will be assigned. It is assumed that Rake fingers will be assigned to each multipath component within a given channel model [1]. It is also possible to assign Rake fingers only to those channel taps that contain most of the signal power eg. not assign Rake fingers to channel taps that attenuate the transmitted signal more than 10 dB.

A.4 System-Level Evaluation Methodology

This section of the Annex defines one possible methodology for the system-level evaluation methodology of HSDPA channels. This methodology may be used and referenced in submitting evaluations. If this methodology is not used then a description of the methodology employed should be provided.

A.4.1 HSDPA release 5

Figure 48 illustrates a methodology for the system-level evaluation of HSDPA performance that was adopted by many companies during the HSDPA study item. This methodology is especially applicable to the case of low/medium Doppler, i.e. when the channel can be assumed to be constant during a TTI.

On system level, a UE exists within the simulated deployment. Based on the UE position, a short-time-average geometry $\overline{G}$, including the effect of distance-dependent path-loss, shadowing, and thermal noise, is determined for each UE. For each UE and each TTI, an instantaneous channel-impulse response $h(t)$ is generated according to the average channel-delay profile (Pedestrian B, Vehicular A, etc.). In practice, the impulse response $h(t)$ will be a sampled impulse response, e.g. with a sampling time equal to the chip time.

In a time-dispersive environment, the channel will cause intra-cell interference due to loss of downlink orthogonality. Thus, the MCS selection and the corresponding block-error probability depend on both the geometry $\overline{G}$ and the instantaneous channel $h(t)$. To directly map $\overline{G}$ and $h(t)$ to an accurate estimate of the block-error probability would require an overwhelming effort on link level and is not a feasible path. Instead, a well-defined mapping function $SIR_{eff}(\overline{G}; h)$ is introduced, that maps $\overline{G}$ and $h(t)$ to an *effective SIR* (a scalar value). The basic idea is that the interference part of the effective SIR should include not only the inter-cell interference and noise but also the non-orthogonal part of the intra-cell interference. Once the effective SIR is calculated, it can be used to find the block-error probability for different MCS from basic AWGN link-level-performance curves.
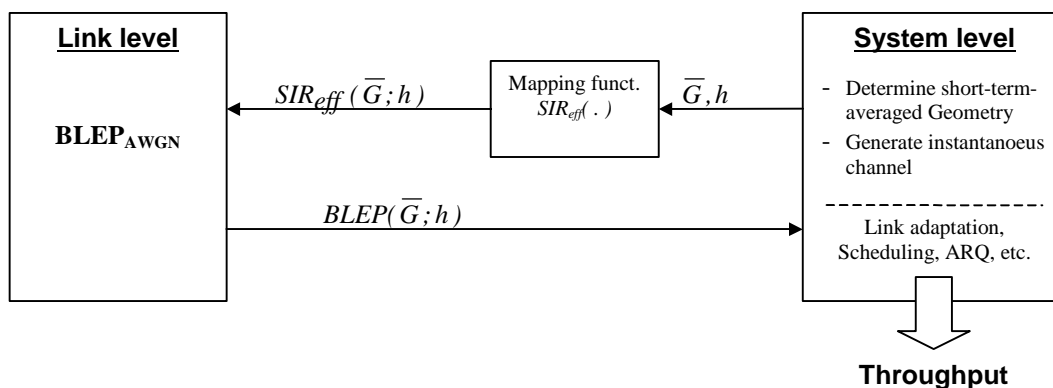
Figure 48: System-level methodology for HSDPA release 5

In case of low/medium Doppler, when the channel can be assumed to be constant over a TTI, it is straightforward to derive the mapping function $SIR_{eff}(\overline{G};h)$ for different linear receiver structures, such as a simple RAKE, a G-RAKE, or a chip-level equalizer using e.g. the MMSE criteria.

In the case of high Doppler, i.e. when the channel cannot be assumed to be constant over the TTI, the above methodology cannot be applied as straightforwardly as for the case of low/medium Doppler. The reason is that, in this case, the effective SIR cannot be assumed to be constant during the TTI. Thus, a more complex mapping function may be needed for accurate performance estimation.

A.4.2 HSDPA using OFDM modulation

For OFDM with a sufficiently large cyclic prefix, there is no intra-cell interference even in case of a time-dispersive channel. However, this does not imply that OFDM performance will not suffer from a frequency-selective (time-dispersive) channel. The reason is that, in case of OFDM and a frequency-selective channel, different coded bits will be subject to different instantaneous channel quality (different SIR). Channel coding and frequency-domain interleaving will reduce the negative effect of a frequency-selective channel on OFDM performance but will not eliminate it completely (the negative effect will be much higher at higher-rate coding, i.e. higher data rates, though).

For a correct system-level comparison between HSDPA release 5 and HSDPA using OFDM modulation, the negative effect of a frequency-selective channel on OFDM performance obviously needs to be taken into account in a sufficiently accurate way. It is also preferred that the methodology used to evaluate the system performance of HSDPA using OFDM modulation is aligned as much as possible with the system methodology used for HSDPA release 5. In this way, irrelevant performance deviations that are due to differences in the methodology are minimized and one can focus on the inherent differences of the different techniques.

Thus, this methodology for evaluating the system-level performance of OFDM modulation consists of the following steps:

- On system level, a UE exists within the simulated deployment and a short-term averaged geometry $\overline{G}$ is calculated for each UE. This step should be *identical* to HSDPA release 5 (same positions, same shadowing, etc.)

- For each UE and each TTI, an instantaneous channel is derived. In the OFDM case, the channel is preferable expressed in the frequency domain, i.e. as a frequency response $H(f)$ (in practice $H(f)$ is sampled in the frequency domain). Note that the channel could still be generated from an identical basic channel (same set of rays) as for HSDPA release 5. Thus, also this step should be fundamentally identical to HSDPA release 5.

- A mapping function $SIR_{eff}(\overline{G};H)$ is introduced that maps the geometry $\overline{G}$ and the frequency response $H(f)$ to an effective SIR value (a scalar value).

- The effective SIR is used to find the block-error probability from AWGN link-level-performance curves, exactly as for HSDPA release 5.
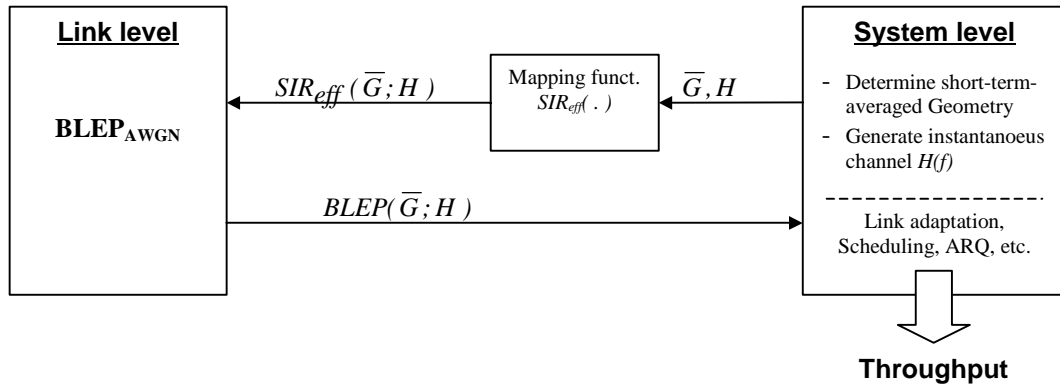
Figure 49: System-level methodology for HSDPA using OFDM modulation

A.4.3 Effective SIR Mapping Functions

A.4.3.1 Effective SIR Mapping Function for WCDMA

A.4.3.1.1 Effective SIR Mapping Function for WCDMA RAKE Receivers

The vector of finger outputs for a RAKE receiver, **y**, may be expressed as a sum of a signal part and a noise plus interference part as follows

$$\mathbf{y} = \mathbf{h}s + \mathbf{u}.$$

Here, s is the desired symbol, **h** is the channel response vector, and **u** models the overall noise and interference. The vector **u** is assumed to consist of complex Gaussian random variables with zero mean and covariance:

$$\mathbf{R}_u = E\{\mathbf{u}\mathbf{u}^H\}.$$

The channel response vector for the finger with delay d_j is given by the expression:

$$h(d_j) = \sqrt{E_0} \sum_{l=0}^{L-1} g_l R_p(d_j - \tau_l)$$

where,

- E_0 is the energy of the desired symbol (the symbol s itself is assumed to be normalized, i.e. $|s|^2 = 1$),
- L is the number of channel paths,
- g_l is the complex gain of the ℓth path ($\ell=1,\ldots,L$),
- τ_l is the delay of the ℓth path, and
- $R_p(d_j - t_\ell)$ is the autocorrelation of the pulse shape evaluated at the difference in delay between the jth finger and the ℓth path.

The calculation of the total noise plus interference covariance matrix $\mathbf{R}_u$ is as described in reference [9]. To summarize this development, the total covariance matrix consists of the sum of three other covariance matrices:

$$\mathbf{R}_u = E_0 \mathbf{R}_{\mathbf{ISI}} + (E_{TOT} - E_0)\mathbf{R}_{\mathbf{MCI}} + N_o \mathbf{R}_{\mathbf{n}}.$$

In this equation,

- $\mathbf{R}_{\mathbf{ISI}}$ is the covariance of the inter-symbol interference,
- $\mathbf{R}_{\mathbf{MCI}}$ is the covariance of the multi-code interference,
- $\mathbf{R}_{\mathbf{n}}$ is the covariance of the noise,
- E_o is the transmitted energy in the desired symbol,
- E_{TOT} is the total energy in the transmitted symbols, and
- N_o is the one-sided power spectral density of the noise.

With $\mathbf{h}$ and $\mathbf{R}_u$ defined, the effective SIR for a RAKE receiver may be calculated as

$$SIR = \frac{\mathbf{h}^H \mathbf{h} \mathbf{h}^H \mathbf{h}}{\mathbf{h}^H \mathbf{R}_u \mathbf{h}}.$$

A.4.3.1.2 Effective SIR Mapping Function for WCDMA MMSE Receivers

The SIR at the receiver output after MMSE filtering can be calculated as:

$$\mathbf{SIR_C} = \frac{\left\|\mathbf{w}_d \mathbf{h}_d\right\|^2}{\sum_{i=0, i \neq d}^{E+L-1} \left\|\mathbf{w}_d \mathbf{h}_i\right\|^2 + \left\|\mathbf{w}_d\right\|^2 \frac{\delta_n^2}{\delta_x^2}}$$

where δ_x^2 is the variance of the transmitted signal and $\delta_n^2 / 2$ is the additive Gaussian noise variance. $\mathbf{w}_d$ is the vector of MMSE equalizer tap coefficients and $\mathbf{h}_i$ is the ith column of the channel response matrix $\mathbf{\Gamma}$ (see [9] for the details). E is the span of the equalizer, in chips, and L is the delay spread of the channel. The above expression for SIR is an energy-per-chip to noise plus interference density ratio. This can be converted to an energy-per-symbol to noise plus interference density ratio with the expression

$$\mathbf{SIR} = \mathbf{SIR_C} \cdot \frac{SF}{\#codes} \cdot \left(\frac{\text{traffic power}}{\text{total power}}\right).$$

A.4.3.1.3 Effective SIR Mapping Function for WCDMA Receivers with Node B Impairments

The effective SIR for a WCDMA RAKE or MMSE receiver when including the effect of the Tx EVM is determined by

$$SIR = \frac{1}{\dfrac{1}{SIR_{no\,EVM}} + \dfrac{1}{SIR_{EVM}}}$$

where, $SIR_{no\,EVM}$ is the SIR as specified in section A.4.3.1.1 and A.4.3.1.2 for the RAKE and MMSE respectively, and SIR_{EVM} is a constant value specified by,

$$SIR_{EVM} = \frac{1}{EVM^2 \dfrac{K}{SF}\left(\dfrac{P_x}{P_{traff}}\right)}$$

where, EVM is the error vector magnitude value (assumed to be 12.5% as specified as the maximum permitted for 16-QAM transmission), K is the number of codes carrying data, $SF=16$ is the spreading factor of the data, and $\dfrac{P_x}{P_{traff}}$ is the ratio of total transmitted power to traffic power. Therefore, when $EVM=12.5\%$, $K=15$, $SF=16$, and

$$\frac{P_{traff}}{P_x} = 0.8 \text{, then } SIR_{EVM} = 17.4\,\text{dB}.$$

A.4.3.2   Effective SIR Mapping Functions for OFDM

This section contains proposed mapping functions for mapping the current channel conditions in an OFDM system-level simulator to an effective SIR that can then be used to determine the expected BLER from AWGN curves.

A.4.3.2.1   OFDM Exponential Effective SIR Mapping

The OFDM subcarrier SIR for an OFDM receiver may be calculated at the system-level as a function of the subcarrier power (which is a function of the channel's current frequency response), the current geometry ($\overline{G}$), the FFT size (N), and the cyclic prefix length (N_p), the percentage of maximum total available transmission power allocated to the data subcarriers (R_D), the number of data subcarriers per TTI (N_{SD}), and the number of total useful subcarriers per TTI (N_{ST}):

$$\gamma_k = P(k) \times \overline{G} \times \left(\frac{N}{N+N_p}\right) \times \frac{R_D}{N_{SD}/N_{ST}}$$

Assuming that the multi-path fading magnitudes $M_p(t)$ and phases $\theta_p(t)$ are constant over the observation interval, the frequency-selective fading power profile value for the kth subcarrier can be calculated as:

$$P(k) = \left|\sum_{p=1}^{paths} M_p A_p e^{j[\theta_p - 2\pi f_k T_p]}\right|^2 = \left|\sum_{p=1}^{paths} M_p A_p e^{j\theta_p} e^{-j2\pi f_k T_p}\right|^2$$

where p represents the multi-path path index, A_p is the amplitude value corresponding to the long-term average power for the pth path (assuming that the sum of the long-term path powers in the channel model has been normalized), f_k is the

relative frequency offset of the kth subcarrier within the spectrum, and T_p is the relative time delay of the pth path. It is assumed here that the fading profile is normalised such that $E[P(k)] = 1$.

The effective SIR mapping for these channel conditions can then be computed as

$$SIR_{eff} = -\beta \ln\left(\frac{1}{N_u}\sum_{k=1}^{N_u} e^{-\frac{\gamma_k}{\beta}}\right),$$

where β is a parameter that must be optimized from link-level simulation results for every modulation and coding rate combination. Note that a subset of the N_u useful subcarriers could also be used to evaluate the effective SIR for reasons of computational efficiency.

A.4.3.2.2 Effective SIR Mapping Function for OFDM with Node B Impairments

The effective SIR for OFDM when including the effect of the Tx EVM is determined by computing the SIR for each sub-carrier m with the expression

$$\gamma_m = \frac{1}{\dfrac{1}{\gamma_{m,\text{no EVM}}} + \dfrac{1}{\gamma_{m,\text{EVM}}}}$$

where $\gamma_{m,\text{no EVM}}$ is the SIR of sub-carrier m without the EVM as specified in section A.4.3.2.1 and $\gamma_{m,\text{EVM}}$ the constant value specified by,

$$\gamma_{m,\text{EVM}} = \frac{T_u F_c}{EVM^2 N_D\left(\dfrac{P_x}{P_{traff}}\right)}.$$

where, *EVM* is the error vector magnitude value (assumed to be 12.5% as specified as the maximum permitted for 16-QAM transmission), F_c is WCDMA spreading rate, N_D is the number of data symbols per OFDM symbol, T_u is the useful OFDM symbol duration, and $\dfrac{P_x}{P_{traff}}$ is the ratio of total transmitted power to traffic power. Therefore, for parameter set 2 and with *EVM*=12.5%, $N_D = 7200/12 = 600$, and $\dfrac{P_{traff}}{P_x} = 0.8$, then $\gamma_{m,EVM} = 17.1\,\text{dB}$. Once the SIR is determined for all of the sub-carriers, the effective SIR can be computed with, for instance, the exponential mapping,

$$SIR_{eff} = -\beta \ln\left(\frac{1}{N_u}\sum_{k=1}^{N_u} e^{-\frac{\gamma_k}{\beta}}\right).$$

A.4.4   System-Level HARQ Modelling

A.4.4.1   Chase-Combining HARQ Modelling for OFDM

The effects of chase-combining HARQ for OFDM can be modelled at the system-level using the following steps.

1. For each TTI, calculate the signal strength for each OFDM subcarrier (QAM symbol) from the channel frequency response for the corresponding OFDM symbol.
2. Calculate the interference-plus-noise power for each OFDM subcarrier (QAM symbol) in the TTI.
3. Permute the signal strength and interference-plus-noise power values according to the physical channel mapping and user multiplexing that is in effect for the current TTI in order to place the QAM symbols in the correct order for QAM demapping.
4. Perform HARQ combining by adding the signal magnitudes for the just received TTI to those present from any previous HARQ combining for that particular data block, and then calculate the power of the combined signal for each QAM symbol.
5. Sum the interference-plus-noise powers for multiple transmission attempts of the same data block.
6. The individual SIR values on the HARQ-combined QAM symbols may then be used to perform the effective SIR mapping mapping.

For greater computational efficiency, the following simplifying assumptions may be made if appropriate.

- For slowly varying channels (e.g. 3 km/h pedestrian channels), the channel frequency response can be assumed to be the same for all OFDM symbols in a given TTI. For a higher velocity channel, it may be necessary to recalculate the current channel frequency response for each OFDM symbol.
- A subset of equally-spaced representative subcarriers (or corresponding QAM symbols) may be used in place of all of the subcarriers (or QAM symbols) within a TTI.
- The interference-plus-noise power will be the same for all subcarriers (or QAM symbols) within a TTI if flat fading is assumed from the interfering cells and all cells (both the target cell and interfering cells) are assumed to be fully loaded. Otherwise, it will be necessary to calculate the interference-plus-noise power individually for each subcarrier (or QAM symbol).

A.4.5   Reference AWGN TTI BLER Curves for System-Level Simulations

Figure 50 and Figure 51 contain reference AWGN TTI BLER curves for use when modelling link-level performance within a system-level simulator. These curves are for a payload size corresponding to 15 data units (7200 QAM symbols per TTI) , and are valid for **both OFDM and WCDMA** (given the same MCS). For greater accuracy, the specific points on the TTI BLER curves are also listed in Table 22 and Table 23. Note that the columns labeled SIR in the tables refer to post-receiver SIR (as measured at the output of the receiver or, equivalently, at the input to the CCTrCH decoder). The turbo decoder used for these link-level simulations used a log-MAP decoding algorithm. A maximum of eight iterations were used, although an early stopping criterion was also in effect if the turbo decoder converged prior to the maximum number of decoding iterations being performed.
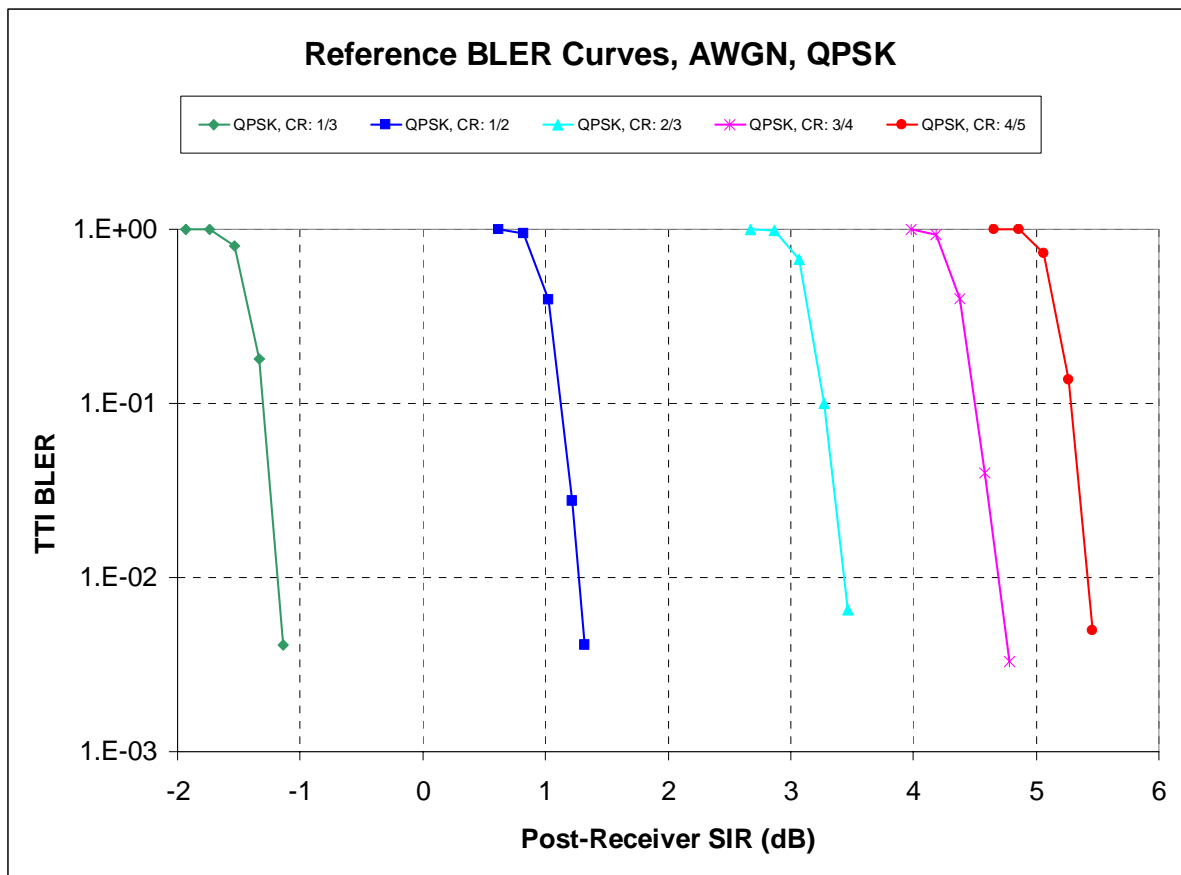
Figure 50: Reference TTI BLER curves in an AWGN channel (QPSK link modes)
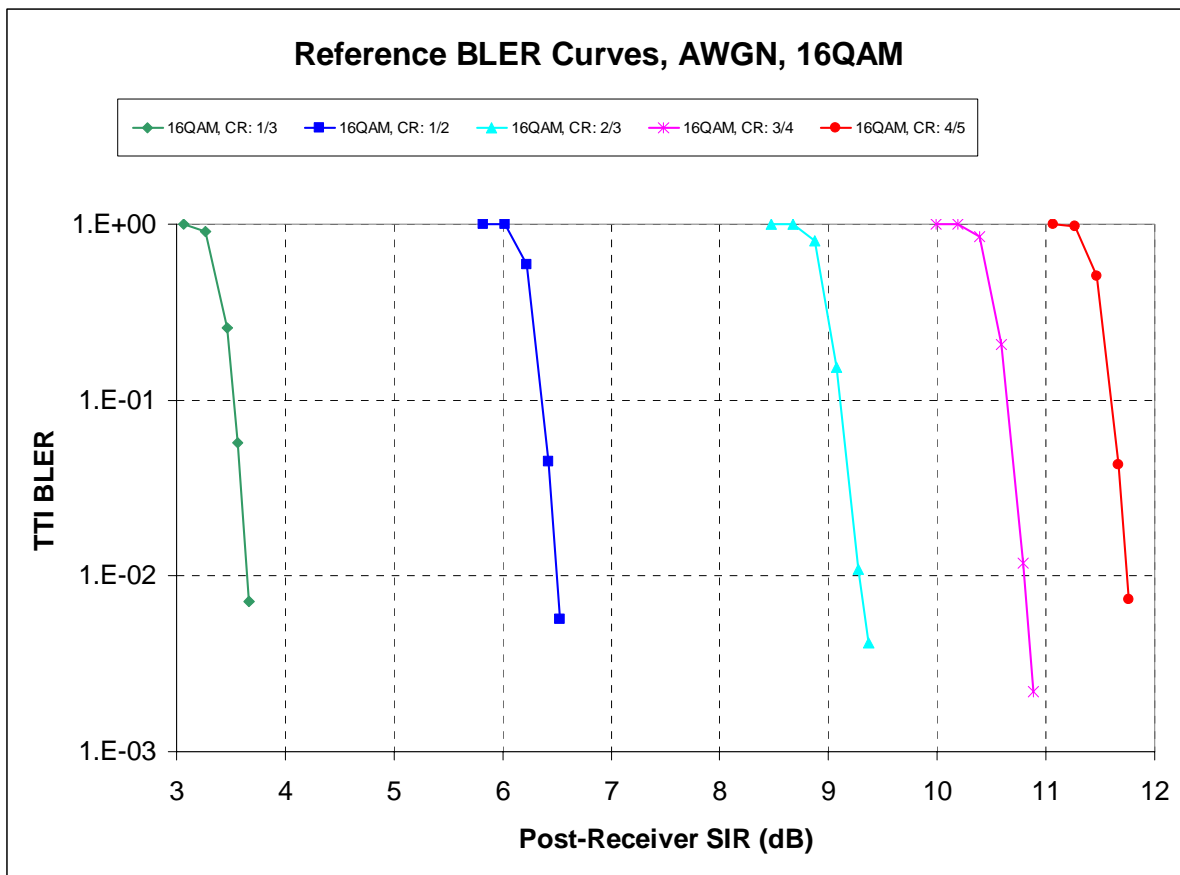
Figure 51: Reference TTI BLER curves in an AWGN channel (16QAM link modes)

QPSK, Rate 1/3		QPSK, Rate 1/2		QPSK, Rate 2/3		QPSK, Rate 3/4		QPSK, Rate 4/5	
SIR (dB)	BLER	SIR (dB)	BLER	SIR (dB)	BLER	SIR (dB)	BLER	SIR (dB)	BLER
-1.94	1.00E+0	0.62	1.00E+0	2.67	1.00E+0	3.98	1.00E+0	4.66	1.00E+0
-1.74	9.95E-1	0.82	9.45E-1	2.87	9.90E-1	4.18	9.40E-1	4.86	9.94E-1
-1.54	8.03E-1	1.02	3.95E-1	3.07	6.76E-1	4.38	3.98E-1	5.06	7.28E-1
-1.34	1.79E-1	1.22	2.76E-2	3.27	9.97E-2	4.58	3.97E-2	5.26	1.38E-1
-1.14	4.10E-3	1.32	4.13E-3	3.47	6.50E-3	4.78	3.30E-3	5.46	4.97E-3

Table 22: Reference TTI BLER curve points for an AWGN channel (QPSK link modes)

16QAM, Rate 1/3		16QAM, Rate 1/2		16QAM, Rate 2/3		16QAM, Rate 3/4		16QAM, Rate 4/5	
SIR (dB)	BLER	SIR (dB)	BLER	SIR (dB)	BLER	SIR (dB)	BLER	SIR (dB)	BLER
3.06	1.00E+0	5.82	1.00E+0	8.47	1.00E+0	10.18	1.00E+0	11.07	1.00E+0
3.26	9.14E-1	6.02	9.94E-1	8.67	9.92E-1	10.38	8.95E-1	11.27	9.51E-1
3.46	2.58E-1	6.22	5.89E-1	8.87	6.67E-1	10.58	2.79E-1	11.47	3.60E-1
3.56	5.72E-2	6.42	4.49E-2	9.07	1.08E-1	10.78	2.00E-2	11.67	2.42E-2
3.66	7.15E-3	6.52	5.70E-3	9.27	1.11E-2	10.98	1.57E-3	11.77	3.30E-3
				9.37	3.80E-3				

Table 23: Reference TTI BLER curve points for an AWGN channel (16QAM link modes)

A.4.6 Reference β Values for the OFDM EESM Approach in System-Level Simulations

A.4.6.1 Reference β Values Using a Random OFDM Subcarrier Interleaver

Table 24 contains a reference set of β values that may be used with the OFDM Exponential Effective SIR Mapping (EESM) technique described in Section A.4.3.2.1 for performing OFDM system-level simulations with the reference AWGN BLER curves from Section A.4.4. Note that these β values were estimated from link-level simulations using a random OFDM subcarrier interleaver.

Modulation	Code Rate	β
QPSK	1/3	1.49
	1/2	1.57
	2/3	1.69
	3/4	1.69
	4/5	1.65
16QAM	1/3	3.36
	1/2	4.56
	2/3	6.42
	3/4	7.33
	4/5	7.68

Table 24: Estimated values for the β parameter in the Exponential Effective SIR Mapping (EESM) for each link mode using a random OFDM subcarrier interleaver

A.5   System Simulation Results

A.5.1 Reference Performance (White Interference, No Impairments)

The following tables summarize the results of system-level performance evaluations that were conducted according to the simulation assumptions and methodologies described earlier in this Annex. Note that no code/unit division multiplexing has been performed, i.e. 15 units are assigned to a single user in each TTI. Note also that the results are based on the following assumptions:

- The interference can be modelled as AWGN.
- Node B/UE impairments are not modelled.
- Ideal channel estimation is used.

The channel models that were evaluated include Ped A and Ped B, both at 3km/h, while the traffic models that were evaluated include full-queue, FTP, and HTTP. Both the maximum throughput and round-robin scheduling algorithms were evaluated.

Technology	Users Per Sector	Average OTA Thruput (Mbps)	Ave. Packet Call Thruput (kbps)	Average Residual BLER	Average Packet Delay (sec)
OFDM	10	10.77	1077	0.000	–
	20	11.35	567	0.000	–
	40	11.51	288	0.000	–
	60	11.52	192	0.000	–
	80	11.52	144	0.000	–
	100	11.52	115	0.000	–
WCDMA (MMSE)	10	10.75	1075	0.000	–
	20	11.38	569	0.000	–
	40	11.50	287	0.000	–
	60	11.51	192	0.000	–
	80	11.52	144	0.000	–
	100	11.52	116	0.000	–
WCDMA (Rake)	10	6.14	614	0.000	–
	20	6.77	338	0.000	–
	40	7.17	179	0.000	–
	60	7.32	122	0.000	–
	80	7.43	93	0.000	–
	100	7.51	75	0.000	–

Table 25: System-level performance results for full queue traffic in Ped A with maximum throughput scheduling

Technology	Users Per Sector	Average OTA Thruput (Mbps)	Ave. Packet Call Thruput (kbps)	Average Residual BLER	Average Packet Delay (sec)
OFDM	10	5.16	516	0.006	–
	20	4.86	243	0.003	–
	40	4.66	116	0.001	–
	60	4.74	79	0.001	–
	80	4.63	58	0.001	–
	100	4.72	47	0.001	–
WCDMA (MMSE)	10	5.12	512	0.007	–
	20	4.76	238	0.003	–
	40	4.56	114	0.001	–
	60	4.65	77	0.002	–
	80	4.53	57	0.002	–
	100	4.60	46	0.002	–
WCDMA (Rake)	10	3.08	308	0.009	–
	20	2.94	147	0.004	–
	40	2.85	71	0.003	–
	60	2.89	48	0.003	–
	80	2.86	36	0.002	–
	100	2.88	29	0.003	–

Table 26: System-level performance results for full queue traffic in Ped A with round robin scheduling

Technology	Users Per Sector	Average OTA Thruput (Mbps)	Ave. Packet Call Thruput (kbps)	Average Residual BLER	Average Packet Delay (sec)
OFDM	10	10.29	1029	0.000	–
	20	11.16	558	0.000	–
	40	11.46	286	0.000	–
	60	11.50	192	0.000	–
	80	11.51	144	0.000	–
	100	11.52	115	0.000	–
WCDMA (MMSE)	10	7.78	778	0.000	–
	20	8.57	428	0.000	–
	40	9.33	233	0.000	–
	60	9.62	160	0.000	–
	80	9.92	124	0.000	–
	100	10.08	102	0.000	–
WCDMA (Rake)	10	3.92	392	0.000	–
	20	4.23	211	0.000	–
	40	4.49	112	0.000	–
	60	4.62	77	0.000	–
	80	4.71	59	0.000	–
	100	4.77	48	0.000	–

Table 27: System-level performance results for full queue traffic in Ped B with maximum throughput scheduling

Technology	Users Per Sector	Average OTA Thruput (Mbps)	Ave. Packet Call Thruput (kbps)	Average Residual BLER	Average Packet Delay (sec)
OFDM	10	5.24	524	0.001	–
	20	5.14	257	0.000	–
	40	5.03	126	0.000	–
	60	5.04	84	0.000	–
	80	4.99	62	0.000	–
	100	5.01	50	0.000	–
WCDMA (MMSE)	10	3.89	389	0.000	–
	20	3.86	193	0.001	–
	40	3.73	93	0.000	–
	60	3.76	63	0.000	–
	80	3.72	47	0.000	–
	100	3.78	38	0.000	–
WCDMA (Rake)	10	2.36	236	0.001	–
	20	2.34	117	0.000	–
	40	2.31	58	0.000	–
	60	2.31	39	0.000	–
	80	2.30	29	0.000	–
	100	2.31	23	0.000	–

Table 28: System-level performance results for full queue traffic in Ped B with round robin scheduling

Technology	Users Per Sector	Average OTA Thruput (Mbps)	Ave. Packet Call Thruput (kbps)	Average Residual BLER	Average Packet Delay (sec)
OFDM	10	3.99	3363	0.021	1.30
	20	4.28	3034	0.016	1.40
	40	4.75	2128	0.011	2.02
	60	5.49	1425	0.005	2.98
	80	6.55	911	0.001	4.61
	100	7.57	596	0.000	6.51
WCDMA (MMSE)	10	3.88	3252	0.024	1.33
	20	4.10	2399	0.020	1.47
	40	4.72	2098	0.011	2.00
	60	5.56	1366	0.005	3.09
	80	6.59	880	0.001	4.65
	100	7.54	593	0.000	6.55
WCDMA (Rake)	10	2.77	2154	0.027	2.01
	20	3.04	1743	0.018	2.51
	40	3.66	1016	0.007	4.22
	60	4.54	524	0.001	7.60
	80	5.14	322	0.000	11.25
	100	5.57	224	0	13.54

Table 29: System-level performance results for FTP traffic in Ped A with maximum throughput scheduling

Technology	Users Per Sector	Average OTA Thruput (Mbps)	Ave. Packet Call Thruput (kbps)	Average Residual BLER	Average Packet Delay (sec)
OFDM	10	3.90	3055	0.021	1.41
	20	3.87	2237	0.022	2.00
	40	4.03	1042	0.018	4.32
	60	4.09	351	0.009	12.23
	80	4.08	165	0.004	24.07
	100	4.17	116	0.003	31.41
WCDMA (MMSE)	10	3.79	2942	0.026	1.44
	20	3.77	2157	0.026	2.03
	40	3.86	884	0.022	5.02
	60	3.95	329	0.012	12.92
	80	3.94	158	0.006	24.93
	100	4.02	108	0.004	33.47
WCDMA (Rake)	10	2.65	1860	0.029	2.38
	20	2.62	1138	0.030	3.90
	40	2.75	336	0.018	12.84
	60	2.66	127	0.008	30.28
	80	2.76	83	0.005	40.37
	100	2.75	62	0.004	48.61

Table 30: System-level performance results for FTP traffic in Ped A with round robin scheduling

Technology	Users Per Sector	Average OTA Thruput (Mbps)	Ave. Packet Call Thruput (kbps)	Average Residual BLER	Average Packet Delay (sec)
OFDM	10	3.80	3153	0.004	1.38
	20	4.01	2702	0.002	1.61
	40	4.45	1802	0.002	2.33
	60	5.10	1026	0.001	3.97
	80	6.11	601	0.000	6.28
	100	6.90	413	0.000	8.20
WCDMA (MMSE)	10	3.27	2636	0.003	1.68
	20	3.39	2100	0.003	2.07
	40	3.83	1170	0.002	3.56
	60	4.67	636	0.000	6.38
	80	5.45	366	0.000	9.57
	100	6.04	274	0.000	10.86
WCDMA (Rake)	10	2.32	1664	0.004	2.63
	20	2.47	1210	0.002	3.58
	40	3.03	490	0.000	8.54
	60	3.58	246	0.000	14.61
	80	3.88	161	0.000	19.22
	100	4.10	119	0.000	23.39

Table 31: System-level performance results for FTP traffic in Ped B with maximum throughput scheduling

Technology	Users Per Sector	Average OTA Thruput (Mbps)	Ave. Packet Call Thruput (kbps)	Average Residual BLER	Average Packet Delay (sec)
OFDM	10	3.77	2956	0.003	1.46
	20	3.85	2233	0.003	1.99
	40	3.89	905	0.002	4.96
	60	4.02	338	0.001	12.62
	80	4.22	180	0.000	22.36
	100	4.32	123	0.000	29.87
WCDMA (MMSE)	10	3.09	2239	0.005	2.02
	20	3.12	1548	0.004	2.93
	40	3.25	544	0.003	8.14
	60	3.34	200	0.001	20.55
	80	3.37	118	0.001	31.54
	100	3.49	85	0.000	39.57
WCDMA (Rake)	10	2.15	1401	0.005	3.25
	20	2.23	827	0.004	5.46
	40	2.25	190	0.002	21.86
	60	2.25	96	0.001	37.37
	80	2.27	63	0.000	48.48
	100	2.29	48	0.000	55.55

Table 32: System-level performance results for FTP traffic in Ped B with round robin scheduling

Technology	Users Per Sector	Average OTA Thruput (Mbps)	Ave. Packet Call Thruput (kbps)	Average Residual BLER	Average Packet Delay (sec)
OFDM	10	2.87	456	0.027	0.14
	20	2.89	448	0.027	0.12
	40	2.91	442	0.026	0.15
	60	3.00	435	0.023	0.14
	80	3.06	426	0.021	0.16
	100	3.13	414	0.019	0.17
WCDMA (MMSE)	10	2.73	442	0.034	0.14
	20	2.78	446	0.031	0.13
	40	2.84	438	0.029	0.15
	60	2.91	427	0.027	0.15
	80	2.98	422	0.025	0.16
	100	3.06	416	0.022	0.19
WCDMA (Rake)	10	2.16	436	0.038	0.19
	20	2.14	428	0.038	0.23
	40	2.17	408	0.035	0.23
	60	2.27	394	0.029	0.23
	80	2.34	382	0.026	0.27
	100	2.44	362	0.022	0.29

Table 33: System-level performance results for HTTP traffic in Ped A with maximum throughput scheduling

Technology	Users Per Sector	Average OTA Thruput (Mbps)	Ave. Packet Call Thruput (kbps)	Average Residual BLER	Average Packet Delay (sec)
OFDM	10	2.93	451	0.027	0.12
	20	2.87	457	0.028	0.15
	40	2.94	454	0.026	0.16
	60	2.86	436	0.027	0.20
	80	2.91	428	0.026	0.21
	100	2.93	412	0.026	0.25
WCDMA (MMSE)	10	2.76	442	0.032	0.13
	20	2.75	447	0.034	0.14
	40	2.81	449	0.031	0.17
	60	2.84	436	0.031	0.20
	80	2.85	425	0.032	0.24
	100	2.86	409	0.030	0.26
WCDMA (Rake)	10	2.11	426	0.041	0.19
	20	2.13	420	0.040	0.22
	40	2.12	405	0.039	0.23
	60	2.13	389	0.037	0.30
	80	2.18	370	0.035	0.42
	100	2.20	338	0.034	0.56

Table 34: System-level performance results for HTTP traffic in Ped A with round robin scheduling

Technology	Users Per Sector	Average OTA Thruput (Mbps)	Ave. Packet Call Thruput (kbps)	Average Residual BLER	Average Packet Delay (sec)
OFDM	10	3.00	469	0.005	0.16
	20	3.19	466	0.003	0.13
	40	3.12	453	0.004	0.14
	60	3.18	442	0.003	0.15
	80	3.17	432	0.003	0.17
	100	3.24	424	0.003	0.19
WCDMA (MMSE)	10	2.66	446	0.005	0.15
	20	2.65	453	0.005	0.18
	40	2.67	443	0.005	0.20
	60	2.71	422	0.005	0.18
	80	2.73	407	0.004	0.21
	100	2.78	389	0.004	0.23
WCDMA (Rake)	10	1.94	424	0.005	0.24
	20	1.97	423	0.005	0.26
	40	2.01	400	0.005	0.29
	60	2.08	380	0.004	0.31
	80	2.09	351	0.004	0.36
	100	2.19	320	0.003	0.42

Table 35: System-level performance results for HTTP traffic in Ped B with maximum throughput scheduling

Technology	Users Per Sector	Average OTA Thruput (Mbps)	Ave. Packet Call Thruput (kbps)	Average Residual BLER	Average Packet Delay (sec)
OFDM	10	3.06	468	0.004	0.13
	20	3.11	468	0.004	0.14
	40	3.11	461	0.004	0.16
	60	3.06	448	0.004	0.17
	80	3.12	440	0.004	0.20
	100	3.13	430	0.003	0.25
WCDMA (MMSE)	10	2.64	464	0.005	0.16
	20	2.60	458	0.005	0.19
	40	2.57	438	0.006	0.21
	60	2.63	429	0.005	0.23
	80	2.64	416	0.005	0.29
	100	2.66	395	0.005	0.35
WCDMA (Rake)	10	1.95	432	0.006	0.24
	20	1.96	427	0.006	0.25
	40	1.94	408	0.005	0.32
	60	1.98	387	0.005	0.42
	80	1.97	346	0.005	0.49
	100	1.99	296	0.004	0.80

Table 36: System-level performance results for HTTP traffic in Ped B with round robin scheduling

A.5.2 Reference Performance (White Interference, Node B Impairments)

The following tables summarize the results of system-level performance evaluations that were conducted according to the simulation assumptions and methodologies described earlier in this Annex. Note that no code/unit division multiplexing has been performed, i.e. 15 units are assigned to a single user in each TTI. Note also that the results are based on the following assumptions:

- The interference can be modelled as AWGN.
- Node B impairments are modelled according to the methodology described in Section A.4.3.
- UE impairments are not modelled.

The channel models that were evaluated include Ped A and Ped B, while the traffic models that were evaluated include full-queue, FTP, and HTTP. Both the maximum throughput and round-robin scheduling algorithms were evaluated.

Technology	Users Per Sector	Average OTA Thruput (Mbps)	Ave. Packet Call Thruput (kbps)	Average Residual BLER	Average Packet Delay (sec)
OFDM	10	10.53	1055	0.000	–
	20	11.27	563	0.000	–
	40	11.47	287	0.000	–
	60	11.51	192	0.000	–
	80	11.52	144	0.000	–
	100	11.52	115	0.000	–
WCDMA (MMSE)	10	10.44	1046	0.000	–
	20	11.19	559	0.000	–
	40	11.47	287	0.000	–
	60	11.51	192	0.000	–
	80	11.51	144	0.000	–
	100	11.52	115	0.000	–
WCDMA (Rake)	10	5.88	588	0.000	–
	20	6.38	319	0.000	–
	40	6.81	170	0.000	–
	60	6.97	116	0.000	–
	80	7.07	88	0.000	–
	100	7.12	71	0.000	–

Table 37: System-level performance results for full queue traffic in Ped A with maximum throughput scheduling

Technology	Users Per Sector	Average OTA Thruput (Mbps)	Ave. Packet Call Thruput (kbps)	Average Residual BLER	Average Packet Delay (sec)
OFDM	10	4.94	493	0.005	–
	20	4.74	237	0.002	–
	40	4.48	112	0.001	–
	60	4.56	76	0.001	–
	80	4.52	56	0.001	–
	100	4.57	46	0.001	–
WCDMA (MMSE)	10	4.95	495	0.007	–
	20	4.49	224	0.003	–
	40	4.41	110	0.001	–
	60	4.46	74	0.002	–
	80	4.43	55	0.001	–
	100	4.47	45	0.002	–
WCDMA (Rake)	10	2.99	299	0.009	–
	20	2.83	142	0.005	–
	40	2.74	68	0.003	–
	60	2.75	46	0.003	–
	80	2.73	34	0.003	–
	100	2.76	28	0.003	–

Table 38: System-level performance results for full queue traffic in Ped A with round robin scheduling

Technology	Users Per Sector	Average OTA Thruput (Mbps)	Ave. Packet Call Thruput (kbps)	Average Residual BLER	Average Packet Delay (sec)
OFDM	10	10.00	1007	0.000	–
	20	10.88	544	0.000	–
	40	11.35	284	0.000	–
	60	11.46	191	0.000	–
	80	11.49	144	0.000	–
	100	11.50	115	0.000	–
WCDMA (MMSE)	10	7.43	743	0.000	–
	20	8.09	405	0.000	–
	40	8.75	219	0.000	–
	60	9.09	151	0.000	–
	80	9.27	116	0.000	–
	100	9.43	94	0.000	–
WCDMA (Rake)	10	3.75	375	0.000	–
	20	4.04	202	0.000	–
	40	4.30	108	0.000	–
	60	4.45	74	0.000	–
	80	4.53	57	0.000	–
	100	4.59	46	0.000	–

Table 39: System-level performance results for full queue traffic in Ped B with maximum throughput scheduling

Technology	Users Per Sector	Average OTA Thruput (Mbps)	Ave. Packet Call Thruput (kbps)	Average Residual BLER	Average Packet Delay (sec)
OFDM	10	5.07	507	0.001	–
	20	4.90	245	0.000	–
	40	4.80	120	0.000	–
	60	4.84	81	0.000	–
	80	4.79	60	0.000	–
	100	4.84	48	0.000	–
WCDMA (MMSE)	10	3.85	385	0.001	–
	20	3.78	189	0.000	–
	40	3.62	91	0.000	–
	60	3.67	61	0.000	–
	80	3.63	45	0.000	–
	100	3.68	37	0.000	–
WCDMA (Rake)	10	2.28	228	0.001	–
	20	2.21	111	0.000	–
	40	2.23	56	0.000	–
	60	2.22	37	0.000	–
	80	2.20	27	0.000	–
	100	2.21	22	0.000	–

Table 40: System-level performance results for full queue traffic in Ped B with round robin scheduling

Technology	Users Per Sector	Average OTA Thruput (Mbps)	Ave. Packet Call Thruput (kbps)	Average Residual BLER	Average Packet Delay (sec)
OFDM	10	3.81	3195	0.020	1.37
	20	4.09	2845	0.016	1.51
	40	4.61	2040	0.010	2.09
	60	5.41	1304	0.004	3.30
	80	6.55	798	0.001	5.19
	100	7.37	551	0.000	7.05
WCDMA (MMSE)	10	3.90	3292	0.023	1.26
	20	4.03	2790	0.019	1.55
	40	4.49	1926	0.012	2.18
	60	5.45	1249	0.004	3.42
	80	6.43	818	0.001	5.03
	100	7.33	527	0.000	7.33
WCDMA (Rake)	10	2.68	2094	0.027	2.08
	20	2.93	1698	0.019	2.54
	40	3.54	904	0.006	4.76
	60	4.37	475	0.001	8.71
	80	4.98	300	0.000	11.54
	100	5.36	208	0.000	14.25

Table 41: System-level performance results for FTP traffic in Ped A with maximum throughput scheduling

Technology	Users Per Sector	Average OTA Thruput (Mbps)	Ave. Packet Call Thruput (kbps)	Average Residual BLER	Average Packet Delay (sec)
OFDM	10	3.67	2892	0.021	1.59
	20	3.74	2143	0.021	2.05
	40	3.87	938	0.018	4.80
	60	3.98	315	0.009	13.81
	80	3.96	160	0.004	24.51
	100	4.02	109	0.003	33.05
WCDMA (MMSE)	10	3.85	3016	0.023	1.44
	20	3.55	2015	0.027	2.13
	40	3.78	788	0.019	5.67
	60	3.92	309	0.011	13.78
	80	3.84	152	0.005	25.57
	100	4.02	109	0.004	32.77
WCDMA (Rake)	10	2.51	1747	0.031	2.51
	20	2.55	1139	0.030	3.93
	40	2.62	296	0.017	14.62
	60	2.61	121	0.008	31.06
	80	2.64	77	0.005	42.42
	100	2.65	59	0.004	49.84

Table 42: System-level performance results for FTP traffic in Ped A with round robin scheduling

Technology	Users Per Sector	Average OTA Thruput (Mbps)	Ave. Packet Call Thruput (kbps)	Average Residual BLER	Average Packet Delay (sec)
OFDM	10	3.83	3169	0.003	1.37
	20	3.89	2655	0.003	1.60
	40	4.32	1637	0.001	2.60
	60	5.07	942	0.000	4.42
	80	5.97	549	0.000	6.82
	100	6.72	378	0.000	8.73
WCDMA (MMSE)	10	3.11	2518	0.005	1.73
	20	3.35	2099	0.003	2.06
	40	3.78	1081	0.001	3.81
	60	4.54	596	0.000	6.58
	80	5.32	358	0.000	9.96
	100	5.90	254	0.000	11.72
WCDMA (Rake)	10	2.25	1628	0.003	2.71
	20	2.43	1086	0.002	4.02
	40	3.00	432	0.000	9.64
	60	3.50	225	0.000	15.63
	80	3.77	151	0.000	20.14
	100	3.94	112	0.000	24.34

Table 43: System-level performance results for FTP traffic in Ped B with maximum throughput scheduling

Technology	Users Per Sector	Average OTA Thruput (Mbps)	Ave. Packet Call Thruput (kbps)	Average Residual BLER	Average Packet Delay (sec)
OFDM	10	3.54	2701	0.003	1.67
	20	3.82	2268	0.003	1.99
	40	3.82	820	0.002	5.52
	60	3.93	311	0.001	13.86
	80	4.12	168	0.000	23.27
	100	4.21	118	0.000	31.37
WCDMA (MMSE)	10	3.15	2314	0.004	1.98
	20	3.06	1478	0.004	2.96
	40	3.20	548	0.003	7.95
	60	3.31	203	0.001	20.12
	80	3.33	115	0.000	31.66
	100	3.41	81	0.000	41.27
WCDMA (Rake)	10	2.15	1386	0.004	3.25
	20	2.17	781	0.003	5.78
	40	2.18	193	0.001	21.17
	60	2.16	88	0.001	39.84
	80	2.17	60	0.000	50.42
	100	2.20	46	0.000	57.40

Table 44: System-level performance results for FTP traffic in Ped B with round robin scheduling

Technology	Users Per Sector	Average OTA Thruput (Mbps)	Ave. Packet Call Thruput (kbps)	Average Residual BLER	Average Packet Delay (sec)
OFDM	10	2.82	460	0.027	0.14
	20	2.89	460	0.026	0.14
	40	2.89	442	0.025	0.13
	60	2.97	430	0.023	0.15
	80	2.99	418	0.021	0.16
	100	3.11	416	0.018	0.18
WCDMA (MMSE)	10	2.71	457	0.033	0.14
	20	2.72	446	0.031	0.13
	40	2.80	440	0.028	0.15
	60	2.84	429	0.026	0.17
	80	2.93	423	0.025	0.16
	100	3.00	408	0.022	0.18
WCDMA (Rake)	10	2.04	430	0.041	0.22
	20	2.12	423	0.036	0.22
	40	2.17	407	0.033	0.22
	60	2.25	396	0.029	0.25
	80	2.31	374	0.025	0.27
	100	2.40	360	0.022	0.32

Table 45: System-level performance results for HTTP traffic in Ped A with maximum throughput scheduling

Technology	Users Per Sector	Average OTA Thruput (Mbps)	Ave. Packet Call Thruput (kbps)	Average Residual BLER	Average Packet Delay (sec)
OFDM	10	2.74	449	0.029	0.13
	20	2.79	459	0.028	0.15
	40	2.80	448	0.027	0.16
	60	2.78	432	0.027	0.19
	80	2.84	419	0.026	0.21
	100	2.90	410	0.025	0.25
WCDMA (MMSE)	10	2.74	456	0.033	0.14
	20	2.73	453	0.031	0.16
	40	2.76	447	0.031	0.17
	60	2.73	427	0.031	0.20
	80	2.80	422	0.030	0.24
	100	2.78	402	0.031	0.30
WCDMA (Rake)	10	2.02	425	0.041	0.21
	20	2.03	419	0.043	0.25
	40	2.11	405	0.037	0.27
	60	2.10	389	0.037	0.32
	80	2.10	362	0.036	0.44
	100	2.13	324	0.034	0.57

Table 46: System-level performance results for HTTP traffic in Ped A with round robin scheduling

Technology	Users Per Sector	Average OTA Thruput (Mbps)	Ave. Packet Call Thruput (kbps)	Average Residual BLER	Average Packet Delay (sec)
OFDM	10	3.04	464	0.003	0.14
	20	3.08	454	0.004	0.13
	40	3.10	449	0.003	0.15
	60	3.05	435	0.004	0.16
	80	3.13	432	0.003	0.18
	100	3.22	420	0.003	0.19
WCDMA (MMSE)	10	2.60	452	0.005	0.18
	20	2.65	455	0.004	0.18
	40	2.61	433	0.005	0.18
	60	2.63	417	0.005	0.21
	80	2.70	406	0.004	0.22
	100	2.76	389	0.004	0.28
WCDMA (Rake)	10	1.93	435	0.005	0.26
	20	1.93	416	0.005	0.24
	40	1.98	403	0.004	0.30
	60	2.01	371	0.004	0.32
	80	2.04	343	0.004	0.39
	100	2.15	313	0.003	0.46

Table 47: System-level performance results for HTTP traffic in Ped B with maximum throughput scheduling

Technology	Users Per Sector	Average OTA Thruput (Mbps)	Ave. Packet Call Thruput (kbps)	Average Residual BLER	Average Packet Delay (sec)
OFDM	10	3.15	476	0.003	0.13
	20	3.05	463	0.004	0.14
	40	3.00	456	0.004	0.17
	60	3.02	447	0.004	0.19
	80	3.04	438	0.004	0.22
	100	3.04	422	0.004	0.28
WCDMA (MMSE)	10	2.47	449	0.008	0.18
	20	2.58	451	0.006	0.21
	40	2.58	439	0.005	0.21
	60	2.59	429	0.005	0.25
	80	2.62	412	0.005	0.29
	100	2.61	389	0.004	0.41
WCDMA (Rake)	10	1.93	432	0.005	0.23
	20	1.89	416	0.007	0.26
	40	1.89	399	0.006	0.35
	60	1.92	377	0.005	0.46
	80	1.92	332	0.005	0.62
	100	1.94	280	0.004	0.90

Table 48: System-level performance results for HTTP traffic in Ped B with round robin scheduling

A.6   RF Aspects

A.6.1   W-CDMA Low Pass Filter: modelling and impact

A.6.1.1   LPF modelling

The LPF used for this study is a 5th order Chebyshef filter, type1. The case of 0.1dB ripple is considered for which gain and phase response versus frequency are shown in Figure 52.
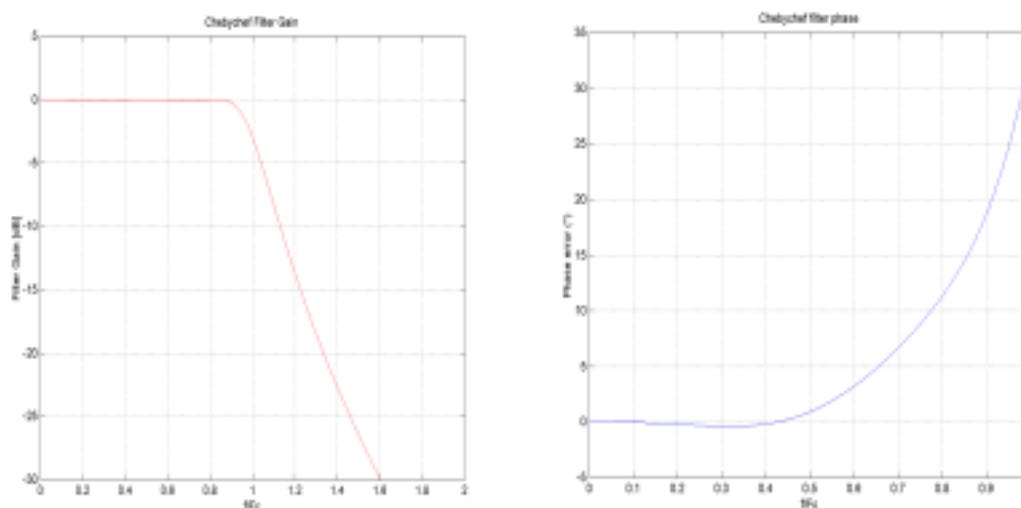

Figure 52: Gain and phase frequency response of the LPF Chebyshef used filter

As we can notice, the phase error increases at the borders of the considered frequency band. In W-CDMA reception chain, this impairment might be corrected by using another filter which compensates only the phase of the LPF. In OFDM technology, since the total frequency band is divided into smaller sub-band, correction may be done by means of the equalizer on every single sub-band without any additional complexity.

The Power Spectral Density of the resulting LPF filtered OFDM signals are presented in Figure 53. Amplitude degradations start to be relevant for Fc < 2.2MHz. Phase error is not presented.
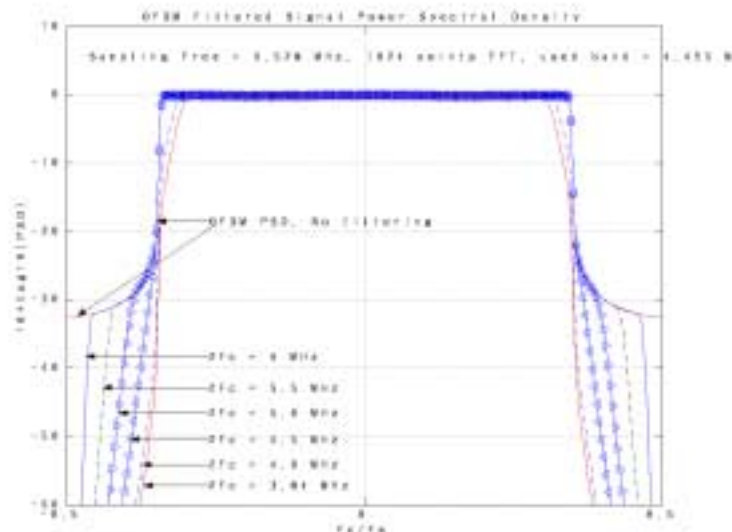
Figure 53: Power Spectral Density for LPF filtered-OFDM signals

A.6.1.2   Simulation assumptions

The Filtered-OFDM simulation chain is presented in Figure 54. The main functionalities are presented. Propagation channel and LPF are calculated by considering the same physical access layer.
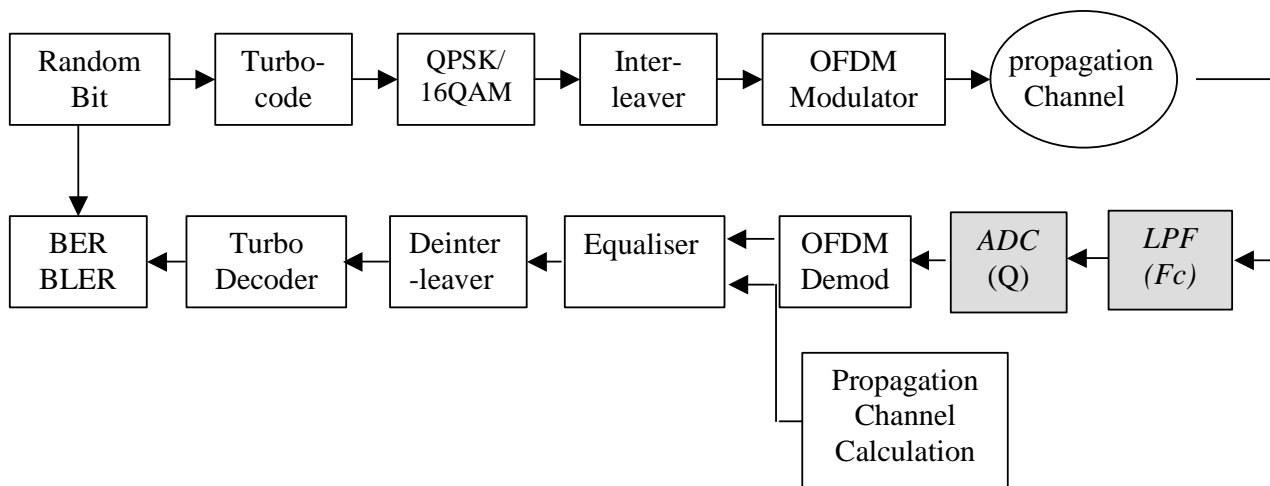

Figure 54: LPF Filtered-OFDM simulation chain

Simulation parameters are the following:

- Turbo-code rate is 1/2,
- Modulation QPSK and 16QAM.
- 15 Blocs of 480 symbols are sent in every TTI of 2ms.
- Interleaving is done over the entire TTI period.
- In case of QPSK: Transport bloc size is 450, this gives [(450+24)*2+12]/2=480 symbols.
- In case of 16QAM: Transport bloc size is 930, this gives [(930+24)*2+12]/4=480 symbols.

- OFDM modulation parameters is conformed to set2 in Table 1.
- The equalizer is a single symbol equalizer requiring only one tap for each sub-carrier.
- Turbo decoding is performed by a max-log-map algorithm.
- LPF cut-off frequency is 1.92MHz.
- No AGC is used.
- Quantification is done over 12 bits, the input dynamic = 3*A (QPSK) and 8*A (16QAM), where A is the mean amplitude signal.
- Propagation Channel is calculated (Perfect Channel Estimation).
- Comparison results are expressed in term of BLER after signal decoding.

The main advantage of the OFDM signal is to transform the multi-path channel into multiplicative channel, thus equalization is simplified and it is done by multiplying each single sub-carrier by a coefficient related to the effect of the propagation channel at this specific time/frequency localization. When considering this, the LPF effect may be assimilated to the channel effect, thus, propagation channel calculation (or estimation) considers both LPF and physical channel propagation and calculates their combined effect and thus no additional calculation is required.

A.6.1.3   LPF effect on multi-path fading channel

For this sake, simulations are done for the worst case cutting frequency value, namely Fc = 1.92 MHz. Simulated propagation channels are OI-A and OI-B for 3 Km/H, Vehicular A for 30Km/H and Vehicular A for 120 Km/h for both QPSK and 16QAM modulation. The LPF ripple value is 0.1dB. Results are presented in the following figures.
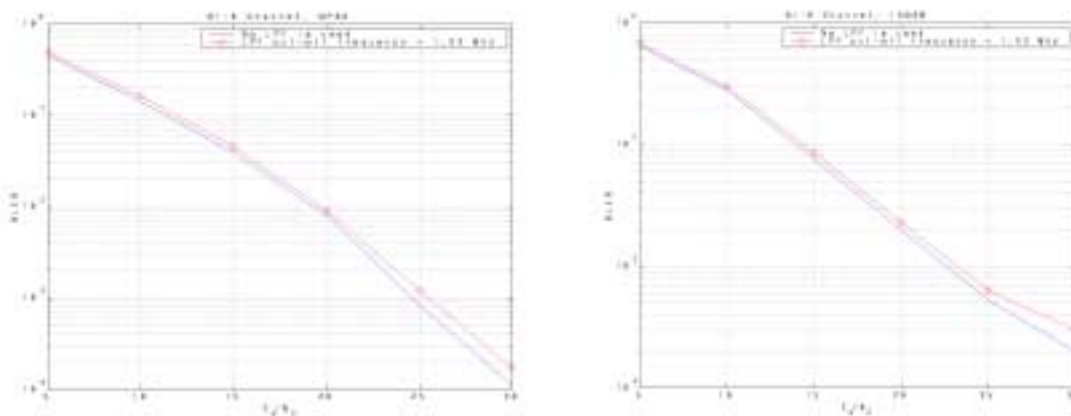

Figure 55: OI-A channel@3 Km/h, Quantization on 12 bits, no AGC, QPSK and 16 QAM modulation, with and without low pass filtering
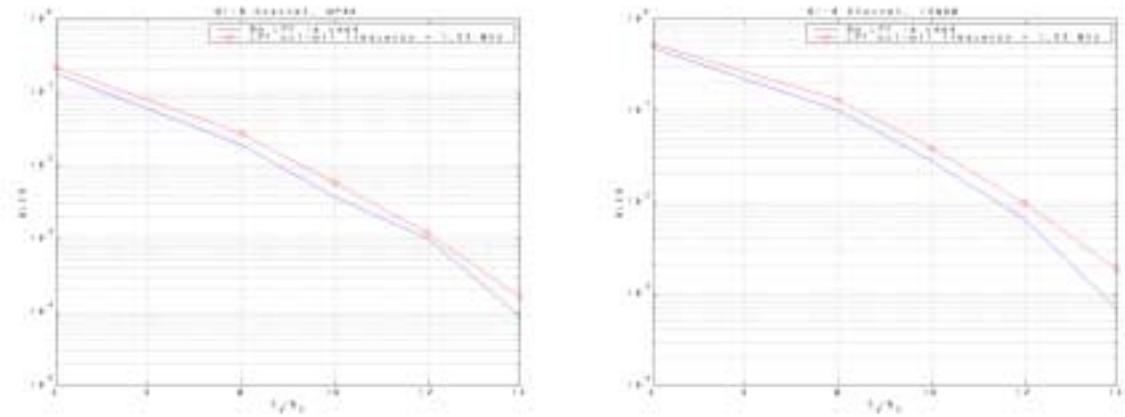
Figure 56: OI-B channel @ 3 Km/h, Quantization on 12 bits, no AGC, QPSK and 16 QAM modulation, with and without low pass filtering
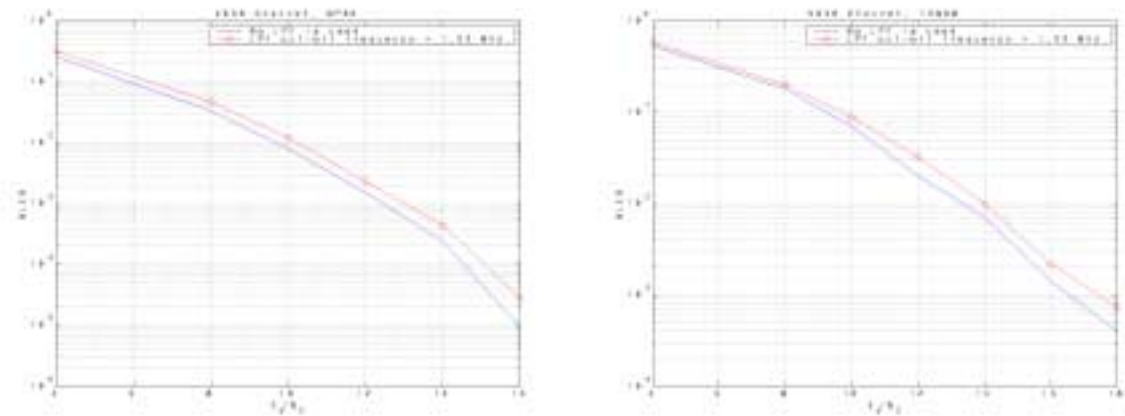

Figure 57: VA channel @ 30 Km/h, Quantization on 12 bits, no AGC, QPSK and 16 QAM modulation, with and without low pass filtering
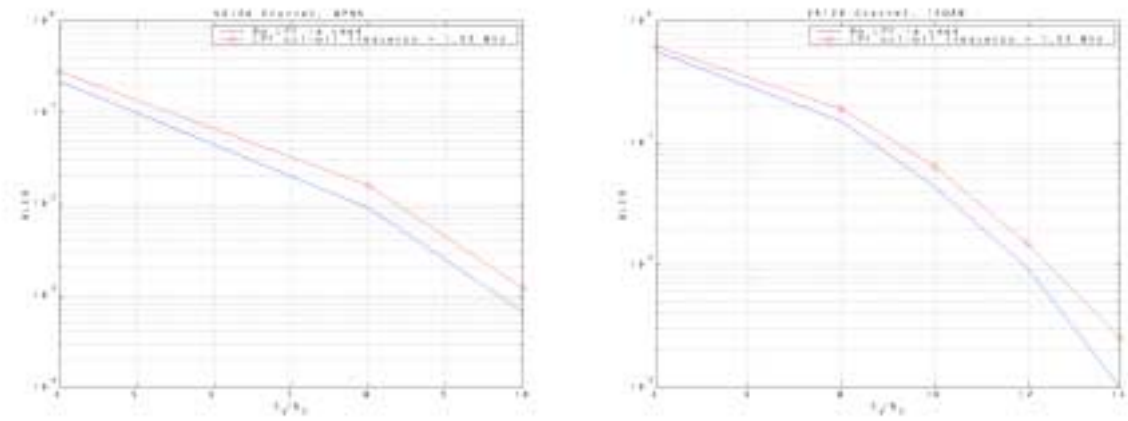
Figure 58: VA channel @ 120 Km/h, Quantization on 12 bits, no AGC, QPSK and 16 QAM modulation, with and without low pass filtering

Annex B:
Change history

Date	TSG #	TSG Doc.	CR	Rev	Subject/Comment	Old	New
05.07.02	RAN1#27	R1-020931			Initial draft presented for discussion		V0.0.1
23.10.02	RAN1#29	R1-021257			Update of the outline after discussions in RAN1#28bis	V0.0.1	V0.0.2
07.02.03	RAN1#31	R1-030227			Inclusion of approved text from R1-030135	V0.02	V0.0.3
19.02.03	RAN1#31	R1-030312			Removed revision marks.	V0.0.3	V0.1.0
20.02.03	RAN1#31	R1-030378			Inclusion of approved text from R1-030149, R1-030166, R1-030169 and R1-030328	V0.1.0	V0.1.1
28.03.03	RAN1#31	R1-030383			Modification to the OFDM sampling frequency definition	V0.1.1	V0.1.2
31.03.03	RAN1#31	R1-030384			Removal of revision marks	V0.1.2	V0.2.0
26.05.03	RAN#32	R1-030632			Inclusion of approved text from R1-030524, R1-030616, R1-030625 and R1-030627	V0.2.0	V0.2.1
28.08.03	RAN1#33	R1-030917			Removed revision marks	V0.2.1	V0.3.0
01.09.03	RAN1#33	R1-030655			Inclusion of modified text from R1-030655 according to agreement reached during the meeting Inclusion of approved text from R1-030804 and R1-030923	V0.3.0	V0.3.1
09.10.03	RAN1#34	R1-031141			Approval of revisions	V0.3.1	V0.4.0
10.10.03	RAN1#34	R1-031150			Inclusion of approved text from R1-031127	V0.4.0	V0.4.1
20.11.03	RAN1#35	R1-031391			Removed revision marks	V0.4.1	V0.5.0
21.11.03	RAN1#35	R1-031409			Fixed section numbering problem in V0.5.0	V0.5.0	V0.5.1
03.12.03	RAN1#35	R1-031436			Inclusion of approved text from R1-031172, R1-031296, R1-031299, R1-031370, R1-031392, R1-031420, R1-031431.	V0.5.1	V0.5.2
28.01.04	Rel6 Ad Hoc	R1-040003			Removed revision marks	V0.5.2	V0.6.0
28.01.04	Rel6 Ad Hoc	R1-040004			Inclusion of approved text from R1-040005, R1-040006, R1-040040, R1-040045 and R1-040091.	V0.6.0	V0.6.1
19.02.04	RAN1#36	R1-040369			Approval of revisions	V0.6.1	V1.0.0
19.02.04	RAN1#36	R1-040373			Inclusion of approved text from R1-040210, R1-040211, R1-040212, R1-040262, R1-040292, R1-040293, R1-040294, R1-050295.	V1.0.0	V1.0.1
05.03.04	RAN1#36	R1-040394			Removed revision marks	V1.0.1	V1.1.0
11.05.04	RAN1#37	R1-040636			Inclusion from approved text from R1-040504, R1-040506, R1-040511, R1-040512, R1-040510, R1-040513, R1-040508, R1-040507, R1-040625	V1.1.0	V1.1.1
25.04.04	RAN1#37	R1-040655			Approved revision marks	V1.2.0	V1.1.0

Presentation of Specification to TSG or WG

Presentation to:	**TSG RAN Meeting #24**
Document for presentation:	**TR25.892, Version 2.0.0**
Presented for:	**Information**

Abstract of document:

This TR is RAN1's working document for the Study Item "Feasibility Study of OFDM for UTRAN enhancement" RInImp-FSOFDM. This study considers the feasibility of introducing OFDM in UTRAN and compares OFDM performance with HSDPA.

As agreed in RAN Plenary, the analysis has considered only textbook OFDM and excluded other OFDM techniques. The study has been on a comparison of the WCDMA physical layer by a OFDM physical layer in DL with 5MHz channelisation in a HSDPA data-only cell. The services to upper layers i.e. Transport channels, measurements, have been basically kept so as to minimise impacts and ease the comparison.

The feasibility study is structured as follows:

- General introduction of OFDM technology (fundamentals, signal generation, reference OFDM and WCDMA scenarios for the study)

- Reference set of parameters for the evaluation

- Feasibility aspects: spectrum compatibility, physical layer structure, handover and synchronisation, frequency re-use, UE and node B complexity aspects, impact on L2 and L3 protocols.

- Simulation assumptions and results (annex)

Changes since last presentation to TSG RAN Meeting:

The TR has been completed to cover compatibility with WCDMA carriers, frequency re-use aspects, mobility and handover, impacts on the UL, impacts on L2 and L3 protocols, performance with node B impairments and coloured interference. The conclusion for the Study Item has also been drawn by RAN1.

Outstanding Issues:

None

Contentious Issues:

None